

Searching for the QCD Dark-Matter Axion

Masha Baryakhtar

Physics Department, University of Washington, Seattle, WA 98195-1560, USA

E-mail: mbaryakh@uw.edu

Leslie Rosenberg

Physics Department and Center for Experimental Nuclear Physics and Astrophysics,
University of Washington, Seattle, WA 98195-1560, USA

E-mail: ljrberg@uw.edu

Gray Rybka

Physics Department and Center for Experimental Nuclear Physics and Astrophysics,
University of Washington, Seattle, WA 98195-1560, USA

E-mail: grybka@uw.edu

16 April 2025

Abstract. Proposed half a century ago, the quantum chromodynamics (QCD) axion explains the lack of charge and parity violation in the strong interactions and is a compelling candidate for cold dark matter. The last decade has seen the rapid improvement in the sensitivity and range of axion experiments, as well as developments in theory regarding consequences of axion dark matter. We review here the astrophysical searches and theoretical progress regarding the QCD axion. We then give a historical overview of axion searches, review the current status and future prospects of dark matter axion searches, and then discuss proposed dark matter axion techniques currently in development.



This review is dedicated to the memory of Ann Elizabeth Nelson. A brilliant theoretical physicist, Ann contributed much to the theory and phenomenology of charge and parity symmetry, including axion physics. She is loved and missed. Photo courtesy D. B. Kaplan.

Contents

1	Introduction	4
2	Theory	6
2.1	The Axion Mass	6
2.2	Axion Interactions with Standard Model Matter and Radiation	7
3	Cosmology	9
3.1	Axion Misalignment	9
3.2	Axion String Networks	10
3.3	Inferences on the Preferred Axion Mass from Dark Matter Density	12
3.4	Additional Cosmological Signatures of Axion Dark Matter	13
3.5	Modifications of Axion Cosmology	14
3.6	Axion Dark Matter Structure Formation	15
4	Astrophysics	16
4.1	The Sun	17
4.2	Red Giants and Horizontal Branch Stars	19
4.3	White Dwarfs	20
4.4	Neutron Stars	20
4.5	Black Holes	22
5	Laboratory Experiments	26
5.1	Relevant Length Scales	26
5.2	Early Searches, Limits and Bounds	27
5.3	Microwave Cavity Haloscopes	32
5.4	Next Steps for Cavity Haloscopes	43
5.5	Electromagnetic Searches Beyond Microwave Cavities	45
5.5.1	LC Circuit Haloscopes	45
5.5.2	Heterodyne Detection	47
5.5.3	Broadband Reflectors	48
5.6	Axion-Nucleon Coupling Experiments	48
5.6.1	ARIADNE	48
5.6.2	CASPEr	49
6	Summary and Outlook	49

1. Introduction

The particle now known as the Quantum ChromoDynamics (QCD) axion was first proposed in the late 1970s [1–3]. It originated as the low-energy manifestation of the Peccei-Quinn (PQ) mechanism [1, 4] devised to solve the puzzle of the undetectable smallness of the amount of charge-parity (CP) violation in the strong interactions in the Standard Model (SM) of particle physics. The CP-violating QCD field strength term has not yet been observed in exquisitely sensitive experiments and is consistent with zero. On the other hand, it is allowed by all the known symmetries of the standard model and produces physical effects such as a non-zero neutron electric dipole moment (EDM) [5–7].

This CP violation is characterized by the dimensionless parameter θ , which is the sum of the QCD topological angle $\mathcal{L} \supset \theta_0 G_{\mu\nu} \tilde{G}^{\mu\nu}$ and the common quark mass phase $\theta = \theta_0 + \arg \det M_q$. While the underlying physics of these two terms is unrelated, with the latter potentially obtaining contributions from CP-violating electroweak physics, they nonetheless appear to cancel to exquisite precision: Among other observables, θ contributes to the neutron EDM $d_n \sim 3 \times 10^{-16} \theta$ e cm [8–10]. The latter has been experimentally bounded to be $d_n < 1.8 \times 10^{-26}$ e cm (90% C.L.) [11], leading to a constraint on the CP-violating QCD field strength parameter of $\theta \lesssim 5 \times 10^{-11}$. Recently, it has been noted that θ provides a contribution to electron EDM observables which currently places constraints two orders of magnitude weaker than neutron EDMs [12] but may provide a cross-check on the underlying physics in the event of a detection.

The QCD axion, a , is a pseudo-Nambu-Goldstone boson whose potential is minimized at the CP-preserving minimum [13], up to small electroweak corrections that lie beyond the current experimental sensitivity [14]. The QCD axion’s potential [15] is largely described by a single parameter, the decay constant f_a , which sets its mass at zero temperature and chemical potential to [16]

$$m_a = 5.691(51) \mu\text{eV} \left(\frac{10^{12} \text{GeV}}{f_a} \right). \quad (1)$$

The leading self-interaction is a quartic one, with value [17]

$$\lambda \simeq 10^{-50} \left(\frac{10^{12} \text{GeV}}{f_a} \right)^4, \quad (2)$$

which, while typically negligible, can have an impact at high axion field densities such as in the early universe or near astrophysical black holes.

The decay constant also parametrizes the axion’s interactions with standard-model particles at energies below the electroweak scale, including gluons, photons and fermions (Figure 1),

$$\mathcal{L} \supset \frac{a}{f_a} \frac{\alpha_s}{8\pi} G_{\mu\nu} \tilde{G}^{\mu\nu} + \frac{g_{a\gamma\gamma}}{4} a F_{\mu\nu} \tilde{F}^{\mu\nu} + \frac{g_{a\psi}}{2} \partial_\mu a \bar{\psi} \gamma^\mu \gamma_5 \psi, \quad (3)$$

where $G_{\mu\nu}$ ($\tilde{G}^{\mu\nu}$) is the gluon field-strength tensor (and its dual) and $F_{\mu\nu}$ ($\tilde{F}^{\mu\nu}$) is the electromagnetic field strength tensor (and its dual). The coupling constants are

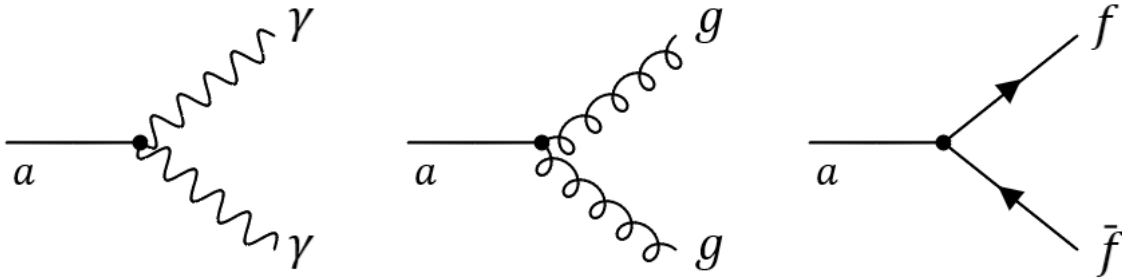


Figure 1: Feynman representation of fundamental axion interactions with gluons, photons, and fermions.

parametrized as

$$g_{a\gamma\gamma} = C_{a\gamma\gamma} \frac{\alpha}{2\pi f_a}, \quad g_{a\psi} = \frac{C_\psi}{f_a}, \quad (4)$$

where α is the electromagnetic fine structure constant and $C_{a\gamma\gamma}, C_\psi$ are dimensionless coefficients, typically order-one or generated at one-loop level in generic models, as discussed further in Section 2.

By itself, the PQ mechanism does not much constrain the axion mass [Eq. (1)], which is to say the $U(1)_{PQ}$ symmetry-breaking scale f_{PQ} (related to the decay constant f_a above by the details of the PQ symmetry and its breaking) is largely undetermined. As the axion straddles the physics of weak and strong interactions, it seemed plausible at the time of the original proposals to consider the electroweak or perhaps the QCD scale as the scale for the $U(1)_{PQ}$ symmetry breaking. Strong-scale axions imply axion masses in the MeV range and axion couplings to normal matter and radiation that would have likely rendered those axions easily detectable in terrestrial experiments and in astrophysical environments—essentially a new neutral pion-like particle would have been observed. In the early 1980’s, not long after the PQ mechanism and the axion were proposed, the weak-scale axion was also experimentally ruled out by beam-dump, accelerator, and astrophysical searches.

As a result of these early bounds, the axion scale f_a was pushed far above the electroweak scale. These extraordinarily feeble couplings to normal matter and radiation would make the axion perhaps the most feebly-coupled particle (excepting the graviton). Indeed, the lifetime of such an axion into its dominant two-photon decay channel is considerably longer-lived than even the lifetime of the proton in a GUT scenario and many orders of magnitude longer than the age of the universe, and can reach up to 10^{77} years for the lightest QCD axions. So these are very feebly-coupled particles indeed. Such axions were, perhaps derisively, called ‘invisible axions’ owing to what was presumed to be the impossibility of their detection [18–20].

A few years after the axion was first proposed as a new particle, it also became apparent that it would provide an inevitable contribution to the energy density of the universe [21–23]. The previously ‘invisible’ axion with a high f_a scale turned out to

have properties that make it an attractive dark-matter candidate. Such axions would thus not only arise in a solution to the strong-CP problem, they would also address the profound question of the nature and composition of dark matter. And so, the axion became one of the rare dark matter candidates to solve an unrelated theoretical issue, the strong-CP problem.

Further, the axion has more recently been found to commonly arise in high-energy extensions to the SM with non-trivial topology in extra dimensions, such as string theory [24, 25]. The dual theoretical and experimental motivations for the QCD axion make it one of the best-motivated candidates for a new particle beyond the SM. Therefore, the detection of the axion would yield much beyond a new particle discovery: it would advance our understanding of symmetries and provide access to the highest energy scales yet observed, as well as open the door to early universe cosmology and the local structure of dark matter in our galaxy.

The last decade has seen tremendous progress in axion physics on both the theoretical and experimental fronts. We point the reader to a number of recent reviews on the theory [26–28], experimental searches [29–32], and astrophysics and cosmology [33–35] of the QCD axion and the broader parameter space of axion-like-particles for further detail and background material; see also the PDG review [36] and an online repository of recent constraints [37]. This review focuses on recent experimental achievements and proposals, as well as new theoretical developments—with a focus on the dark matter QCD axion—while providing relevant context. We give a summary of axion theory in Section 2, axion dark matter cosmology in Section 3, searches in astrophysical compact objects in Section 4, and provide a detailed review of axion laboratory experiment history, recent progress with an emphasis on cavity haloscopes, and future directions toward the dark matter QCD axion in Section 5. We conclude and comment on the outlook for the future in Section 6.

2. Theory

The details of the axion solution to the strong-CP problem have been established for several decades. In this section, therefore, we provide an outline of the essential theory background relevant for establishing the axion parameter space and subsequent discussion, in particular its mass and couplings to the SM. We also comment briefly on the more recent theoretical progress.

2.1. The Axion Mass

The axion mass is determined by how the QCD vacuum energy depends on the CP-violating θ parameter,

$$m_a^2 = \frac{\chi_{\text{top}}}{f_a^2} + \mathcal{O}(m_\pi^2/f_a^2) \quad (5)$$

where χ_{top} , the topological susceptibility, is the second derivative of the free energy with respect to the θ angle at $\theta = 0$. This is a non-perturbative quantity in QCD and has been

computed on the lattice to be $\chi_{\text{top}} = 75$ MeV with a few percent uncertainty [16,38,39]‡. Furthermore, the fact that the physical angle θ is the sum of the QCD topological angle $\bar{\theta}$ and the common quark mass phase $\arg \det M_q$ allows the θ parameter to be fully rotated into the light quark mass matrix using quark field phase redefinitions. Then at leading order in the chiral expansion all the non-derivative dependence on the axion is contained as phases in the pion mass terms, which in turn allows the use of tools of chiral Lagrangian perturbation theory with inputs from the lattice to compute the axion mass very precisely at zero temperature [17]. Using $N_f = 2$ chiral theory at NNLO with QED corrections [16] gives the mass prediction of Eq. (1).

At finite temperature, the topological susceptibility is an important quantity in determining the early universe evolution of the axion and therefore its late-time abundance. The axion begins behaving as dark matter in the early universe when the axion mass is of order the Hubble parameter; the axion mass is itself a function of the background temperature. The high-temperature regime $\chi_{\text{top}}(T) \gg T_c$ is largely well-approximated by the dilute instanton approximation while at lower temperatures, the lattice has been used to determine $\chi_{\text{top}}(T)$. A shallower power law with temperature would imply a larger f_a coupling constant for a fixed dark matter abundance and initial misalignment angle. While in some work [38,40], the power law suppression was found to be a much smaller than the dilute instanton gas prediction, $\chi_{\text{top}}(T) \sim T^{-8}$, later lattice results seem to agree with the instanton gas approximation scaling at temperatures close to the QCD phase transition in pure Yang-Mills [41,42] and QCD [39,43–45] for three light flavors, although to date calculations of the overall magnitude of the susceptibility are not yet in agreement. The lattice calculations which capture the temperature dependence $\chi_{\text{top}}(T)$ over the relevant range point to a post-inflationary misalignment axion mass of $28 \pm 2 \mu\text{eV}$ [39]. Other work estimates the present uncertainties in the topological susceptibility to translate to an uncertainty in the dark matter axion mass of a factor of 2 [46].

The understanding of the QCD axion potential at finite nuclear density (or chemical potential) is far more uncertain. At densities approaching nuclear density, the potential is expected to be suppressed [47] due to a reduction in the quark condensate [48]. How this suppression—and the resulting effect on the axion mass and interactions—evolves at and beyond nuclear density remains unclear but may have implications for axion physics in dense objects such as neutron stars [49–51].

2.2. Axion Interactions with Standard Model Matter and Radiation

The axion solution to the strong-CP problem relies only on the coupling of the axion to the gluon field strength. However, this coupling is unfortunately the most difficult to probe quantitatively, due to the non-perturbative nature of QCD at low energies. Our inability to access free gluons and quarks and the lack of precision predictions

‡ The lattice calculation is in the isospin-symmetric limit and the quoted quantity is corrected to take into account deviations from $m_u = m_d$.

and measurements of their low-energy manifestations—nucleons and nuclei—make this coupling a challenge to pursue. Nevertheless, in recent years there have been several detection ideas, including Casper Electric [52–54] and the more recent Axioelectric effect [55, 56] to search for axion dark matter through the fundamental QCD coupling.

It was quickly realized that in typical ultraviolet models the axion also inherits interactions to other SM particles [57–62]. One of the more generic, and most promising for detection, is the coupling to pairs of photons. Since part of the coupling to photons comes from low-energy QCD, it is challenging to entirely tune away the axion interaction with photons. There are two original benchmark classes of models yielding photon coupling predictions: KSVZ (or “hadronic”) [57, 58] and DFSZ [59, 60], which have different field content creating the anomaly that yields the two-photon coupling. These envelope an expected band of interactions [16],

$$g_{a\gamma\gamma} = \frac{\alpha}{2\pi f_a} \left(\frac{E}{N} - 1.92(4) \right), \quad (6)$$

with E (N) the electromagnetic (color) anomaly of the PQ symmetry. Searches for the photon coupling has driven most of the experimental effort in the search for the QCD axion, see Section 5.

In addition to photons, axions also have a derivative interaction with nuclei N , with interactions at low energies of the form,

$$\mathcal{L} \supset \frac{\partial_\mu a}{2f_a} c_N \bar{N} \gamma^\mu \gamma_5 N, \quad \text{with } N = \{n, p\}, \quad (7)$$

where the couplings to protons p and neutrons n depend on the model and have been computed using chiral EFT methods with lattice input to be [17],

$$\text{KSVZ} : c_p = -0.47(3), \quad c_n = -0.02(3). \quad (8)$$

$$\text{DFSZ} : c_p = -0.617 + 0.435 \sin^2 \beta \pm 0.025, \quad c_n = 0.254 - 0.414 \sin^2 \beta \pm 0.025. \quad (9)$$

In the DFSZ models there are direct couplings to the quarks in the UV theory, and $\tan \beta$ characterizes the ratio of vacuum expectation values in a two-Higgs doublet model.

The typical couplings to electrons is $\sin^2 \beta/3$ in DFSZ models, and if zero at tree level in the UV is generated at loop level at low energies to be $C_e \sim \mathcal{O}(\alpha^2)$ [61, 62]. Finally, in a CP-violating background, axions can mediate new Yukawa-type forces [63]. These new forces are being searched for in experiments including ARIADNE [64, 65].

There have been many recent theoretical developments potentially broadening the parameter space of couplings outlined above, including enhanced couplings using the clockwork mechanism [66]; for a detailed recent review of models see [27]. However, in grand unified theories, even axion-like particles are expected to have photon couplings close to or below the QCD axion line, further motivating experimental searches that target QCD axion sensitivities [67–69].

3. Cosmology

Just a few years after the axion particle was identified as a solution to the strong-CP problem, it became apparent that it could easily solve another outstanding problem in the Standard Model: the absence of a cold dark matter candidate [70, 71]. Several groups pointed out that the so-called invisible axion—with decay constant above that constrained by stellar evolution, $f_a \gtrsim 10^8$ GeV [72–74]—would have a non-trivial cosmological abundance [21–23].

Cosmology with an axion field goes as follows: Initially, the temperature of the universe is above f_a and particle physics is Peccei-Quinn symmetric. As the universe cools below f_a , Peccei-Quinn symmetry is broken, and, below the scale of the QCD crossover transition, an energetically preferred value of $\theta \equiv a/f_a$ arises. The misalignment between the initial θ_i value and the preferred minimum of the axion potential corresponds to a large energy density being stored in the axion field. Additionally, because θ is 2π periodic, topological defects known as axion strings thread the universe upon PQ breaking and, at the time of the QCD transition, regions of different θ are bounded by domain walls. The strings and domain walls evolve and ultimately annihilate, emitting axion radiation. If this process takes place before the end of inflation, and PQ symmetry is not subsequently restored, then the expected number of strings and domain walls within our visible universe is negligible. At no time is the axion field in thermal equilibrium with the rest of the SM particles, and the axion couplings are so small that axions produced via misalignment or topological defect decay persist today as dark matter, either smoothly distributed or potentially in part in residual clumps formed in the QCD phase transition.

A detailed description of axion cosmology is available in [33, 34]. Here we summarize the aspects above, with a focus on addressing the question of what astrophysical measurements of dark matter can tell us about QCD axion parameters, and discuss current developments beyond the standard axion cosmological story.

3.1. Axion Misalignment

If PQ symmetry is broken before inflation ends, a range of initial conditions is possible, and the energy density in axion dark matter depends on the initial value θ_i in the patch from which our universe originated [75]. If PQ symmetry is broken after inflation ends, then all possible θ_i 's are populated in our observable universe and the initial energy density arises from the average axion field misalignment oscillating around its minimum value. This gives $\Omega_a h^2 \approx 0.12 (28 \pm 2 \mu\text{eV}/m_a)^{1.165}$, averaged over a flat initial θ distribution in the $(-\pi, \pi)$ range[§]. Calculations with instanton and chiral EFT techniques suggest a larger uncertainty of $\sim 25\text{--}45 \mu\text{eV}$ [46]. In the post-inflationary case, axions from string and domain wall decay also add to the misalignment

[§] The ‘effective’ initial misalignment for the QCD axion potential, $\sqrt{\langle\theta_i^2\rangle} \sim 2.155$, deviates slightly from the $\sqrt{\langle\theta_i^2\rangle} = \pi/\sqrt{3}$ result for a cosine potential [17, 39].

contribution which likely shifts the prediction to higher masses; see the following section. This scenario can be more difficult to implement in some string axion models due to the nonperturbative nature of the topological defects [76–78], although see recent constructions [79, 80].

If PQ symmetry is never restored after inflation ends, the vacuum misalignment scenario estimates the dark matter density as $\Omega_a h^2 \approx 0.12 (7 \mu\text{eV}/m_a)^{1.165} \theta_i^2$, where θ_i is an arbitrary initial angle randomly seeded by primordial fluctuations in the range $(-\pi, \pi)$; note this scaling is modified for $\theta \sim \pi$ due to nonlinearities in the axion potential [81].

3.2. Axion String Networks

The axion arises from a spontaneously broken global symmetry, $U(1)_{\text{PQ}}$. If this symmetry is broken after the end of inflation, topological defects which form during the phase transition can be relevant to axion cosmology and final dark matter abundance [82–85].

The equations of motion for the axion and radial fields admit a string solution where the phase of the axion field winds around from 0 to 2π and the PQ symmetry is restored at the center of the string. The size of the string core is set by the radial mode mass m_ρ , and away from the string the field is equal to its expectation value. The energy per unit length of the string in the core is of order $\mu \sim f_a^2$. Additional energy is stored in the gradient of the axion field away from the string core. This energy is logarithmically divergent along the direction away from the string, in contrast to the case of a broken local symmetry, in which the variation of the field outside the string core is pure gauge and carries no energy. The divergence is naturally regulated by the nearest string of opposite orientation, the string loop radius, or the size of the Hubble patch.

The dynamics of the string network in an expanding universe, illustrated in fig. 2, are complicated but can be qualitatively understood as being driven by two processes. The string length and thus energy density per Hubble volume increase as more strings enter a given Hubble volume due to the expansion of the universe. On the other hand, the strings can intersect and recombine with one another, and form loops and high-curvature kinks; they already have high curvature components due to the random formation process which is uncorrelated across Hubble patches. High curvature strings and loops radiate axions, radial modes, and to a lesser extent gravity waves (GWs) [86–89]. Since a higher density of strings results in more crossings and radiation, the network is believed to reach a scaling solution of $\mathcal{O}(1)$ strings per Hubble volume, assuming efficient recombination and radiation of the strings, as the length of strings entering the Hubble patch is converted into axion radiation. The total energy per unit length of the string is given by $\mu \sim \pi f_a^2 \log(\eta m_\rho/H)$, where H^{-1} is the Hubble length, m_ρ^{-1} the size of the string core and η is an $\mathcal{O}(1)$, potentially slowly-time-varying number which captures the number of strings per Hubble volume [90]. A larger number of strings per volume

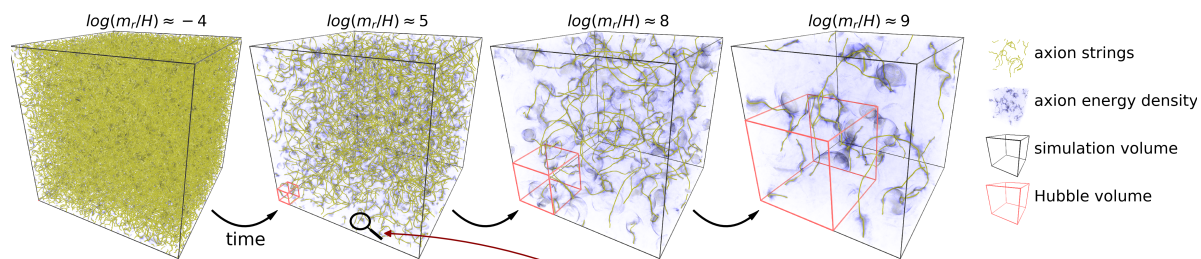


Figure 2: Illustration of the evolving axion string network in the background of an expanding universe. The growing Hubble volume is shown in red. Figure from [91].

results in a larger amount of axion dark matter at late times.

These radiated axions have momenta distributed between the effective infrared cutoff, which is provided by approximately the Hubble scale H , and the effective ultraviolet cutoff set by the string width m_ρ . For momenta between these two scales the radiation spectrum is expected to follow a power-law, $\propto (k/H)^{-q}$ for $H \ll k \ll m_\rho$ and a scaling index q . The axions then redshift, acquire mass during the QCD crossover transition—during which domain walls form and annihilate and potentially produce more axion radiation—and contribute to the dark matter abundance.

Most recent simulations have established the logarithmic growth of the number of strings per Hubble volume [90–96], first observed in [90]. A remaining source of uncertainty is the momentum spectrum of axions radiated by the strings, as this dictates the number of axions (and in the end the axion dark matter abundance). The extraction of the power law is uncertain since the UV and IR cutoffs must be far enough apart to allow for a robust extraction of the power law component of the momentum spectrum, and choices related to the cutoff and grid spacing are subject to numerical errors [91, 93, 94, 96].

It has been argued the the spectrum should be scale invariant ($q = 1$) based on observations of rapidly collapsing string loops [97, 98], or peaked in the IR ($q > 1$), based on the similarities of the dynamics of axion strings to local strings at late times [85, 99, 100]. It appears unlikely to be UV dominated. It has also been observed that the power law itself may evolve logarithmically with time as the universe expands, $q \sim q_0 + q_1 \log(m_\rho/H)$ [90, 93]. Even a small positive coefficient for the logarithmic term would lead to an IR-dominated spectrum at late times and predict a large axion number density and an axion mass at the meV scale from the string abundance [93]. Other groups have observed evolution consistent with the logarithmic growth of the power law, predicting an axion dark matter energy density dominated by string decays [94, 95]; see also [94] for a discussion of different scaling laws with time. On the other hand, a momentum spectrum constant over the evolution, extracted from recent simulations using adaptive mesh refinement techniques with large dynamic range, gives an axion string contribution which only slightly dominates the misalignment value, resulting in an estimated axion mass of tens of μeV [91, 96].

It is evident that there is considerable uncertainty in the calculation of the energy

density of axions from string and domain wall decay. The main difficulty comes in the huge dynamical range of the problem. Placing the evolution of the complex scalar field on a grid, one must simultaneously have a small enough spacing d in order to accurately resolve string core dynamics, $d \ll m_\rho^{-1}$, and large enough “box” volume to capture cosmic string evolution and range of momentum scales, $L \gg H^{-1}$. By the time the string network is destroyed at the QCD transition, the number of grid points to evaluate in principle should reach $(L/d)^3 \gg (m_\rho/H)^3 \sim e^{200}$, an unimaginable task. Thus any simulation results have to be extrapolated from smaller grid sizes which only capture the early stages of string network evolution.

Further uncertainties arise due to the complex nature of the formation and collapse of the domain wall network. The domain walls form when the axion potential turns on during the QCD crossover transition. The value of the axion θ angle jumps from 0 to 2π at the domain wall. The system then consists of strings connected by domain walls, as well as closed or infinite wall surfaces without strings. The dynamics then depend on the vacuum structure, i.e., the number of minima N in the axion potential. A single minimum corresponds to unstable domain walls, whereas a higher number of minima can result in a frustrated network which is stable; to make $N > 1$ viable, a breaking of the PQ symmetry is required, small enough to not reintroduce the strong-CP problem. The contribution of this process to dark matter axion abundance is not yet well understood but may well be larger than the string production [93, 96, 101].

3.3. Inferences on the Preferred Axion Mass from Dark Matter Density

In principle, with perfect understanding of the mechanisms above, the energy scale f_a and thus the axion mass could be inferred from density of dark matter today. Unfortunately, this has challenges in both the case where PQ symmetry is broken before and after inflation. In the pre-inflationary case, the dark matter density depends strongly on the initial θ in our universe. A typical, $\mathcal{O}(1)$, misalignment angle suggests an axion dark matter mass scale $\sim 1\text{--}30 \mu\text{eV}$, the focus of resonant cavity experiments since the 1980s. However, misalignment angles exponentially close to 0 or π can yield axion dark matter mass scales ranging from peV to meV [75, 81, 102].

In the post-inflationary PQ symmetry breaking case, there is in principle a unique dark matter abundance prediction as a function of axion mass. To find it, it is important to establish the dynamics of the axion string network; both the number of strings per Hubble volume as a function of time, and the spectrum of axions that are radiated, all of which suffer from the uncertainties mentioned above. Over the last several decades, both numerical and analytical approaches have been applied and reached a range of conclusions, from the strings contributing a smaller or similar number of axions relative to the initial misalignment value, which would point to a scale of $f_a \sim 2 \times 10^{11} \text{ GeV}$ [91, 92, 96, 97, 103–105], to the contribution of the string network dominating the axion production by about an order of magnitude, resulting in an axion mass necessary to achieve the right relic abundance on the order of 0.5 meV [90, 93, 95, 99, 100, 106, 107].

In summary, we feel it will likely never be possible to fully simulate the evolution of the complex dynamics giving rise to axion dark matter production from strings and domain walls. However, there have been new results achieved due to the combination of increased computational power, improved numerical techniques such as adaptive mesh refinement achieving impressive dynamic range [91,96], and a connection with analytical arguments which can inform the extrapolation to unachievably high dynamic ranges. Recent advancements in the scale of these simulations suggest higher axion masses from string production than those predicted by the vacuum misalignment mechanism alone. Buschmann and Benabou et. al. find a mass range of 40–180 (45–65) μeV for KSVZ [91,96]. Spectra consistent with IR-dominated momenta at late times yield larger masses: Gorghetto et. al. [93] find $m_a \sim 500 \mu\text{eV}$ for the KSVZ model (domain wall number $N = 1$) and $\sim 3500 \mu\text{eV}$ for the DFSZ model ($N = 6$); Saikawa et. al. [94] report a best fit mass from 95–450 μeV , and Kim et. al. ~ 420 –470 μeV [95]. Klaer and Moore, on the other hand, find a lower value $26.2 \pm 3.4 \mu\text{eV}$ [104] from a different string implementation than the other approaches. A consensus of the community could provide interesting input to the search for axion dark matter. As there are likely to be additional contributions from domain wall collapse [93,96], these mass ranges should be taken as lower bounds for post-inflationary dark matter axions.

It is important to keep in mind of course that the pre-inflationary scenario is perfectly consistent with everything we know about axions and the early universe and can significantly broaden the range of axion masses for which the axion is a motivated dark matter candidate.

3.4. Additional Cosmological Signatures of Axion Dark Matter

There are cosmological bounds on the axion parameter space, which apply to the QCD axion as well as more general axion-like particles. In the pre-inflationary scenario, the axion is present as a light scalar field during inflation, which undergoes its own fluctuations independently from the inflaton, leading to contributions to isocurvature fluctuations [108,109]. The amplitude of fluctuations is proportional to $(H_I/f_a)^2$ where H_I is the value of the Hubble scale during inflation, and are constrained to be small by measurements of the Cosmic Microwave Background (CMB) [110]. This results in the requirement that if $f_a > H_I$ and PQ symmetry is not restored after inflation, then $f_a \gg H_I$, that is the scale f_a has to be far enough above the scale of inflation to suppress isocurvature contributions.

Regardless of the production mechanism of axion dark matter, a small abundance of relativistic axions can be produced in the early universe and contribute to the amount of radiation today, typically parametrized as an equivalent increase in the number of neutrino species, N_{eff} . At high enough temperatures, the abundance of axions produced can be significant enough to place constraints on axion parameter space from the non-observation of extra relativistic radiation in the BBN, CMB, and large scale structure analyses [111–118]. Future CMB surveys could probe N_{eff} to a high enough precision

to exclude or observe axions with a low enough f_a . These constraints assume a high reheating scale, but would otherwise be competitive with constraints from the cooling of astrophysical objects [117]. The couplings of axions to fermions below the electroweak symmetry breaking scale, on the other hand, are dominated by low energies, and are therefore insensitive to the scale of inflation, but at the moment do not produce competitive bounds [119, 120].

3.5. Modifications of Axion Cosmology

There have been several recent developments in the theoretical aspects of the cosmological history of axions that can affect the prediction of axion DM abundance today as a function of its mass and decay constant. These fall into two categories: increased abundance due to early universe dynamics, or decreased abundance through depletion mechanisms. In addition, as in any dark matter model, the cosmological history will affect the final axion abundance; for example an era of early dark matter domination can enhance axion abundance as well as axion substructure [121, 122].

One way to achieve an axion abundance larger than the minimal prediction is to place the axion field close to the top of its potential, delaying the start of oscillations and red-shifting. In the large misalignment mechanism [81], it was pointed out that large initial field values (exponentially close to the maximum of a cosine potential, or generically for potentials which are relatively ‘flatter’ at large field values) can result in a parametric increase in the dark matter density. In addition, the larger self-interactions which result from probing the non-quadratic part of the potential give rise to interesting dynamics, including parametric resonance of certain axion momentum modes and enhancement of structure on small scales. Several models which implement the above initial conditions have been proposed [123–125].

Another way to increase axion abundance is to give the axion non-zero kinetic energy at the start of oscillations which can be used as an additional energy source. This kinetic misalignment mechanism has the initial axion field with non-zero angular momentum in field space, which then gets translated into a kinetic energy of the axion Goldstone boson [126]. This mechanism can lead to additional structure as well as GW production.

Finally, an additional energy source for the axion can enhance its abundance. One mechanism is where a heavy axion field decays into light axions through parametric resonance [127]. Another is axion “friendship” [128, 129], in which two coupled axions with nearby masses can exchange energy, with the axion with lower decay constant inheriting more energy from the one with higher decay constant. The latter mechanism does not appear to be applicable to the case of the QCD axion, but energy can be transferred by level crossing as the QCD axion mass turns on during the QCD transition [130].

Suppressed axion abundance can be achieved through rearranging the axion’s energy into other degrees of freedom, for example decays into relativistic matter that

redshifts away quickly. One example is the axion decay to dark photons through parametric resonance [131], which reduces its abundance and potentially produces GWs and additional radiation.

3.6. Axion Dark Matter Structure Formation

While the QCD axion is indistinguishable from cold dark matter with current observations, there are interesting structure formation differences due to the initial fluctuations of axions as well as due to their wavelike nature. For ultralight axions, beyond the standard QCD axion range, the wavelength becomes astrophysically relevant and has been explored in the context of the ‘fuzzy dark matter’ regime [132–135]. The strongest current constraint with purely gravitational interactions of the axions is $m \gtrsim 3 \times 10^{-19}$ eV [136] due to wave interference resulting in order-one density and thus gravitational potential fluctuations, causing heating of the stellar population dynamics. A range of other constraints from $m \gtrsim 10^{-22}$ eV to $\gtrsim 10^{-19}$ eV arises from suppressed power on short scales and altered stellar dynamics; for further details see e.g., refs. [33, 133–135].

In many ‘more visible’ axion models described above which have with enhanced abundance compared to the traditional order-one axion misalignment abundance, the axion can have an enhanced matter power spectrum [81, 128, 129, 137]. This results in new compact structures which go by the names of ‘oscillons’, ‘solitons’, ‘axion stars’, and ‘minihalos’. If these structures survive into the present day they can dramatically change detection prospects compared to a smooth cold dark matter axion background; estimates result in an order-one fraction of dark matter in structure.

Potentially even the standard QCD axion can impart unusual structure in our universe which may be observable. First, if PQ symmetry is broken after inflation, the resulting strings and domain walls can radiate axions which may contribute to a dark radiation component. In addition, as the universe passes through the QCD phase transition, large overdensities of axions form ‘miniclusters’ [92, 138–143], as seen in figure 3. These large overdensities are thought to have mostly dispersed by the present day but may have an impact on structure formation. In the case of the QCD axion string formation scenario, it was recently pointed out that an order-one fraction of the dark matter today could be present in axion stars [144].

There are open questions regarding the fraction of axions in substructure and the resulting impact on searches and search strategies. It is important to establish how generically these structures form and survive until late times. They seem to be more prevalent in ‘more visible’ axion models, where the axion density is enhanced beyond that from misalignment. Their detection may thus require the development of new astrophysical searches as well as new laboratory search strategies.

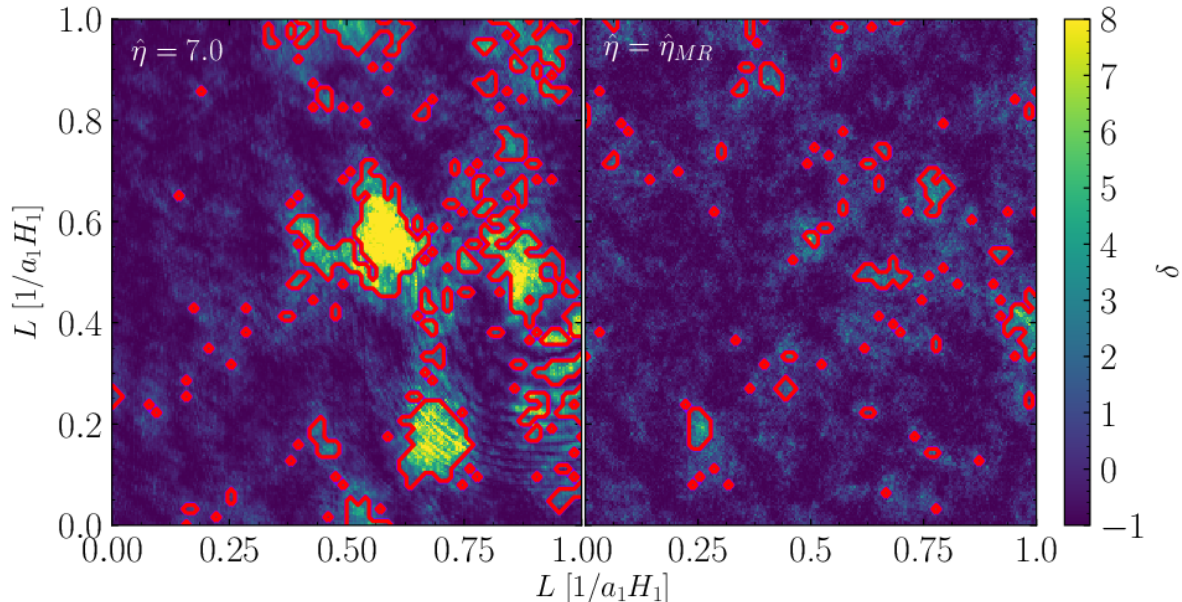


Figure 3: The overdensity of the axion field over the course of its evolution is shown as a 2D slice. *Left*: A portion of a 2D slice through the overdensity field at the end of the QCD crossover transition. Bright regions indicate large overdensities, and rings of relativistic radiation are visible as these overdensities decay. Clustered ‘minihalos’ are outlined in red. *Right*: As in left panel, but the overdensity field is shown at matter-radiation equality. At this time the large overdensities have dispersed, and the axion field is nonrelativistic. Figure from 92.

4. Astrophysics

Shortly after the axion was postulated, it was realized that tight constraints on the axion parameter space could be extracted from observations of astrophysical objects. A very early publication inaugurated bounds on Higgs and axions from big bang nucleosynthesis, microwave background and the abundances of red giants [145]. Although by more recent standards those early bounds were not highly constraining, perhaps surprising was that the most restrictive bound came from the axion’s effects on red giant evolution. Further important early astrophysical bounds used observables of our Sun’s nuclear energy power emission [72] and the terrestrial neutrino flux from supernovae [146].

These early bounds relied on the fact that the evolution of any star is throttled by the rate at which thermal energy (carried away by photons, neutrinos, or, say, axions) can escape. Owing to the relatively short photon interaction length within stellar matter, stellar cooling is dominated by radiation from a relatively thin photosphere surface layer. This applies as well to the core-collapse supernova SN1987A, where core neutrinos are trapped and escape only from a relatively thin outer layer. However, feebly-coupled axions can have interaction lengths greater than the size of the star and readily escape.

Since all the energy from axions produced anywhere within the bulk of the star escapes, this radiation can be a significant cooling mechanism even if the axion is only rarely produced. As a result of adding axion production to normal stellar-evolution processes, the star can either become colder or hotter, depending on the details. The latter case arises when the star’s gravitational potential energy becomes heat when the additional axion cooling reduces the outward photon radiation pressure thereby resulting in partial collapse. Many of these, and other, early astrophysical bounds were detailed in Georg Raffelt’s seminal 1996 book “Stars as Laboratories for Fundamental Physics” [147].

The general path for establishing astrophysical bounds is to test observations against the predictions of stellar evolution with the axion added. Of course, astrophysical predictions can have large uncertainties. Hence, conservatism calls for reserving the claim of discovery to clear discrepancies between stellar evolution models and observables. Since the early energy-loss constraints, many ideas have been developed to search for evidence of the axion in astrophysical systems. New techniques and observables, from indirect observation of axions produced and converted to photons in stars and compact objects to superradiance clouds of axions produced by black hole spindown, have been realized and continue to extend the reach of astrophysical probes. In this Section, we summarize the most important astrophysical searches and constraints which can impact the QCD axion parameter space, starting from less compact astrophysical objects such as the Sun and red giants (Sections 4.1, 4.2), and increasing in compactness to white dwarves (Section 4.3), neutron stars (Section 4.4), and finally black holes (Section 4.5). An overall summary of the bounds on the axion-photon coupling is shown in figure 4 and the QCD axion parameter space can be found in figure 17.

4.1. The Sun

The Sun’s luminosity: At the center of the sun, axions would be created in the Compton process $e + \gamma \rightarrow e + a$. For DFSZ axions, the resulting axion total axion power density is about $10 (m_a/\text{eV})^2$ erg/g/s. Although our knowledge of the Sun’s core thermodynamics from its ${}^4\text{He}$ abundance, luminosity and age is imperfect, it is very unlikely the axions at present could significantly contribute, readily bounding the DFSZ axion mass to less than about an eV [72].

Per the discussion above, an added axion energy transport channel would serve to increase the temperature of the Sun’s core thereby increasing the Sun’s neutrino flux measured on Earth. However, no such neutrino excess is observed and such arguments rather robustly exclude axions above around 1 eV, where the production rate in the core is too small, up to a few keV, the solar core temperature. One could quibble with details, especially as they apply to stellar opacity, and thus exactly where to place the mass bounds.

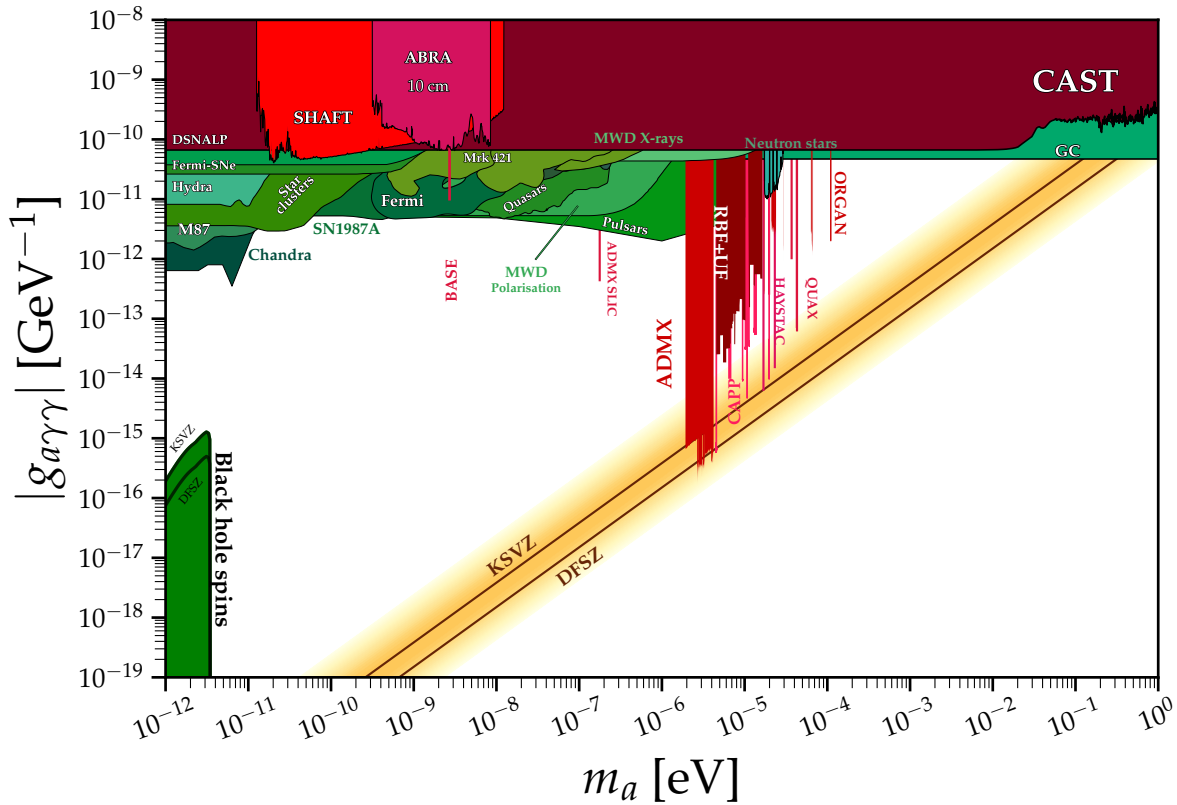


Figure 4: Astrophysical (green) and experimental (red) bounds on axion-photon coupling as a function of axion mass. See section 4 and section 5 for details of the constraints. The QCD axion benchmark parameters (KSVZ, DFSZ) are shown as a diagonal line from the lower left to the upper right. Modified from Ciaran O’Hare [37]. For further details, see e.g., the PDG review [36, 148].

Direct detection of axions from the Sun: In addition to the cooling and stellar evolution based constraints described above, there are laboratory experiments on Earth that are capable of detecting a flux of axions from the Sun and placing some of the strongest constraints across a wide range of parameter space of axion-like particles. The CAST experiment uses a large magnet to convert the axion flux from the Sun into x-ray photons, which would then be detected in an otherwise near-zero background environment [149] and has set constraints most recently in 2017 of $g_{a\gamma\gamma} < 0.66 \times 10^{-10} \text{GeV}^{-1}$ at 95% confidence for axion masses below $\sim 10^{-2}$ eV (figure 4). Upgrades to BabyIAXO and IAXO could gain several orders-of-magnitudes with larger “target” volumes, higher-field magnets and improved x-ray detectors [150]. The theoretical uncertainties of the solar flux are at the $\sim 5\%$ level and have been recently updated to include effects previously neglected, including the partial degeneracy of electrons [151].

In addition to CAST, WIMP dark-matter experiments are also sensitive to axions produced in the hot solar core and then absorbed in, e.g., a Xenon atom through the axioelectric effect [152]. Recent results from Xenon nT set joint constraints on the

$g_{a\gamma\gamma} < 5 \times 10^{-10} \text{GeV}^{-1}$ and $g_{ae} < 2 \times 10^{-12}$ couplings; the latter is a factor of a few weaker than the constraints from red giant cooling and white dwarf cooling (Sections 4.2, 4.3) but constitutes an important complementary bound [153].

While the bulk of stellar emission into axions is into relativistic modes, heavy axions with mass on the order of the solar temperature (keV) populate “solar-basin” bound orbits and can eventually exceed the relativistic flux of axions [154]. The energy density can be detectable in Earth-based laboratory experiments, allowing for direct or indirect detection of heavy axions without the assumption of a dark matter abundance.

4.2. Red Giants and Horizontal Branch Stars

As main-sequence stars age, more and more hydrogen in the core is fused into ^4He . If the star has sufficient mass and enough ^4He builds up, then ^4He fusion processes in the core proceed rapidly and the star evolves into a red giant. These red giants are quite large, but with low temperature and luminosity. The red giant ^4He supply is “burned” quickly at a core temperature around 10 keV; the lifetime of such red giants is short, only around 100 Myr. After the ^4He supply is exhausted, the red giant then continues evolving, eventually becoming a compact object.

Axions would be produced in the cores of red giants by a Primakov-like process whereby a real thermal photon scatters off a virtual photon near a nucleus, the two photons thereby becoming an axion. The axion readily transports energy out of the red giant, thereby shortening the time the star spends in the red giant phase.

One observable used in placing axion bounds is the fraction of red giants in certain stellar populations, the effect of axion emission would be to reduce this fraction. This argument, applied to the red giant populations in clusters gives a relatively robust upper axion-mass bound of a few eV [73].

Should the axion be DFSZ (or otherwise have couplings to leptons), then the axion-Compton process $e + \gamma \rightarrow e + a$ is important and the dynamics becomes more complicated. In slightly more detail, the ^4He core of the red giant is supported against collapse by electron degeneracy pressure. As the star burns ^4He , the star shrinks thereby converting gravitational potential energy into heat and the star gets hotter. Of course, there are still normal neutrino transport process at play, cooling the core, but this neutrino cooling is relatively slow. However, as is the case for neutrino production, the axion production rate in the core is a high power of the core temperature, and these axions could effectively transport energy out of the core. Hence, heavier and thereby more strongly-coupled axions remove more energy and depress the core temperature, and as the axion mass increases, the ^4He burning is increasingly quenched, thereby increasing the red giant lifetime. Models of red giant dynamics, including the effect of DFSZ axions, exclude such axions with masses between around 10^{-2} eV where the production rate is too low, and the core temperature around 10 keV [74]. This, too, is a fairly robust bound but it, too, has uncertainties in the modeling leading to “fuzziness” on exactly where to place the mass bounds.

Current constraints using production of axions in red giants and horizontal branch stars use observations of old globular clusters (GC) in the galaxy and compare the numbers of horizontal branch stars to the number of red giant stars [155,156]. The ratio of these populations would be significantly affected by axion production in the cores of the stars. Most recent stellar evolution simulations quantify the uncertainties of stellar modeling and constrain $g_{a\gamma\gamma} < 0.47 \times 10^{-10} \text{GeV}^{-1}$, which is comparable to CAST and places the leading constraint on axion-photon couplings at the high end of QCD axion parameter space, as shown in figure 4 [156].

4.3. White Dwarfs

White dwarfs are an interesting environment in which to search for axions, where the main focus of the search is in details of the white-dwarf luminosity function. Axion emission, mainly from electron bremsstrahlung, in the white dwarf atmosphere would speed up cooling and skew the luminosity function. A somewhat recent study on white dwarfs in the the galactic disk suggested that DFSZ axions with masses above around 10 meV are excluded [157]. However the white-dwarf atmosphere model has considerable uncertainties and the bounds may therefore be weak. It is intriguing that an earlier analysis had best fit to the luminosity function when a DFSZ axion with mass of a few meV was added the white-dwarf cooling [158]. This analysis, while interesting, has not generated huge excitement as the effect of this axion is small and the uncertainties are large.

Another probe for axion effects in white dwarfs is the pulsation period of ZZ-Ceti white dwarfs. The period slowing is related to the white dwarf cooling. Analysis in this way of white dwarf cooling suggests again an extra cooling channel consistent with a DFSZ axion as called for just above [159], again with large uncertainties in the atmosphere model. It is certainly interesting that two different analyses on white dwarfs yield similar results.

On the other hand, such axions emitted from magnetic white dwarfs would convert into x-rays in the white-dwarf magnetosphere and those x-rays then detected in orbiting x-ray observatories. The Chandra x-ray observatory looked for such x-rays from the magnetic white dwarf REJ0317-853 and did not detect any excess [160]. This result is in conflict with the possible axion suggested from a distortion of the white-dwarf luminosity function. See also [161–163] for constraints on axions with white dwarf physics and observations.

4.4. Neutron Stars

The Supernova Bound: The core-collapse supernova SN1987A in the nearby LMC dwarf galaxy released around 10^{53} ergs of gravitational potential energy almost completely in neutrinos from a core temperature of tens of MeV. The underground terrestrial detectors IMB and Kamiokande recorded between them around 19 neutrinos over about a 10 second arrival time. This was a milestone astrophysical observation,

confirming our gross understanding the supernova explosion with three neutrino flavors. Axions can be produced within the core via axion bremsstrahlung off of nucleons: $N + N \rightarrow N + N + a$. Neutrinos in the supernova core are trapped and the duration of the explosion (and the temporal dispersion in the neutrino arrival times) is therefore throttled by energy transport of neutrinos from the core. The effect of adding in axion emission would be to add a new, efficient energy transport channel, thereby shortening the duration of the explosion. Such arguments provide restrictive bounds, excluding axion masses from around 10^{-3} eV, where the axion production is too feeble, up to a few eV, where the axions are trapped and otherwise approach the core temperature [164].

The supernova bound has model uncertainties, particularly the effect of nuclear properties on axion emission. Hence, here, too, there is uncertainty in exactly where to place the mass bounds, though it has been argued axions with masses above around 10^{-2} eV are likely forbidden [35, 165]. Recent calculations exclude hadronic axion masses above 15 – 60 meV, closing the hadronic (KSVZ) axion window at heavier masses [166, 167]. Moreover, recent improvements in understanding pion populations in supernovae and mergers suggests that pion production may actually dominate axion bremsstrahlung from nuclei, through the process $\pi^- + p \rightarrow n + a$. If confirmed in simulations, pion emission further strengthens the axion mass bound from 1987A by a factor of about 2 [168]. Finally, observations of the 1987A remnant with ALMA [168, 169] and more recently JWST [170] has yielded firm evidence for the presence of the neutron star (NS) resulting from the supernova, putting these constraints on even more robust footing. In addition, studies of axion emission including higher-order chiral perturbation theory terms and finite density corrections have shown that there is a model-independent constraint on the QCD axion, yielding $m_a < 53_{-13}^{+73}$ meV [51].

Neutron Star Cooling: In addition to the neutrino signal from Supernova 1987A, axions can also contribute to the long-term cooling of NSs. Young, hot NSs have been used to place constraints; Cassiopeia A from the seventeenth century supernova has been used to constrain axions with decay constants comparable to those from SN1987A with some assumptions on the details of the NS interior [171–173]. Analysis of cooling data from NS HESS J1731-347 has yielded $f_a > 6.7 \times 10^7$ GeV for KSVZ and $f_a > 1.7 \times 10^9$ GeV for DFSZ axions [174], although there are some uncertainties on the nature of this compact object. The strongest constraints come from a set of five NSs which are hundreds of thousands of years old with precise age measurements, resulting in an upper mass bound of 16 meV for KSVZ models and $m_a > 10 - 30$ meV for DFSZ models (equivalent to couplings of $g_{an} < 1.3 \times 10^{-9}$, $g_{ap} < 1.5 \times 10^{-9}$ at 95% confidence) [175].

Neutron Star Conversion: Axion dark matter passing through the magnetospheres of NSs can convert into radio photons in the large magnetic field. Additionally, the conversion is resonant when the axions pass through the region near the NS where the mass of the axion matches the photon plasma mass [176] (see also [177, 178]). This allows NSs to act as targets for indirect axion detection with radio telescopes in the range $\sim 0.2-$

40 μeV . Improved treatment of the NS magnetosphere and environment [179], as well as 3D modeling of the axion to photon conversion [180] is expected to make the constraints more robust. Searches for signals from NSs have been performed in the data, with reach below the CAST bound but still far from the QCD axion expectation [181–183].

In addition to axion dark matter converting in the large magnetic fields of neutron stars, neutron stars themselves can source axions, either through the nuclear emission processes described above, or through only the electromagnetic coupling in regions with large electric and magnetic fields (pulsar polar-cap cascades) [184, 185]. These axions can again be observed once converted through photons in magnetic fields. Observations of neutron stars have already placed constraints for emission in the neutron star [182] and in the polar caps [184]. Interestingly, these observations lie in the radio band and in the event of a detection could provide motivation for haloscopes to zoom in on a particular region of axion mass and test this axion hypothesis.

Neutron Star Constraints on Exceptionally Light QCD Axions: Finite density effects change the axion potential. A lighter-than-expected axion can change properties of dense matter [47, 186]; if the axion has a tuned potential while still coupling to QCD, energy is minimized for field values $a \sim \pi f_a$ inside large, dense objects like NSs [47]. In these exceptionally-light axion models, NSs source a non-trivial axion field which gives rise to axion radiation and forces between the NSs for lighter axions [187], and the lack of a NS crust for heavier axions [50, 188, 189], which can be constrained with LIGO-Virgo-KAGRA (LVK) data [187, 190] and NS crust observations [50, 189], respectively. (See also [47, 186] for constraints on similar models from white dwarves.) Depending on the impact of a non-zero theta on nuclear interactions, these observables can reach to within 10% of the standard QCD axion line [50]; it remains to be seen whether high-density QCD at non-zero theta can be understood sufficiently well for dense matter to impact the profile of the minimal QCD axion.

4.5. Black Holes

Black hole (BH) superradiance is a process through which rotating astrophysical BHs lose energy and angular momentum and build up macroscopic, gravitationally-bound states of axions [25, 191]. Note that superradiance is not limited to axions; it can occur for any sufficiently weakly interacting boson [192–197]; see [198] for a detailed overview. For the purposes of this review we focus only on axions.

Superradiance leads to an exponential growth in the number of particles in the bound state, and can start from quantum fluctuations, thus not requiring a cosmological abundance of axions. Superradiance occurs if the axion mass and bound state numbers satisfy the ‘superradiance condition’ relative to the BH mass and spin: $\alpha \leq m\alpha_*/\left(2 + \sqrt{1 - \alpha_*^2}\right)$, where $\alpha \equiv G_N M_{BH} \mu$ is the dimensionless parameter governing the properties of growth rates and bound states, proportional to the axion mass μ and BH mass M_{BH} . The BH spin a_* is a property of the Kerr metric and

ranges from 0 (Schwartzchild BH) to 1 (extremal BH). The integer m corresponds to the angular momentum along the rotation axis of the BH per axion in the bound state. States with lower total angular momentum have parametrically faster growth rates, so generally the lowest allowed m -value state dominates the evolution at a given time.

As the cloud grows, the BH spins down until the superradiance condition for the given level is saturated; most of the mass and angular momentum loss from the BH occurs in the last e -folding. The resulting bound state has on the order of 10^{77} axions for stellar mass BH's, leading to new search strategies. We summarize three classes of signatures: BH spin-down; gravitational wave (GW) emission; and gravitational impact of the cloud on dynamics near the BH, and then comment on effects of non-gravitational axion couplings.

Black Hole Spin Constraints: As superradiance causes BHs to spin down on a characteristic timescale set by the axion mass, highly-spinning BHs can be used to constrain the parameter space of light, weakly-coupled axions [191,199]. Measurements of BH spins and masses have been performed generally in binary systems, either by measuring the innermost stable circular orbit by observing the accretion disk from the companion star or by fitting gravitational waveforms to identify the BH spin. Several BHs in X-ray binaries have been observed to have very high spins, which can be used to constrain axion parameter space as shown in figure 4. Conservative constraints on axion parameter space from BH spin measurements are shown [196] with the standard conversion between $1/f_a$ and $g_{a\gamma\gamma}$ for the KSVZ and DFSZ models, constraining QCD axion masses to be above $\sim 6 \times 10^{-12}$ eV from measurements of Cygnus X-1 and slightly weaker constraints from other black holes. More stringent constraints which combine data from multiple BH measurements with specific assumptions about systematics and error covariance increase the reach to higher axion masses [200]; a full statistical analysis with M33 gives $m_a \gtrsim 3 \times 10^{-12}$ eV [201].

It is also possible to use statistical analyses of the BHs merging in LIGO data to constrain—or search for signatures of—superradiant spin down [206]. Gaining reliable evidence for the axion hypothesis likely requires hundreds of events [206,207]; on the other hand, a factor of 2 exclusion in axion mass, 1.3×10^{-13} eV– 2.7×10^{-13} eV (assuming sufficiently weak self-interactions and sufficiently long BH merger times) has been placed, driven largely by two systems, GW190412 and GW190517, which were observed to have non-zero initial BH spin at high significance [208].

Measurements of supermassive BHs can probe ultralight axions [199,200,206,209–211]. However, the spin measurements of supermassive BHs are more uncertain, and superradiant evolution times become comparable to astrophysical timescales such as accretion and mergers, so bounds have to be interpreted with extreme care.

Searches with Gravitational Waves: The axion bound states around the BH constitute an enormous energy density with both angular and time dependence. In general relativity, these clouds then necessary source GWs. Specifically, the components of the

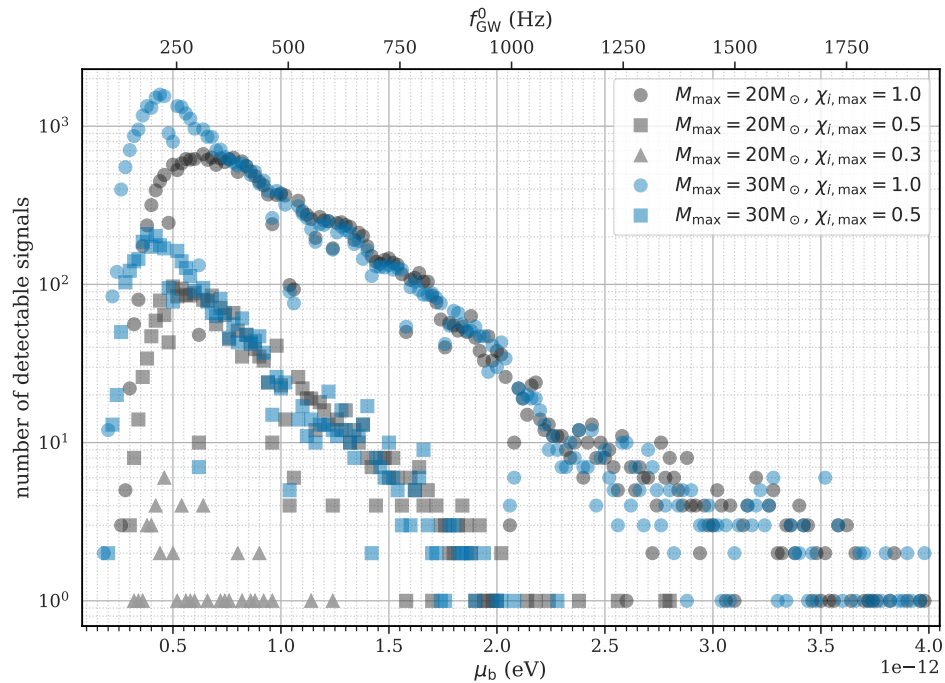


Figure 5: Number of gravity wave signals with amplitudes above the detectability level of recent all-sky searches for continuous GWs [202–204], for bosons in the mass range 1×10^{-13} eV to 4×10^{-12} eV. We consider the standard (black circles) and heavy (blue circles) BH populations, as well as the moderate (gray squares), heavy moderate (blue squares) and pessimistic (gray triangles) spin populations. The fluctuations are due to stationary lines and other artifacts in the detectors, which decrease the CW search sensitivity in nearby frequency bins. Figure from [205].

stress energy tensor with quadrupole or higher angular dependence, and non-zero time dependence, source GWs. At the particle level, the high-frequency terms correspond to annihilations of two bound-state axions to a single graviton with frequency of order twice the axion mass, and are always present, while low frequency terms correspond to transitions from a higher-energy level to a more deeply bound one, and are present when multiple levels are simultaneously populated [191, 199]. The latter are thus more rare except in the case where axions self-interact to a significant extent [196, 199].

These GWs lead to energy loss from the axion cloud, on timescales parametrically slower than the superradiance rate. Thus the peak ‘annihilation’ signal takes place once the cloud has finished growing through superradiance and can last for a period ranging from days to millions of years, depending on the axion and BH masses. The signals from individual BHs can be observed in blind [199, 206] or directed [206, 212] continuous wave searches in LVK data [213]. Alternatively, a large population of BHs which are all emitting GWs can manifest as excess stochastic noise in a frequency band around twice the axion mass [214–216]. Both the blind and stochastic signals have a strong dependence on the properties of the BH population (in the Milky Way and beyond), in

particular the formation rate of BHs, and their mass and especially spin distributions at formation [205]. With current data and standard BH population assumptions, between several and several hundred monochromatic continuous wave signals for axions of around 10^{-13} eV in mass would be expected in LVK data and all searches have been null to date [204, 205, 217]; however any exclusion in axion parameter space is conditional on the unmeasured properties of Milky Way BHs.

Directed searches, following up a merger with a newly born BH, is the “golden observation” for exclusion or detection of a new particle. The BH formation time and properties being well-measured, the superradiance waveform can be calculated as a function of axion mass. Most likely, next-generation GW observatories will be required for such searches for axions [206, 212, 218], but present detector sensitivity is already promising for vector particles [219].

In addition to the currently ongoing BH spin and GW measurements, future observations may be able to shed light on the presence of the cloud around BHs, such as the modification of BH inspirals [220–223], back reaction of the cloud to create ‘floating orbits’ [224, 225], and the imprint of superradiance on hierarchical BH mergers [226, 227].

Non-Gravitational Interactions: Superradiance is a fundamentally gravitational process and thus does not depend on any interactions of the particle other than its mass and spin. However, the large field amplitudes that are formed in the final stages of superradiant growth can impede or otherwise change the dynamics of superradiance in the presence of non-gravitational couplings [191]. In the case of axions, the most relevant is the self-interaction, at leading order a quartic (Section 1). The self-interaction leads to new dynamics in the cloud, enabling the axion field to source new bound angular momentum levels as well as non-relativistic and relativistic axion waves; the former could be seen in future earth-based laboratory experiments searching for axion DM [196]. The self-interactions also limit the maximum field value of the cloud [196, 228–230], which slows down spin extraction from the BH and thus relaxes the bounds for lower- f_a axions [196] and reduces GW signals [196, 231]. There has been uncertainty in the literature regarding the existence of a ‘bosenova’, a violent collapse of the cloud under self-interactions; it was recently demonstrated that for small enough axion masses relative to BH size, the bosenova does not occur [196, 230]. Further work is needed to establish dynamics of higher angular momentum levels and relativistic clouds, which introduce additional uncertainties but could extend the reach of BH superradiance to heavier QCD axions by a factor of about 2 [196, 201, 232].

The axion coupling to photons can in principle lead to parametric resonance decays of the cloud to photons, although the finite size of the cloud [233] and the presence of interstellar plasma [234] impede this process in realistic situations [196]. The large axion field can also act as a type of magnetic field acting on spins in the BH vicinity; however, the maximal values do not exceed a fraction of a gauss, which is negligible compared to, e.g., accretion disk B fields [191]. For photon couplings enhanced by several orders of magnitude compared to the KSVZ and DFSZ expectations, a complete analysis in a

realistic BH environment has yet to be performed.

5. Laboratory Experiments

As discussed throughout this review, the coupling of the axion to normal matter and radiation is extraordinarily feeble. It would be perhaps therefore surprising that laboratory axion searches would be promising for direct detection of the QCD dark-matter axion. Nonetheless, laboratory experiments have been demonstrated to be exquisitely sensitive and are a promising path to discovery.

We first place the axion scales relevant for experiments in context in Section 5.1. Before we discuss the more recent developments in axion experiment, it is worthwhile to review the outcome of the early terrestrial accelerator and reactor experiments launched in the decade or two after the axion was postulated (Section 5.2). Early on, it was appreciated that bounds on axions and other hypothetical particles could be established by their observable effects on stellar evolution and were many orders of magnitude more restrictive than these searches (see Section 4). It was not until the microwave cavity concept that attention returned to terrestrial QCD axion dark-matter experiments. This line of inquiry remains very active today (Section 5.3) and is being continuously developed as described in Section 5.4. We summarize other approaches to detect the dark matter axion through the electromagnetic coupling in Section 5.5 and outline ongoing and proposed searches for axion-nucleon couplings in Section 5.6.

5.1. Relevant Length Scales

For the small masses left unexplored by early laboratory and astrophysics searches, the axion is distinct from most subatomic particles in that its relevant length scales can be much larger than those of the detector. Axions, depending on their mass, have characteristic length scales that are somewhat smaller than, comparable to, or larger than the experimental apparatus. This leads to a wide variety of techniques, each applicable to only a certain range of masses. The relevant length scales to consider are the Compton wavelength, which is the wavelength of photons created from axion conversion, the de Broglie wavelength, which is the length scale of the axion matter wave, and the correlation length and time, which are the length and time scales over which the phase of the axion field is coherent.

Lower bounds on the correlation length and time can be estimated from the maximum velocity dispersion axions can have in order to make up a virialized dark matter Milky Way halo. For the Maxwellian distribution of a fully virialized halo, all the length scales – the mean and the most probable de Broglie wavelengths as well as the correlation length – are set by the virial velocity v_0 in the halo and are within tens of percent of one another. The correlation time is longer by another factor of c/v_0 . In principle, axions may be much colder with much longer correlation lengths and times. This occurs for example for subcomponents of dark matter that are not virialized such

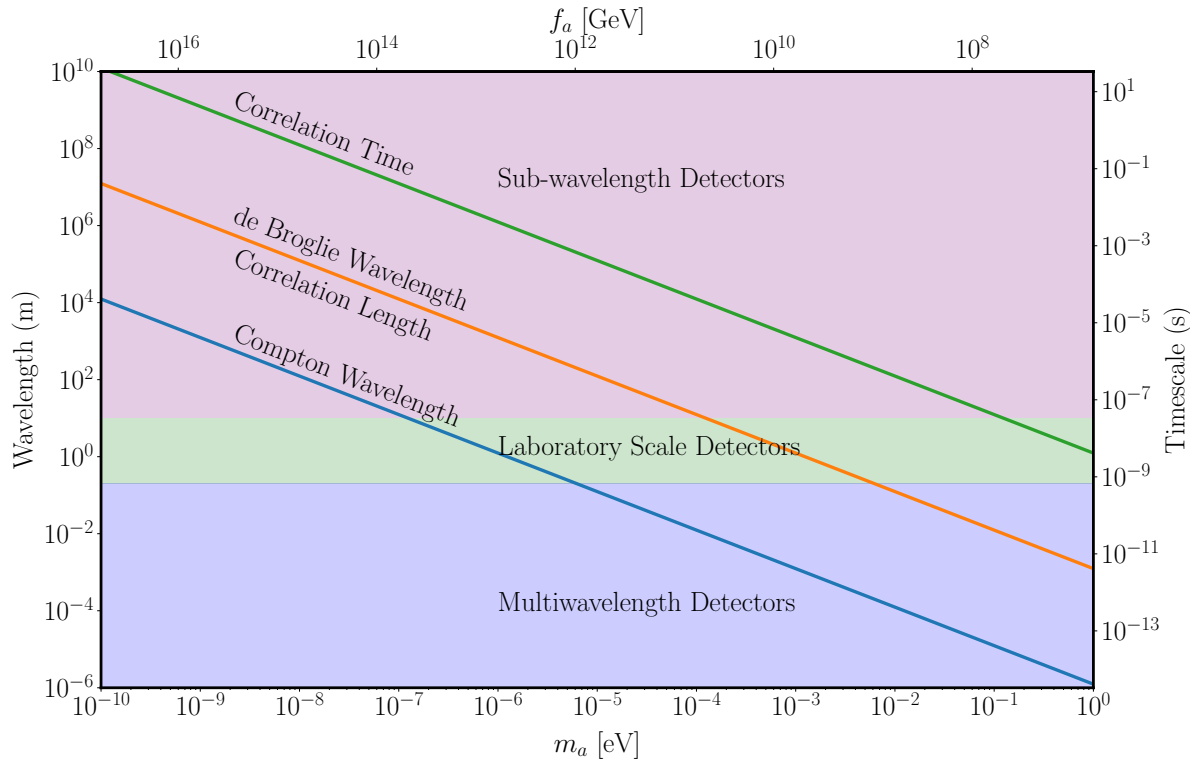


Figure 6: Characteristic lengths and times for virialized axion dark matter as a function of mass. Dark matter is non-relativistic so the scaling of Compton and de Broglie wavelength is a trivial scaling with axion mass and velocity, but the correlation scales are more dependent on assumptions about the dark matter kinematics as described in the main text.

as streams, or axions in self-bound structures such as miniclusters. The relationship between these length scales and the laboratory length scale is shown in figure 6. In the event of a detection, the information from these correlations can be used to extract information about the dark matter halo (e.g., ref. [235]). Existing axion-like particle bounds from astrophysics and laboratory experiments are shown in figure 4, where it is notable that the most sensitive laboratory experiments correspond to the mass range where the Compton wavelength is roughly at the laboratory scale.

5.2. Early Searches, Limits and Bounds

Recall that early searches for axions assumed the PQ scale to be near the electroweak scale, and such axions would be relatively strongly coupled to normal matter and radiation and would have been produced in abundance and detected in reactor and accelerator experiments. The negative searches imply the axion scale f_a is considerably greater than the weak scale. Following, we give an updated summary of these early searches, largely adapted from the reviews [236–238].

The experimental searches into the early 1980's were broadly divided into terrestrial experiments (reactor-based, accelerator-based, etc.) and astrophysical bounds (counting horizontal branch stars, e.g.). Although the early terrestrial experimental bounds played the important role of decoupling the axion scale from the weak scale, the feebleness of the 'invisible' axion couplings now largely render such early search methods (reactors, beam dumps, etc.) obsolete; they lack the required sensitivity to QCD axions in the most plausible mass range by orders of magnitude and other terrestrial technologies have overtaken them. Similar and new concepts are still active today in the search for 'heavy axions' (see, e.g., refs. [239–247]).

Reactor experiments The core of a nuclear reactor is the source of a huge flux of $\bar{\nu}_e$'s. Although the yields can vary considerably, approximately each $\bar{\nu}_e$ is accompanied by a prompt γ ; this γ production is dominated by E1 transitions with a small component of M1 transitions, where most of the M1 γ 's arise from isovector transitions. However, should there be an axion of appropriate mass and coupling, there would as well be a pseudoscalar contribution increasing the M1 rate via direct axion emission. These final-state axions could escape the reactor core and subsequently decay into two photons, which would then be detected by nuclear scintillation detectors. An alternate detection process is for the emitted axion to convert into a photon through the Compton process $a + e^- \rightarrow \gamma + e^-$ where the outgoing γ is detected. In one such experiment [248], (sketched in figure 7) NaI scintillation detectors were positioned approximately 1 m from the Savannah River reactor core. Energy depositions of greater than 1.5 MeV were counted, yielding a background-subtracted counting rate of -160 ± 260 counts/day, whereas the count rate from weak-scale axions would result in rate of over 1000 counts/day. With no excess counts observed, this experiment and other reactor experiments began to strain the weak-scale axion hypothesis.

Other reactor-experiment results were then reinterpreted in the context of axion emission. An even-earlier experiment [249] searched for weak neutral current neutrino-induced disintegrations of deuterium via the process $\bar{\nu}_e + d \rightarrow \bar{\nu}_e + n + p$. An axion with energy in the MeV range would have added approximately 1000 counts/day from the process of induced disintegration from nucleon scattering to the observed background-subtracted count rate -3 ± 7 counts/day. Again, a weak-scale axion would have been readily observable.

Nuclear de-excitations A nucleus in an excited state can de-excite through axion emission, with the emitted axion-nucleus system carrying away spin-parity $J^P = 0^-, 1^+, 2^-, 3^+ \dots$ etc. Specifically, for $J^P = 1^+$, the isoscalar and isovector transition rate has been estimated for several isotopes where the de-excitation has been measured and is well understood [250]. For ${}^7\text{Li}$, ${}^{97}\text{Nb}$ and ${}^{137}\text{Ba}$, the observed deexcitation rates are considerably less than that from a weak-scale axion. These early low-energy nuclear experiments showed promise, but, since the time of these early bounds, we know of no new higher-sensitivity results for nuclear de-excitations in the context of axions.

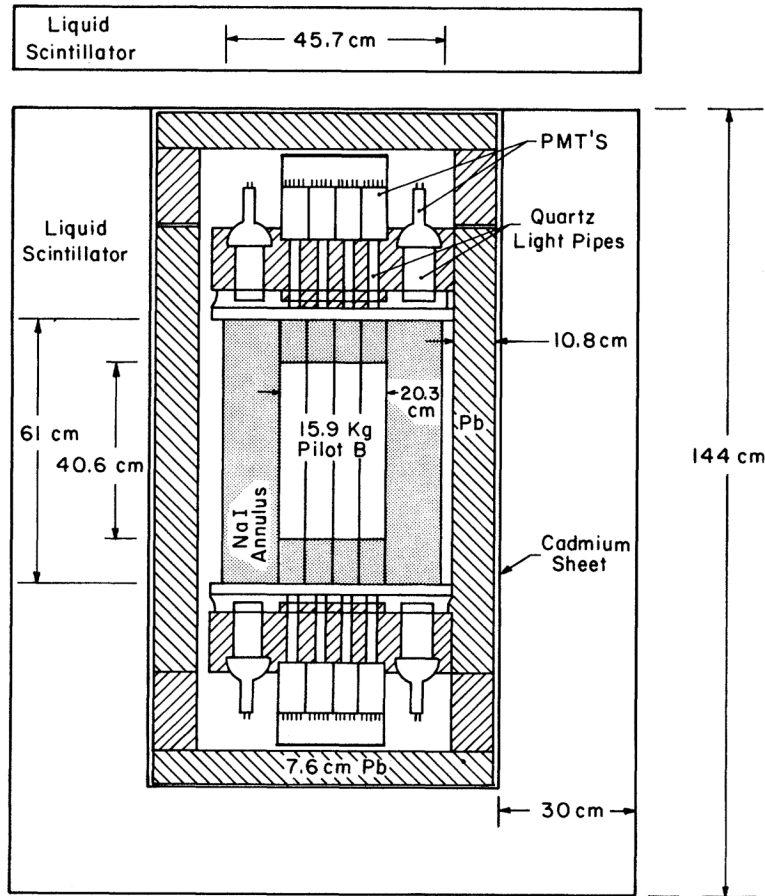


Figure 7: Sketch of the Reines-Gurr-Sobel $\bar{\nu}_e$ scattering experiment at the Savannah River power reactor. The main detector consists of a plastic scintillator target. An axion of appropriate mass and couplings would have resulted in a substantially increased electromagnetic count rate. From [248](#).

Beam dumps Beam dumps have a long history in searching for penetrating particles. The dump mass shields the detector from the source and allows a much-reduced background with a consequent increase in sensitivity. In one type of experiment, axions in such searches would be produced in the source by directing a particle beam into a target. The resulting axions then penetrate an earth berm (the ‘dump’ or ‘shield’). Axions or their decay products then interact with a detector. Early on, SLAC had a major role in these beam-dump axion experiments. In an early search [[252–254](#)], reinterpreted in the context of axions [[255](#)], electrons from the linac were directed onto a target. The beam-dump geometry is shown in figure 8 (upper). In the target, axions would be produced via the axion bremsstrahlung process off the nuclear electromagnetic field. These axions would then pass through a 55 m earth berm and then decay into muon pairs, either in flight or in the berm near the exit. The resulting two-muon event signature is distinctive, and after analysis no muon pairs were detected.

Several CERN groups also searched for axions in beam dumps [[251, 256, 257](#)]. The

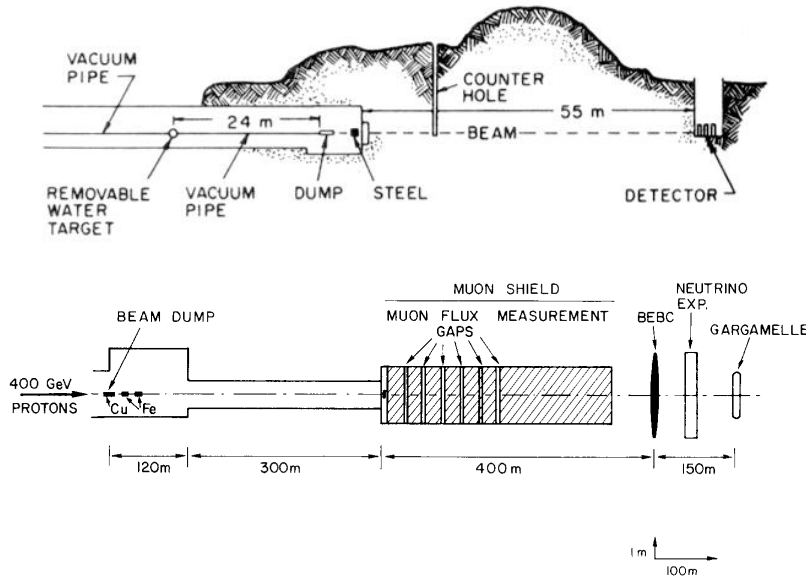


Figure 8: *Top*: Sketch of the Donnelly et al. beam-dump experiment at SLAC end-station A. From 250. *Bottom*: Sketch of the BEBC beam-dump experiment at the CERN SPS. From 251.

axions in this case were produced by directing 400 GeV SPS-produced protons onto a target. Axions, produced by a nuclear bremsstrahlung process in the nuclear field, would then pass through an earth berm and decay into electron, muon or possibly neutrino pairs, either in flight or near the exit of the berm. The detectors were placed approximately 1 km from the target. A small number of observed lepton pairs were attributed to neutral-current dilepton production. However, weak-scale axions would have resulted in a much larger number of pairs than that expected from the neutral current background. The configuration of one such CERN experiment is shown in figure 8 (lower).

Interest in beam dump experiments increased with the reports of anomalous e^+e^- pairs produced in heavy ion fixed-target collisions at GSI (see, e.g., ref. [258]). One interpretation of these pairs was that they arose from the decay of a $1.8 \text{ MeV}/c^2$ axion-like particle produced in the collision. In retrospect, the peaks were likely spurious (see, e.g., ref. [259]). Later SLAC experiments were then targeted at detecting these possible GSI axions. SLAC experiment E-141 directed 9 GeV electrons from the linac onto a combined tungsten target and dump [260]. Again, bremsstrahlung axions would be emitted in the collisions and escape from the exit of the dump. The axions would decay in flight and the decay products would be detected by the venerable SLAC 8 GeV spectrometer. Backgrounds from hadrons and muons were identified with a hydrogen Cerenkov detector and lead-glass calorimeter. By the time those data were analyzed, the ‘onia’ experiments, described below, had already excluded a weak-scale axion in

the accessible mass range. So, the E-141 focus was on an unusual ‘GSI-excess’ axion that would preferentially decay into e^+e^- pairs with lifetime appropriate for the distance between the exit of the dump and the detector. Such ‘leptophilic’ axions do occasionally appear in the literature (ref. [261] is one of many such examples).

Perhaps the most sensitive of these early beam-dump experiments for the purposes of this review was SLAC E-137 [262], schematically shown in figure 9 (upper). Here, 20 GeV electrons from the linac were directed at an Al/H₂O target and axions produced in the target would then penetrate a 179 m earth berm. On the exit side of the berm was the detector consisting of an 8 radiation length electromagnetic shower calorimeter, especially sensitive to electron or photon pairs. Axions with masses greater than about a few 100 keV were thereby excluded, with the limit shown in figure 9 (lower).

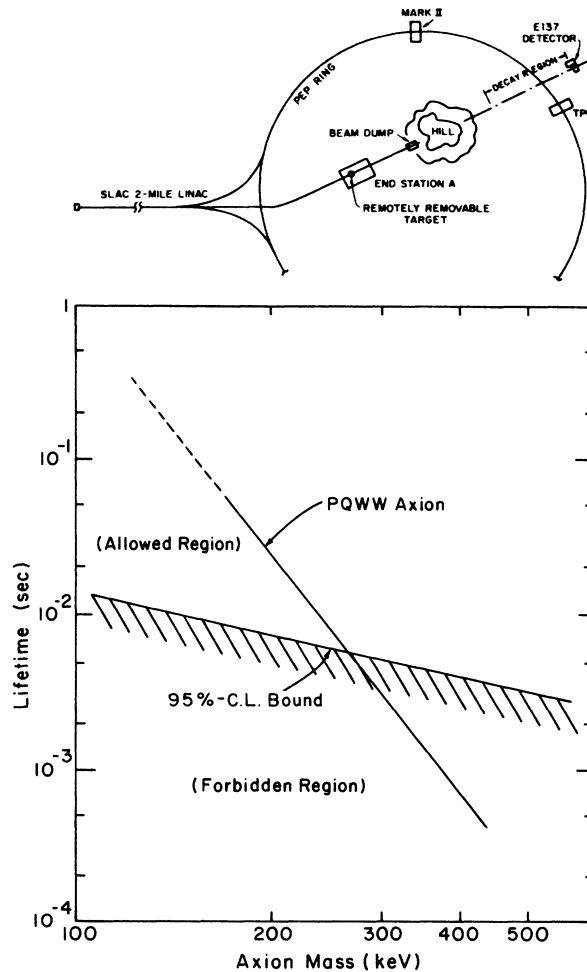


Figure 9: (upper) Sketch of the E-137 beam-dump experiment at SLAC. (lower) E-137 limit on the Peccei-Quinn-Weinberg-Wilczek axion. This weak-scale axion is excluded below the few 100 keV axion mass range. From 262.

‘Onia’ decays The 1⁻ heavy quark ‘onia’ states (the J/Ψ and B states) can decay into $a + \gamma$. If the axion lives sufficiently long, it escapes and the experimental

signature is a distinctive single photon. The ‘onia’ detectors consist of highly segmented electromagnetic calorimeters, thus yielding an almost background-free single-photon signature for axion production. One can also imagine a short-lifetime axion decaying in flight into electromagnetic products before entering the calorimeter, also yielding an almost background-free signature. A series of collaborations: CUSB [263] and CLEO [264] at the CESR e^+e^- storage ring at Cornell, Crystal Ball [265] at the SPEAR e^+e^- storage ring at SLAC, and LENA [266] at the DORIS e^+e^- storage ring at DESY, looked for the single photon event topology and at very high confidence excluded the weak-scale axion. Somewhat later CUSB and CLEO studies excluded shorter-lifetime weak-scale axions with a single photon plus two electromagnetic (e or γ) particle final state [267, 268].

5.3. Microwave Cavity Haloscopes

Given these experimental constraints, as well as the astrophysical bounds described in the previous section, it had been assumed that the extraordinarily feeble couplings of the QCD dark-matter axion (the ‘invisible axion’) to normal matter and radiation would render those axions impossible to detect in experiments, and progress in experimental searches slowed from that point on. However, in 1983 Pierre Sikivie conceptualized the microwave cavity haloscope whereby invisible axions could be detected [269] (also see refs. [270, 271]). The axions to be detected this way are “cosmic axions”, nearby Milky Way halo dark-matter axions. Since these axions are already in great abundance in the vicinity of a terrestrial laboratory (with a prodigious axion number density of $\sim 10^{15}/\text{cm}^3$ at μeV masses), the tiny factor of the axion coupling to normal matter and radiation need not be expended in producing them. The haloscope includes a large right-circular-cylinder high-quality factor RF cavity threaded axially by a large static magnetic field, see figure 10.

From a microscopic physics perspective, a single nearby halo axion scatters off of a “static” virtual photon in the magnetic field, thereby converting into a single real photon populating the TM_{010} cavity mode. The axion field at the relevant mass is coherent over the cavity volume and, for reasonable magnet and cavity parameters, the conversion rate is in the neighborhood of 100 Hz or less for the more-weakly coupled, but highly compelling DFSZ axion. The corresponding signal power is in the yoctoWatt range or less. This axion-conversion process is, in spirit, similar to the inverse of Primakov scattering of neutral pions off a nuclear electromagnetic potential, thereby converting neutral pions into photons in the nuclear electromagnetic field. || The high cavity quality factor Q enhances the conversion rate; one way to picture this Q enhancement is to recall a high quality factor increases the effective density of states near cavity resonant frequency, thereby increasing the conversion rate by that Q -factor in the Golden Rule.

The power from axion conversions incident on the cavity on resonance to a particular

|| This analogy is close since axions and neutral pions can mix.

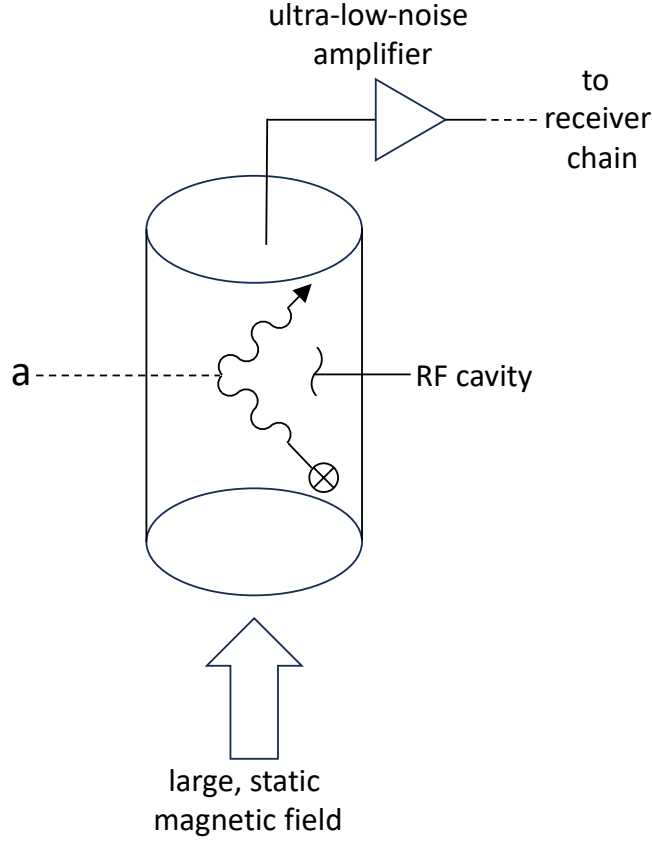


Figure 10: The Sikivie-concept haloscope axion detector. Cosmic halo axions scatter off a large, axial, static magnetic field and thereby convert into a microwave photons inside a tunable high-Q RF cavity. The experimental axion signature is very slight excess cavity electromagnetic power at the frequency of the cavity TM_{010} mode when that mode is tuned to the axion mass.

mode is given by [272]

$$P_{a \rightarrow \gamma} \approx 10^{-22} \text{W} \left(\frac{C_{a\gamma\gamma}}{0.97} \right)^2 \times \left(\frac{V}{136 \text{ L}} \right) \left(\frac{B}{6.8 \text{ T}} \right)^2 \left(\frac{C_{nlm}}{0.4} \right) \left(\frac{\rho_a}{0.45 \text{ GeV/cm}^3} \right) \left(\frac{\nu}{650 \text{ MHz}} \right) \left(\frac{Q}{50000} \right), \quad (10)$$

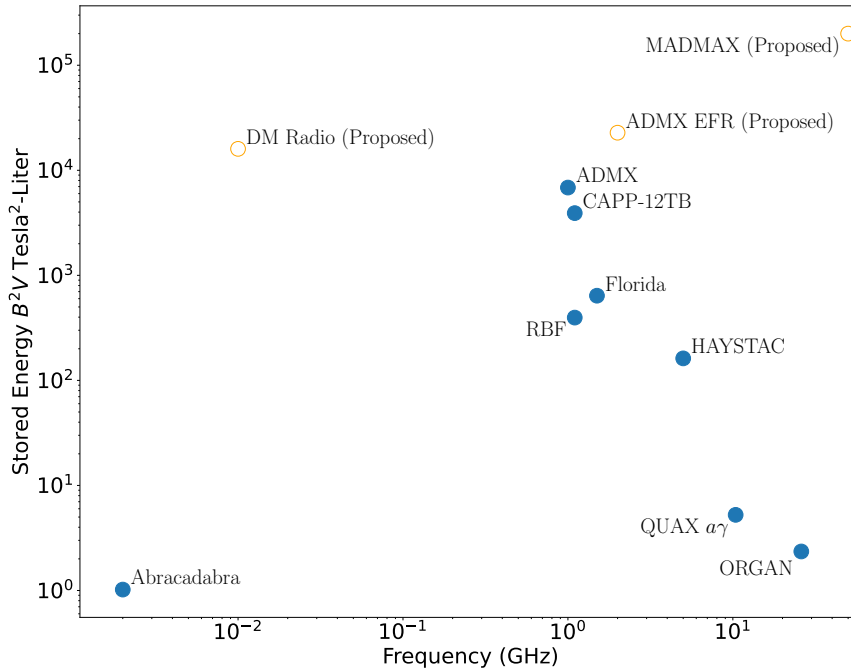
where V is the cavity volume, B is the axial magnetic field within the cavity (for simplicity assumed constant), C_{nlm} is the form factor of the nlm cavity mode, $C_{a\gamma\gamma}$ is the dimensionless coupling of axions to photons (eqs. (3),(4)), ν is the cavity resonant frequency, and Q is the loaded cavity quality factor. The axion energy density is given by ρ_a , chosen to be at a reference value of 0.45 GeV/cm^3 based on early work on galactic dark matter density inferences [273]. While the energy density in the lab itself is not directly measurable, precision astronomical data is continuing to improve: on kiloparsec scales, typical measurements constrain the density to be in the range of $0.4\text{--}0.6 \text{ GeV/cm}^3$, while large-scale galactic inference come in slightly lower at $0.3\text{--}0.5 \text{ GeV/cm}^3$ [274].

A small antenna inserted into the cavity extracts some of this RF power from the TM_{010} mode and delivers that power to the input of an ultra-low-noise amplifier. The output of the first-stage amplifier is applied to a more-or-less conventional receiver chain (either analog heterodyne or digital), and the bandwidth about the cavity resonance is then Fourier-analyzed into a frequency spectrum in the search for an axion signal above the noise. Axions thermally virialized with other galactic components would have a frequency bandwidth of order $\frac{1}{2}m_a v_0^2$ where v_0^2 is the square of the virial velocity dispersion of dark matter near Earth. For m_a in the μeV range (~ 1 GHz), and $v_0 \sim 10^{-3}c$, the axion line width is ~ 1 kHz. A reasonable normal metal loaded cavity Q around 10^5 has a cavity resonance bandwidth ~ 10 kHz. These considerations set the Nyquist parameters for Fourier analysis of the cavity power spectrum.

This idea was quickly applied to relatively small cavity experiments at BNL [275] and the University of Florida (UF) [276], which demonstrated the experimental method and established the path for the current ‘second-generation’ cavity experiments. It was only in the late 2010’s, almost 30 years after the PQ axion was postulated, that ADMX Gen 2 finally demonstrated sensitivity to the highly compelling ‘DFSZ’ dark matter axion in a promising axion-mass region. The modern realization of this technique is the focus of the remainder of this section.

The number and variety of haloscopes, operating, proposed and conceptualized, continues to increase, so this review will necessarily be incomplete by the time of publication. We discuss in detail the development of the oldest operating experiment, ADMX, and provide a limited selection of other notable efforts.

ADMX Overview The Axion Dark Matter eXperiment (ADMX) is the longest-running haloscope and by far has scanned the widest mass-range at DFSZ sensitivity. ADMX was the first experiment to achieve sensitivity to even weaker-than-DFSZ couplings in the few μeV axion-mass range. ADMX began operation in the 1990’s, initially sited at Lawrence Livermore National Laboratory, and built as a conceptual follow-on to the UF pilot haloscope [276]. It was recognized that the early BNL and UF pilot experiments lacked the sensitivity required to detect plausible QCD dark-matter axion models by several orders-of-magnitude. The initial ADMX was a scale-up of the UF design, but with a significantly greater cavity volume. The first generation of ADMX (“Phase 0 ADMX”) used cryogenic transistor first-stage amplifiers (“HFETs”). Although considered low-noise in the general microwave community, these cryogenic HFET amplifiers nonetheless have electronic noise considerably greater (perhaps by a factor of 100) than that allowed by the standard quantum limit (SQL) of $h\nu/2$, with ν the signal frequency. Nonetheless, because of the large cavity volume, this “Phase 0” ADMX achieved sensitivity to the benchmark KSVZ axion for masses in the plausible range of the QCD dark-matter axion [287]. Unfortunately, the DFSZ coupling is almost a factor of 10 weaker in developed cavity signal than that of the KSVZ coupling, and the ADMX Collaboration and others certainly appreciated that what the community



Experiment	Volume (L)	Field (T)	Reference
Florida	10	8	[276]
ADMX	119	7.6	[277]
CAPP-12TB	37	10.3	[278]
HAYSTAC	2	9	[279]
ORGAN	0.048	11.5	[280]
QUAX $a\gamma$	0.08	8.1	[281]
Abracadabra	1.02	1.0	[282]
RBF	11	6	[283]
ADMX EFR (Proposed)	258	9.4	[284]
DM Radio (Proposed)	1000	4	[285]
MADMAX (Proposed)	2000	10	[286]

Figure 11: The total magnetic stored energy (B^2V) for a selection of haloscopes discussed here, spaced as a function of frequency. Solid blue circles are experiments with published results and the volume is for the resonator used in the reference. Hollow orange circles are magnets described in white papers of proposed experiments, and use the total magnet bore volume, not the volume of a particular resonator. The speed at which frequencies can be scanned is proportional to the stored energy squared. Note that the trend so far has been to use smaller bore, higher field magnets with lower stored energies at higher frequencies.

called a “definitive search” ¶ requires sensitivity to DFSZ axions.

Recall, of the parameters that contribute to the haloscope sensitivity [eq. (10)], the magnetic field is perhaps the most obvious parameter one could improve. However, the ADMX Phase 0 magnet is of NbTi conductor construction, and its central field around 8 T is near the maximum practical field for NbTi technology at 4.2 K.

Returning to the parameters contributing to the sensitivity, another promising factor to improve is the system noise (see also section 5.4). In principle, achieving the Standard Quantum Limit (SQL) of noise would improve the sensitivity by a factor of $\times 100$ relative to ADMX Phase 0 at fixed scanning speed and other parameters, though in practice some of the improvement in amplifier noise is lost in downstream electronics and some of the the sensitivity improvement is applied instead on speeding up the search. Nonetheless, it was appreciated during the epoch of ADMX Phase 0 that approaching the SQL in noise would allow ADMX to achieve DFSZ sensitivity over a wide axion-mass range.

Although the idea of there being a lower quantum limit to noise of an amplifier is credited to Heitler in the 1930’s [288], it was not until the development of the maser that such low microwave-amplifier noise could begin to be explored in the laboratory. Throughout the 1960’s, low-noise maser microwave amplifiers were constructed, giving hints of measurable quantum noise buried in the amplifier-noise output. However, the maser amplifiers themselves were not typically operating close to the SQL, they were considerably noisier. Although maser amplifiers were deployed in radio-telescope applications, ultimately, for these frequencies, many radio-telescope receivers transitioned to cryogenic HFET transistor amplifiers by the 1990’s. About that time, amplifiers based on dc Superconducting QUantum Interference Devices (SQUIDs) were demonstrating impressively low noise up to perhaps low-UHF frequencies. However, the standard “Ketchen” SQUID fabrication geometry has a parasitic capacitive coupling between the SQUID input loop and the SQUID washer, and this capacitance rolls-off the SQUID gain with increasing frequency. Early in the 2000’s, it was realized that a modification of this geometry, in which the input loop is replaced by a resonant stripline coupled to the SQUID loop, would allow the parasitic capacitance to be cancelled by the reactance of the input stripline operating slightly off resonance [289]. This concept is distantly related to an old radio-electronics idea of operating a transmitter slightly off of the antenna-feed resonant frequency to cancel parasitic impedances, the so-called “shunt detuned position”. Such Microstrip SQUID Amplifiers (MSAs) demonstrated low noise, nearly down to the SQL at signal frequencies up to at least several GHz. This advance provided the enabling technology for ADMX to achieve DFSZ sensitivity.

Incorporating MSAs into ADMX introduced several technical challenges. First, MSAs, being based on dc SQUID technology, are disturbed by even very tiny ambient

¶ The term “definitive search” is somewhat hyperbolic in that a motivated theorist could certainly conjure a scheme for axions to evade it. Furthermore, the sensitivity to the coupling depends on the assumption about the local dark matter density on Earth, which is not directly determined and is order-one uncertain in standard cosmological models.

magnetic fields. For the MSA to operate near the ADMX RF cavity, it must be shielded from the 8 T field down to field strengths much less than a gauss. Since the magnetic-field gradient near the MSA is high, the resulting force on a magnetic-shield system would be enormous, perhaps several tons. Restraining such forces in a deep cryogenic environment is a challenge. To deal with these forces, the field-cancellation coil surrounding the SQUID is co-axially mounted on a mandrel with a counter-wound coil energized in opposite phase. The two coils are designed to have net-zero force.⁺ Second, achieving low MSA noise requires operation at dilution-refrigerator temperatures.

While cryogenic HFET transistor amplifiers no longer much improve in noise below physical temperatures of a few K, the MSAs continue to improve in noise all the way down to ambient temperatures approaching $h\nu$ (around 50 mK at 1 GHz). Hence, in practice an ADMX incorporating MSAs requires surrounding the cavity and MSA electronics in “1 K” thermal shield outside of the dilution-refrigerator space, which called for a significant re-design of the ADMX experiment insert. A version of ADMX incorporating the field-free region for the MSA plus dilution-refrigerator was proposed. A review deemed the engineering required for operating the MSA in the field-free region to be high risk, and therefore the project would proceed in two sequential stages: “Phase 1a” ADMX would demonstrate the MSA could operate successfully near the 8 T main magnet in its field-free region, and a follow-up “Phase 1b” would retrofit the dilution refrigerator.

The Phase 1a ADMX successfully demonstrated MSA operation at pumped ^4He physical temperatures around 1 K [290]. The resulting system noise was somewhat improved over that of the HFET ADMX Phase 0. With MSA operation demonstrated, ADMX proposed retrofitting the dilution refrigerator, thereby lowering the cavity and amplifier physical temperature to around 100 mK and realizing the low-noise potential of the MSA in a production search, approved in the DOE-HEP “Generation 2” dark-matter-detection call. The dilution-refrigerator ADMX Phase 1b was renamed “ADMX Gen 2”. The ADMX Gen 2 project moved to the University of Washington into a newly refurbished facility. After several preparatory data runs without the dilution refrigerator, the dilution refrigerator was successfully deployed in what was internally called within ADMX “run 1A”. Run 1A was notable for achieving sensitivity to DFSZ axions over a plausible range of QCD dark-matter axion masses, a long-time goal of axion research finally realized [291]. The follow-up run 1B significantly extended the mass range and demonstrated long-term, stable operations at better than DFSZ sensitivity [292]. The current Run 1C continues scanning and in the near-term run 1D will finish the single-cavity ADMX operations. The follow-up scan is run 2A, which will deploy multiple RF cavities to allow a searching at higher axion masses while maintaining good sensitivity.

The various phases of ADMX are described in the literature [293]. The section below expands on details of the current ADMX Gen 2.

⁺ Net-zero force implies net-zero mutual inductance between the coil pair and the main magnet. This is highly desirable: should one of the coils quench the other would not have large induced currents.

ADMX “Gen 2” The currently-operating phase of ADMX is ADMX Gen 2 (“ADMX” in what follows) [277]. ADMX is located at the Center for Experimental Physics and Astrophysics (CENPA) at the University of Washington, Seattle. The main experimental package, the “insert” is located in the bore of a 8 T superconducting solenoidal magnet, see figure 12. The insert consists of a right-circular cylindrical microwave cavity (OFHC copper-plated over stainless steel, approximately 1/2 m diameter, 1 m tall), in which are two movable tuning rods and an adjustable-depth antenna. Above the cavity are components of a dilution refrigerator (for cooling the RF cavity and cryogenic microwave electronics), motion-control components (for rods and antennae). Yet higher up is a liquid-helium reservoir and the cryogenic microwave electronics. In addition to supplying cooling to the insert, the reservoir contains a smaller superconducting solenoid magnet (the “bucking coil”) to “buck” (zero) the magnetic field in the vicinity of the cryogenic electronics. Above the reservoir is the cold head of a pulse-tube cooler that establishes a 50 K thermal shield. In addition, there are two pumped ^4He refrigerators (“pots”), one for the 1.5 K thermal shield surrounding the cavity and electronics, the other condenses the circulating ^3He - ^4He mixture of the dilution refrigerator. A substantial portion of the ADMX infrastructure also includes a dedicated Linde L1410 helium liquefaction system for liquefying helium exhaust gas from the main-magnet and reservoir.

Recall, the enabling technology for ADMX is the quantum amplifier front end of the cryogenic electronics package. The most recent incarnation of ADMX uses a Josephson Parametric Amplifier (JPA) in a “current-pump” mode, fabricated in aluminum, which is based on dc SQUID technology. These devices provide around 20 dB of microwave power amplification with near quantum-limited noise. JPA’s are tunable and dissipate very little power from the bias current. However, since they contain Josephson junctions, they need be shielded from the 8 T main field by the “bucking coil”. The output of the JPA feeds a high-electron mobility cryogenic JFET amplifier (“HFET amplifier”), at which point there is enough low-noise gain for the signal to exit the cryostat. The low-noise gain offered by the JPA is critical: recall that for a fixed scanning time, the sensitivity of the experiment degrades linearly with the JPA noise, and for fixed sensitivity, the scanning time increases quadratically with JPA noise. Without these quantum amplifiers, a search at DFSZ sensitivity over the plausible QCD dark-matter axion-mass range could take centuries.

The microwave signal as well as slow-controls signals are processed by room-temperature data-acquisition electronics. Here, the microwave signal is mixed-down to lower IF frequencies and digitized. The resulting voltage-time series is processed into a power spectrum in the vicinity of the cavity resonance. One power spectrum results from approximately each minute of acquired time series. The time-series is over-sampled, so spectral resolution can be adjusted after-the-fact to, e.g., match the isothermal axion phase space. The achievable frequency resolution is ultimately limited by the stability and noise of the local oscillators and digitizers, around fractional frequency resolution of 10^{-14} . A typical single power spectrum is shown in figure 13. The overall shape is due to

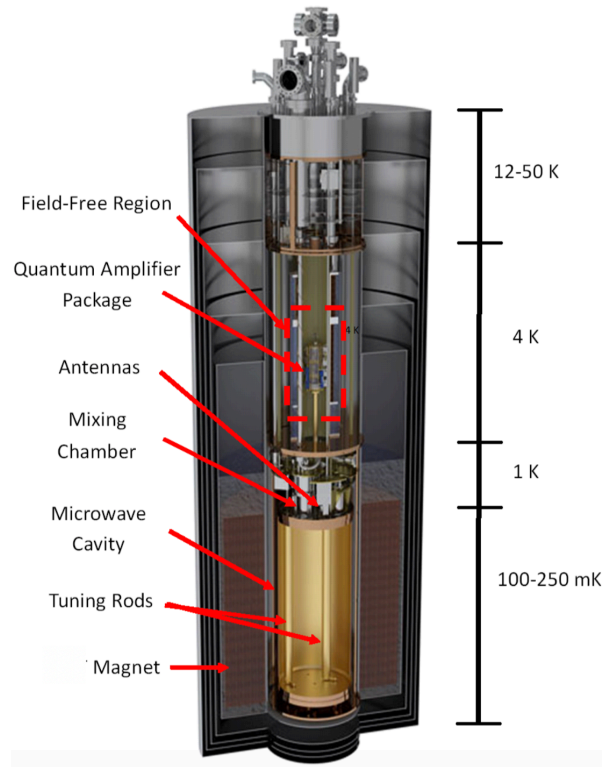


Figure 12: Sketch of the “Gen 2” ADMX experiment insert. The RF cavity near the bottom is in the bore of a large superconducting solenoid magnet. Above the cavity are dilution-refrigerator and quantum-amplifier components. The quantum-amplifier components are situated within a magnetic-field-free region established with a “bucking coil.” From [277](#).

the interaction of the cavity, transmission lines, and device inputs. This overall shape is understood and the analysis searches for relatively narrow small-amplitude peaks, with fractional width around 10^{-6} (for a virialized axion), on top of the overall structure. The experimental cadence is to record such a spectrum on the timescale of minutes, then step the cavity frequency by a small amount (relative to the cavity resonance width), then record another spectrum, then step the cavity frequency, etc. Months of such data are collected and used in a search for axion signals.

A recent set of ADMX limits is shown in figure [14](#), where the horizontal axis is axion mass (upper) or frequency (lower), and the vertical axis is the coupling of the axion to two photons [[277](#)]. The two diagonal lines are the benchmark KSVZ and DFSZ axion models. The blue region shows very early “Phase 0” ADMX limits at KSVZ sensitivity, representing almost a decade of data-taking. The orange shows the later ADMX “Run 1A” limit, representing about a year of data-taking. The orange region is notable for demonstrating DFSZ sensitivity, a long-term goal of axion research. The yet more recent red “Run 1B” limits, also at better than DFSZ, represents about year of data-taking and shows a considerable speed-up. ADMX is near finishing taking data in “Run 1C” and

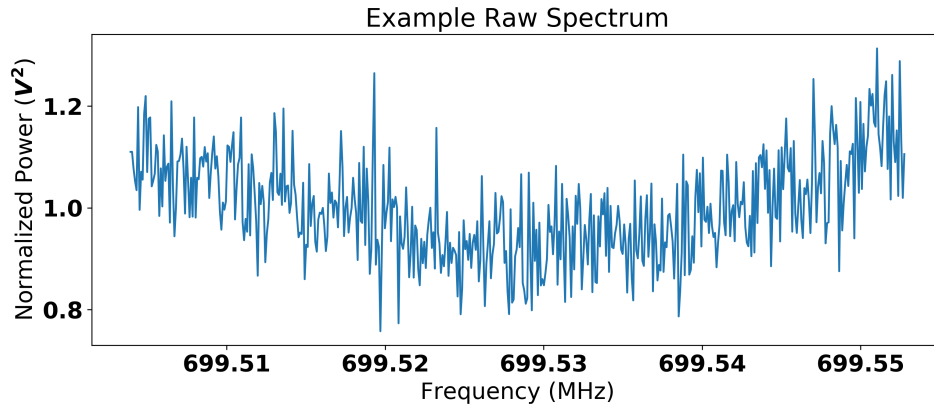


Figure 13: A single “raw” unprocessed power spectrum in ADMX. The overall shape is due to the interaction of the cavity, transmission lines, and device inputs. From [292](#).

is transitioning to “Run 1D”. One subtlety: on close examination, note there are two limits, e.g., light and dark red. The darker color limit assumes an isothermal sphere axion phase-space, the light color assumes the phase space from the N-body model of structure formation [\[294\]](#) and is likely the more realistic.

ADMX continues to take data. The ADMX strategy is to search upwards in frequency. A major upgrade will occur when ADMX is retrofitted with a 4-cavity insert package (“Run 2A”). The smaller-diameter of each cavity moves the search to higher frequencies. Approximately a year after that, ADMX will be fitted with a yet higher-frequency package (“ADMX-EFR”) to allow the search to move into yet higher axion masses [\[284\]](#).

CAPP/CULTASK There is an ambitious program that includes RF-cavity axion research underway at the Center for Axion and Precision Physics Research (CAPP) in Korea [\[296\]](#). This program has several platforms for axion searches and R&D. The flagship platform is CAPP’s Ultra-Low Temperature Search in Korea (CULTASK). The conversion magnet is a 12 T peak-field solenoid. Inside the magnet bore is an approximately 30 liter conversion cavity (radius 0.132 m, height 0.560 m) with a single metallic tuning rod (radius 0.034 m) tuned with piezoelectric actuators. The cavity and cryogenic electronics are cooled with a dilution-refridgerator system operating at temperatures below 50 mK. The front-end of the cryogenic RF electronics is a Josephson parametric amplifier.

Importantly, this system has reported a result at DFSZ sensitivity over a relatively narrow mass range [\[298\]](#). The first 20 MHz wide data-set was taken above 1 GHz (approximately $4.5 \mu\text{eV}$ axion mass) in March 2022. The CULTASK system continues to take data and has recently greatly expanded its DFSZ-sensitive region [\[297\]](#).

The broader CAPP program also reported results from lower-magnetic-field platforms at axion couplings above DFSZ at a variety of masses. The program includes R&D on superconducting cavities and “multi-cell” (multi-cavity) systems [\[299\]](#).

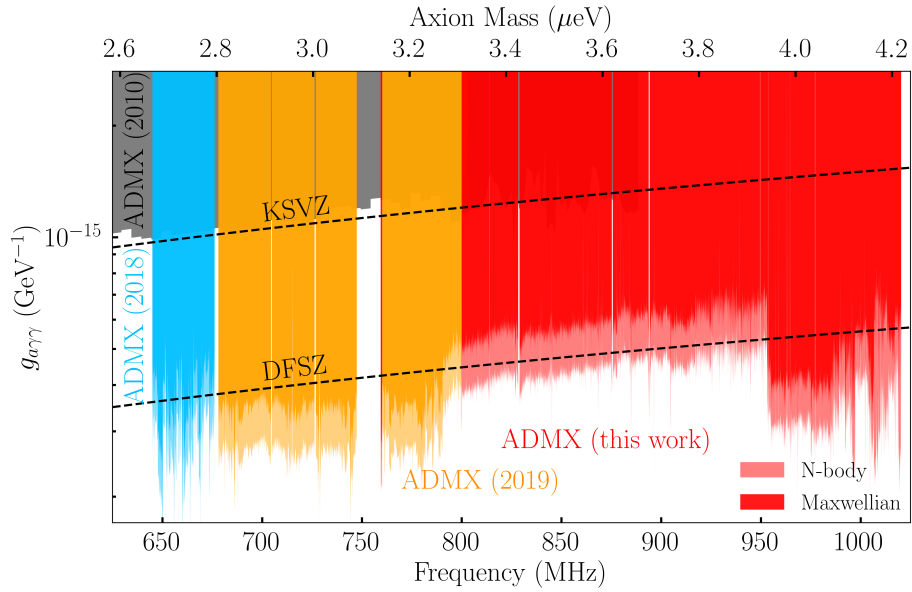


Figure 14: A recent set of ADMX limits. The horizontal axis is axion mass (upper) or frequency (lower), and the vertical axis is the coupling of the axion to two photons. The two diagonal lines indicate benchmark KSVZ and DFSZ axion models. The grey region shows very early ADMX limits at KSVZ sensitivity. The blue shows the later ADMX limit; it is notable for achieving DFSZ sensitivity, a long-term goal is axion research. The more recent orange and red limits are also shown. The dark limits assume an isothermal sphere axion phase-space and $\rho_{\text{DM}} = 0.45 \text{ GeV/cm}^3$. The lightened regions assume a DM density and phase space distribution extracted from N-body simulations of Milky-Way-type galaxy structure formation [294]. From 295.

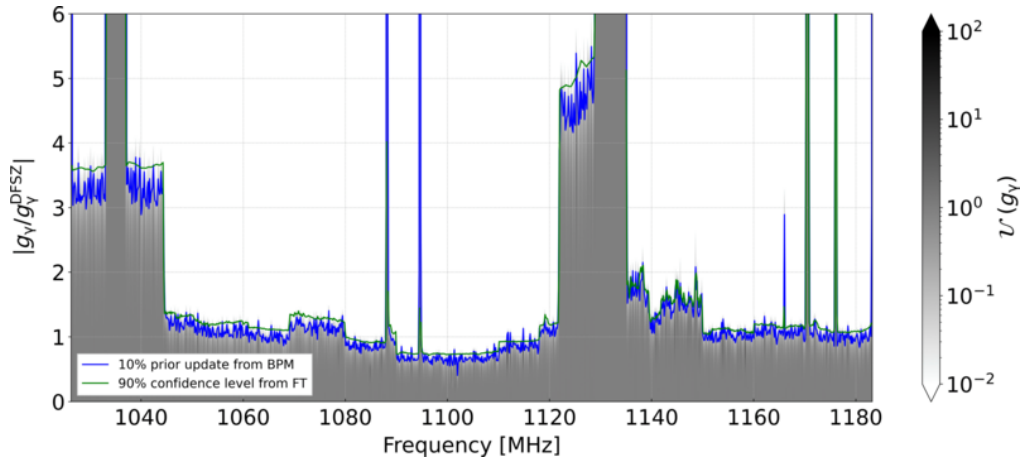


Figure 15: Recently excluded CAPP axion parameter space. From 297.

HAYSTAC: The Haloscope at Yale Sensitive to CDM (HAYSTAC) experiment is a relatively small-volume haloscope with a 25.4 cm long and 10.2 cm inner diameter main cavity with a 5.1 cm diameter tuning rod, in an 8 T magnetic field [279, 300]. The experiment first took data with with a single Josephson parametric amplifier and

reported an exclusion result for masses in the range of 23.15–24.0 μeV and couplings a factor of 2.7 above the KSVZ line [279, 301]. An upgrade to Phase II then covered the mass range 16.96–17.12 and 17.14–17.28 μeV in Phase IIa [300] and 18.44–18.71 μeV in Phase IIb for axion-photon couplings a factor of 2 above KSVZ [302]. Of particular interest in this second phase is that the receiver used vacuum squeezing to evade the standard quantum noise limit [300]. In this case, the squeezing improved the SNR by around $\sqrt{2}$, thereby speeding up the scan by around a factor of 2. This is the first demonstration that state-squeezing could be used to improve haloscope sensitivity (see section 5.4).

RADES: The Relic Axion Dark-Matter Exploratory Setup (RADES) is a haloscope axion search within the bore of the CERN Axion Solar Telescope (CAST) helioscope [303]. The cavity package consists of five right-circular cylindrical cavities in series, coupled at each end with aperture-filters. The cavities were cooled to around 1.8 K and read out by a cryogenic HEMT amplifier. The magnetic field in the neighborhood of the cavity was around 8.8 T. A result was reported for this system at an axion coupling two orders stronger than the CAST bound [303]. What is interesting about this result is the frequency is around 8.4 GHz (34 μeV) and it is now one of the most sensitive direct searches at these relatively high axion masses.

ORGAN: The Oscillating Resonant Group AxionN (ORGAN) is a haloscope aimed at high frequencies (high axion masses) in the range 15-50 GHz (62-207 μeV). The magnet had peak field around 11.5 T and a relatively small cavity volume. ORGAN reported an early result for axion masses in the range 63-67 μeV [280]. Although the sensitivity is for axion coupling far from DFSZ, this is a demonstration of the haloscope technique to what had previously been inaccessible axion masses.

QUAX: The (QUAX) collaboration [304] was conceived to search for the axion-electron coupling with a resonant experiment. Here, a small RF cavity is loaded with a ferromagnetic material. Due to the relative motion of the Earth and axion dark-matter halo, there is an axion gradient interaction which leads to an effective magnetic-field electron-spin interaction. The electrons precess and this, in effect, transfers power from the axion field to the precessing electrons. This resonant power is then re-emitted as electromagnetic radiation inside a tuned RF cavity [305]. A recent QUAX apparatus consisted of a small, non-cylindrical cavity, loaded with GaYIG spheres, with relevant mode frequency near 14 GHz. The system was cooled to mK temperatures and read out with a JPA. The resulting limits were in a narrow axion mass band near 43 μeV with coupling sensitivity still far from the QCD axion coupling. [306]

In the course of developing resonators, the QUAX group has also run searches for the axion-photon coupling as a standard haloscope. Recently, they have demonstrated near-KSVZ sensitivity to dark matter axions in a narrow band around 34 μeV in a system held at 20mK in a 7 T field. [307]

5.4. Next Steps for Cavity Haloscopes

The prospects for improving axion haloscopes with new technologies are good, and can be divided into: larger magnets, lower noise, and improved resonators.

The rate that frequency bandwidth can be scanned is proportional to

$$\frac{d\nu}{dt} \propto QB^4V^2 \frac{1}{T_s^2}, \quad (11)$$

where T_s is the system noise temperature (substantially the sum of the amplifier noise and the cavity physical temperature) and Q is the linewidth of the cavity resonance. In particular, notice the importance of the experimental parameters B , V , and T_s in the scan rate. For a practical search, the physical temperature of the cavity must be very low, the first-stage amplifier must therefore be of extremely low-noise design, and the magnet field strength and volume should be as large as possible. Note that the cavity bandwidth increases as the Q decreases so improvements in cavity Q offer less dramatic improvements in scan time (or sensitivity) compared to increased B or reduced T_s . The Q dependence also becomes more complicated when the cavity linewidth is narrower than the axion linewidth from the velocity dispersion of dark matter: tuning schemes can still gain scan speed, but at the expense of becoming insensitive to axion linewidths narrower than that of the cavity.

Magnets The power as measured by an axion haloscope is proportional to the active volume of the resonator, and to the average magnetic field squared. This translates directly to the stored energy of the magnet: Bigger is better. The stored energy of axion haloscope magnets has been steadily increasing over time, as has their cost. The highest field used to date is 18T with a 70mm bore, 500 mm long [308, 309].

The stored energy for several of the experiments discussed here is shown in figure 11 for comparison. With existing technology, there is a decision for future axion haloscope magnets: an experimental group could choose to use Nb₃Sn superconducting technology to build a magnet with a very high field over a very small volume, or the group could choose a lower field magnet with NbTi superconductor but a much larger volume.

One could conceive of large-bore magnets wound with Nb₃Sn superconductor, a considerably more expensive, fragile and therefore riskier superconductor; the resulting magnet would be perhaps a factor of 10 more expensive per unit of stored energy than that of NbTi. Hence, large volume 20 T magnets are immediately achievable, but at very high cost, and are being investigated [310]. Yet-higher magnetic fields are conceivable with high- T_c superconductors, perhaps even magnets into the 40 T range [311]. There is considerable interest in this high- T_c technology, but the engineering challenges have not yet been surmounted for building high- T_c solenoid magnets with large-volume bores and robust quench-protection. One could perhaps envision, though, such magnets eventually being inexpensive-enough and technically mature-enough to be deployed in a Sikivie-cavity search; this would be a potential “game changer” in haloscope design.

Noise: The current generation of axion haloscopes operates near the standard quantum limit with a noise temperature equivalent $kT \simeq h\nu/2$ [312]. This limit arises from the use of linear amplifiers, which must add a half-photon of noise in amplification to preserve the Heitler phase/photon-number (power) uncertainty relation. Two directions are being pursued to avoid this bound, both based around trading larger phase uncertainty for lower power uncertainty.

The first of these is “squeezing”, in which a special noise source that has “squeezed” most of the noise into one of the “quadratures” provides the background, and the system is read out and amplified in the other quadrature. Interestingly, this cannot directly lower the noise of an axion haloscope; the fundamental noise from the cavity physical temperature cannot be squeezed. What can be done, however, is to over-couple to the detector cavity. In this case, both the signal and the noise from the cavity are reduced, but the cavity covers a larger range of frequencies. The over-coupled antenna also has a noise component that is reflected off the cavity; this is where the squeezed source is used. Thus, in principle, a wider range of frequencies can be explored at once with squeezed noise than with a white noise source, and thus frequencies can be scanned more quickly [313,314]. As mentioned above, this has already been successfully demonstrated in the HAYSTAC experiment [300], with a factor of 2 improvement in scan speed. The limiting factor in this scheme is that any noise from losses between the cavity and amplifier are magnified by the squeezing, and the cavity and amplifier are necessarily separated, both because of the need for intervening RF components and because the amplifier needs a very low-field in which to operate. Improvements in low-loss and field-tolerant RF components amplifiers are needed for further improvement.

The second approach to a post-SQL axion search is to use a non-demolition measurement where the number of photons in the cavity is measured, and the phase information is not. This is well-aligned with present efforts to develop quantum computing hardware and has significant technological overlap. The primary challenge is to couple photons from the detection cavity in a high field, to a readout cavity in zero field to accommodate the readout electronics. A single mode transport system has been demonstrated in a field-free system [315]. A more complicated system that may avoid some of the transport issues has been proposed in [316], and a successful demonstration could potentially lead to an orders of magnitude increase in scan speed.

Resonators: The principal difficulty in the half-wavelength resonators used presently for axion haloscopes is that at higher frequencies, the small size of the resonators and reduced quality factor makes any dark matter signal too feeble to be useful. A number of solutions are in development, as noted below.

Multicavity Systems: For nonrelativistic axion dark matter, the Compton wavelength is much smaller than the de Broglie wavelength. The signals produced from multiple haloscope cavities within the axion de Broglie wavelength will be in-phase, so this suggests that one path to a more sensitive haloscope is to combine the signals from

multiple cavities. This is the proposed technique to utilize a magnet with characteristic dimensions larger than that for a single cavity in the ADMX G2 and ADMX EFR experiments [284]. There have also been efforts made to combine the field from multiple cavities in more complicated geometries to achieve the same effect. Both cases present a challenge that all cavities must be tuned relatively closely in frequency to coherently combine the signals.

High- Q Cavities: For resonant haloscopes, the rate at which frequencies can be explored at constant sensitivity is proportional to the resonant quality factor Q [292], which is limited by the loss of the cavity walls. At present, high-purity copper cavities with unloaded Q s as high as $\sim 100,000$ at 1 GHz have been used in haloscopes [277], and Q scales as $\nu^{2/3}$ at higher frequencies. Much higher quality factors (as high and more as 10^{11}) have been achieved in superconducting cavities, but the superconductor tends to become quite lossy when immersed in magnetic fields of the strengths used in axion experiments. Nevertheless, there have been some reports of cavity geometries that could maintain Q 's a factor of 6 better than copper even in multi-Tesla fields using Nb_3Sn [317] and high-Tc superconductors [318, 319]. If these methods can be successfully implemented in a full-scale axion search, it would enable higher frequencies to be explored on tractable timescales.

Multiwavelength Resonators: In contrast to coherently combining the signal from multiple resonators, one can envision a single resonance that spans multiple wavelengths. For naive geometries, multiwavelength resonances overlap very poorly with the axion wave. However there have been efforts to use dielectrics to shape the electromagnetic resonance to have significant overlap with the axion wavefunction for microwave frequencies above 10 GHz using periodic dielectric structures such as in the ORPHEUS experiment [320, 321], and in the far infrared using thin film deposition with the LAMPOST experiment in the context of dark photon searches [322, 323]. It has also been suggested to use subwavelength metallic structures to emulate the wavelength of photons in a plasma to produce larger volume resonators for a given frequency (the Plasma Haloscope [324, 325]).

Of particular note is the semiresonant system used in the MADMAX experiment [286, 326], where dark matter axions couple to the traveling waves between a series of dielectric plates inside a dipole magnet. Results from a recent small-scale prototype [327] have demonstrated sensitivities to axion couplings below existing limits from solar experiments.

5.5. Electromagnetic Searches Beyond Microwave Cavities

5.5.1. LC Circuit Haloscopes

While the axion haloscope was originally proposed as a resonator with the same length scale as the axion Compton wavelength, there is no fundamental issue with resonant detection of axion wavelengths exceeding the scale of

the detector. One approach which is well-suited to lower frequencies than the microwave cavity searches is to exploit the oscillating effective current induced by the axion field within a static external magnetic field. The “wire in cavity” LC circuit concept was proposed in ref. [328] (see also [329] for a related concept for dark photon detection), wherein an oscillating induced effective current in turn induces a real oscillating magnetic field, which is detected via an induced EMF in a coil. The resonant frequency can be tuned to the axion mass through an LC circuit or similar method. Recently a series of experiments have demonstrated the feasibility of the LC circuit technique [330–333] (ABRACADABRA, ADMX-SLIC, and others) and a set of experiments with significant reach into unexplored axion parameter space are in preparation.

- ABRACADABRA

The first realization of the low-mass axion detection scheme was A Broadband/Resonant Approach to Cosmic Axion Detection with an Amplifying B-field Ring Apparatus (ABRACADABRA) [334]. The ABRACADABRA proposal consisted of a toroidal magnet to source the external magnetic field, resulting in an azimuthal effective current, with the benefit of the physical oscillating magnetic field signal being in a region of zero background magnetic field [334]. The experiment could be run in broadband or resonant mode, with the first prototypes taking broadband data [330, 331]. The recent “10 cm” apparatus consisted of a small toroidal magnet (12 cm diameter, 12 cm tall) with peak field around 1 T. The central magnet bore contains the inductive loop (fig. 16) which is read out by a dc SQUID at temperature around 0.5 K [331]. The latest limits were in the 0.41–8.27 neV mass range for couplings close to and somewhat exceeding the CAST bound [331]. Future improvements could probe the QCD axion in this mass range.

- SHAFT

Another search based on the axion induced current is the Search for Axion-Like Dark-Matter with Ferromagnets (SHAFT) [333]. Here, a pair of independent toroidal coils are wrapped around high-permeability cores. A 1.5 T azimuthal magnetic field is applied, and each coil has its own readout; the induced signal is read out by a dc SQUID. The two-channel scheme allows for enhanced rejection of electromagnetic backgrounds. Limits were placed on 12 peV to 12 neV axion masses, with the lightest range below 0.1 neV just exceeding the CAST constraints. Improvements to the sensitivity by four orders of magnitude could be envisioned, thereby perhaps achieving sensitivity to QCD axions in this mass range.

- DM Radio

To access the lower axion masses at QCD sensitivity, the LC-circuit based DM-Radio [335, 336] has been proposed. This is to proceed in several stages. The first, DM-Radio 50L will demonstrate LC circuit technology on a large scale with a 50 Liter volume and access frequencies as low as 10 kHz, albeit at sensitivity above the QCD axion band. The DM-Radio m³ is a cubic meter instrumented volume projected to cover the 10 to 200 MHz range [337] with QCD axion sensitivity. A future, much larger, DM-Radio-GUT stage with resonant readout is proposed to access frequencies below 10

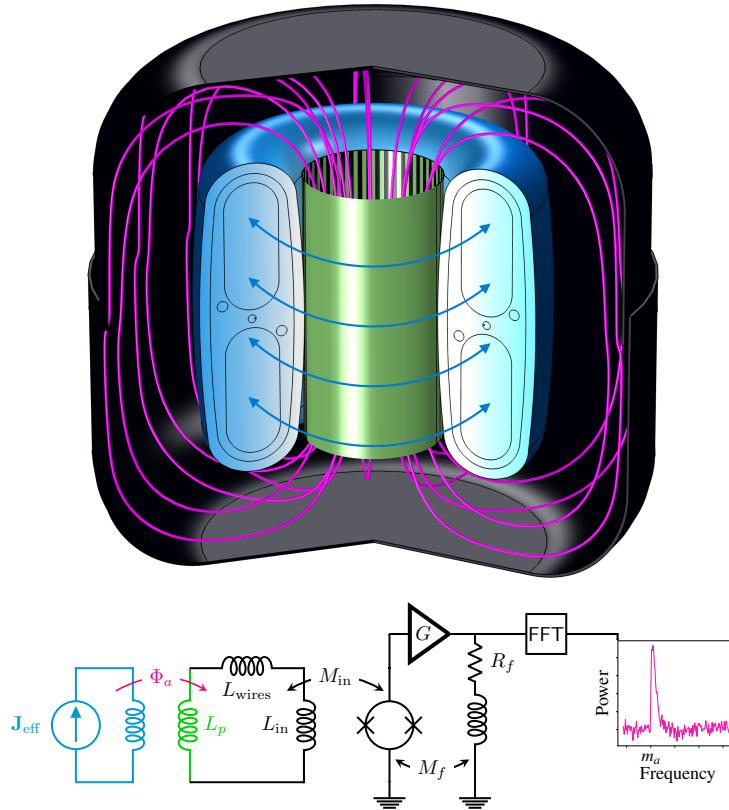


Figure 16: Top: Sketch of an ABRACADABRA prototype showing the effective axion-induced current (blue), sourced by the toroidal magnetic field, generating a magnetic flux (magenta) through the pickup cylinder (green) in the toroid bore. Bottom: Schematic of the signal readout. The pickup cylinder L_p is inductively coupled to the axion effective current. The induced current is read out through a dc SQUID coupled to the circuit through L_{in} . From 331.

MHz with sensitivity to the QCD axion.

5.5.2. Heterodyne Detection In the traditional haloscope detector, the axion field interacts with a static magnetic field to produce a photon at a frequency corresponding to the axion mass ω_a . If the magnetic field is non-static and varying with frequency ω , then photons can be produced at frequencies $\omega \pm \omega_a$. This suggests the possibility of designing a heterodyne haloscope without the usual large superconducting magnet [338–340]. It presents two challenges, however. First, the magnetic fields achievable with oscillating fields are much smaller than those achievable with static magnets, and second, time-varying magnetic fields tend to also vary spatially, so the overlap of the applied magnetic field, the axion field, and the resultant photon electric field must be carefully aligned. A proposed technique is to use high-Q superconducting cavities with engineered TM and TE modes such that the field overlap is non-zero for axion conversion when the

TM mode is excited with a large-power RF signal [341, 342]. This draws from the experience of high-power RF cavity design for accelerator engineering, and the hope is that the high Q achievable with superconducting cavities will compensate for the smaller applied magnetic field. The primary benefit is that, because the difference between the TE and TM mode frequency must correspond to the axion frequency, much smaller axion masses can be probed than would normally be accessible by microwave cavities.

5.5.3. Broadband Reflectors Axion-to-photon conversion can result from any electromagnetic boundary parallel to an applied magnetic field. From this point of view, resonant haloscopes can be viewed as conveniently spaced boundaries for a particular axion frequency [343]. Alternately, one can cede resonant enhancement and instead focus photons produced from axion conversion at boundaries onto a detector for a broadband search [344]. Several experiments have been proposed based on this principle [345], but in general the loss of resonant enhancement makes it difficult to achieve QCD sensitivity. The BREAD experiment uses a reflector design that is compatible with a high-field solenoidal magnet targeting high mass axions [346]. This technique has recently achieved sensitivity beyond the CAST constraint [347] and may be viable to probe the QCD axion pending the development suitably sensitive single-photon far infra-red and THz detectors.

5.6. Axion-Nucleon Coupling Experiments

In addition to the axion-photon coupling that has been the focus of this review, several directions have emerged in recent years toward detecting the interactions of axions with nuclei. This includes the ‘fundamental’ interaction of the axion with the CP violating gluon field strength, as well as derivative (gradient) couplings of axions with nuclear spins [52, 63]. While these interactions are particularly difficult to pursue in precision experiments, progress has been made toward several techniques.

One phenomenon, regardless of the makeup of dark matter, is that the axion-nucleon coupling would manifest as a macroscopic, spin-dependent “5th force”, in addition to a Yukawa force in the presence of CP violation [63]. The magnitude of this force varies between axion models, but current torsion pendula experiments are still many orders of magnitude away from the sensitivity necessary to detect even optimistic forces compatible with the QCD axion [348–351]. A dark matter axion field would induce oscillating nuclear electric dipole moments, as well as having a gradient coupling with nuclear spin [52]. Another manifestation is the proposed ‘piezoaxionic effect’ in which QCD axion dark matter generates oscillatory nuclear Schiff moments, which in a piezoelectric crystal can result in strain, or alternatively which can source axion forces [55, 56].

5.6.1. ARIADNE The Axion Resonant InterAction Detection Experiment (ARIADNE) is a proposal to detect the effect of the weak short-range force mediated by

an axion [64]. The goal is to construct a system with a resonant coupling between a rotating tungsten mass with periodic structure, which sources a slowly oscillating axion field through a Yukawa term (proportional to a small background level of CP violation) and the NMR frequency of polarized ^3He nuclear spins. The axion field sources a fictitious magnetic field which is sensed at a very low level in a magnetically shielded system. This strategy has the potential to probe axion masses between 0.1–10 meV and the technology for this experiment is currently under development [65, 352–354].

5.6.2. CASPEr The Cosmic Axion Spin Precession Experiment (CASPEr) searches for oscillating nuclear spins in the presence of axion dark matter [53, 54, 355]. There are two directions, CASPEr-electric and CASPEr-wind. CASPEr-e searches for nuclear spin precession in the background of a large effective electric field in a solid state system. Here, an oscillating nuclear CP-odd moment (e.g. Schiff moment, nuclear electric dipole moment) arises from the axion-gluon coupling in the background of an oscillating background θ , predicted to be $\sim 4 \times 10^{-19}$ if the QCD axion makes up the local dark matter density. This effect in principle has very little model dependence for the QCD axion, although the precise theoretical calculations of the size of the effect in nuclei and atoms have some uncertainties. Recent experiments have demonstrated the technique in the 162-166 neV mass range [356], currently still well within neutron star and supernova constraints (or alternatively testing a background θ 10^{-6}). In another approach, no evidence of an oscillating EDM at very low masses (less than 10^{-17} eV) has been seen by comparing the ^{199}Hg and ultra cold neutron precession frequencies in neutron EDM experiments [357], though the sensitivity is still within astrophysical bounds and several orders of magnitude away from the expected QCD axion coupling. Several orders of magnitude improvement is expected and further theoretical and experimental development is ongoing [358–360].

CASPEr-wind searches for an oscillating fictitious magnetic field in the presence of axion dark matter, which arises from the gradient coupling and is generically present but more model-dependent. A dedicated series of experiments for gradient couplings using nuclear spin co-magnetometers is underway at very low axion masses, ranging from 10^{-22} - 10^{-12} eV: CASPEr-Wind ZULF [361–363], NASDUCK [364], and others. The most recent results have exceeded astrophysical limits for feV and peV mass axions [365, 366]. The sensitivity of these searches is still many orders of magnitude away from the QCD axion predictions, and is undergoing development.

6. Summary and Outlook

Figure 17 shows the current status of searches for the QCD dark-matter axion. It is clear that we are at the very beginning of the exploration of the QCD axion as a dark matter candidate. In the near future there are two clear paths that seem most likely to lead to a discovery. First, cavity haloscope experiments that have already reached DFSZ sensitivity in the μeV mass range must be expanded as far and deep as possible,

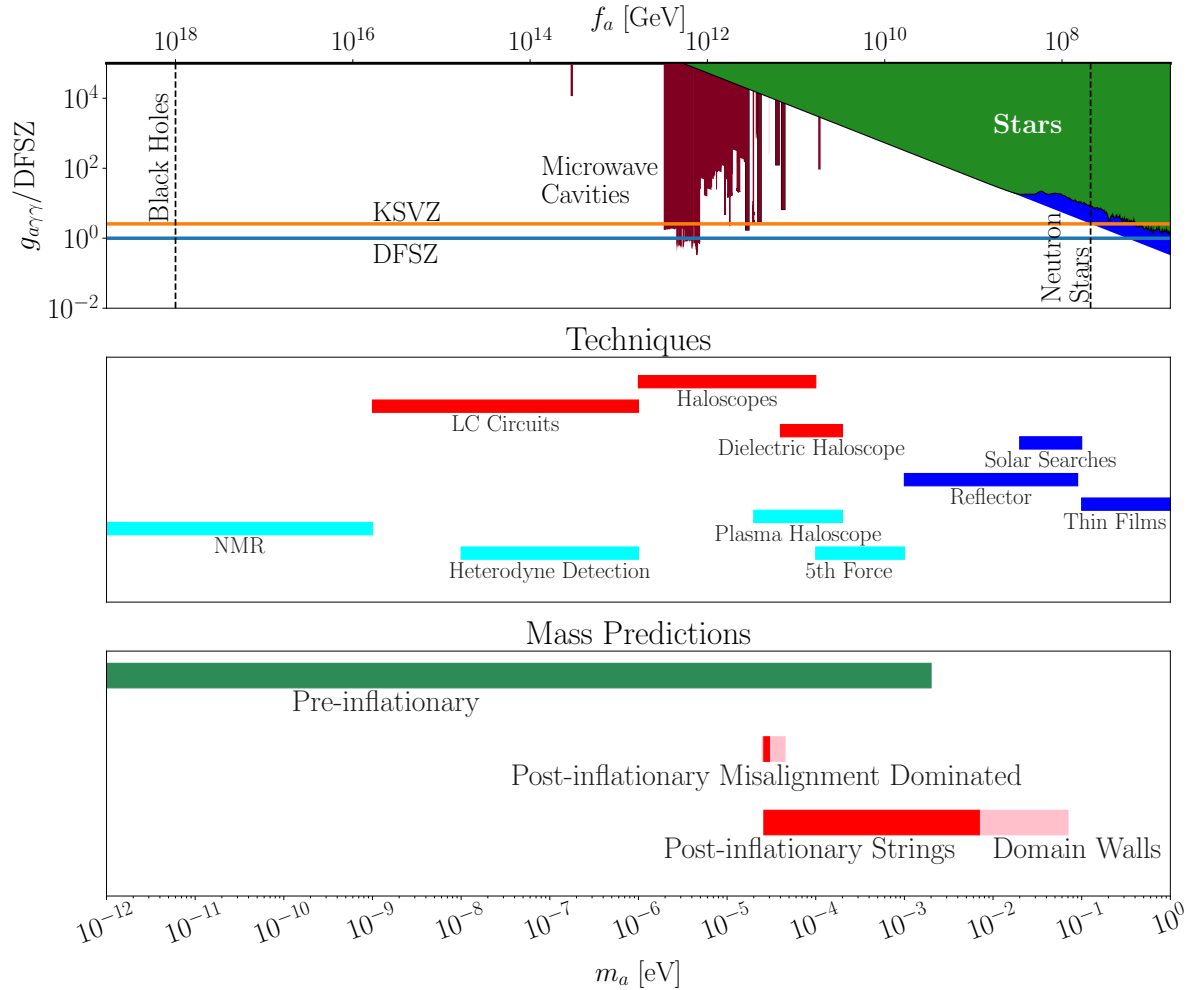


Figure 17: The overall status of searches for the QCD dark-matter axion. The horizontal axis is axion mass (lower axis) and axion scale f_a (upper axis). The vertical axis is the axion to photon coupling in units of the DFSZ coupling. The upper plot shows the currently achieved axion mass and photon coupling bounds, with a local dark matter density of $0.45 \text{ GeV}/\text{cm}^3$ assumed for haloscopes; see Section 5. The vertical dashed lines indicate the approximate lower (upper) bounds on the QCD axion from black hole (neutron star) observations; see Section 4. The middle plot indicates where the various search techniques have optimal sensitivity; see Section 5. The lower plot shows a high-level view of mass predictions grouped into pre-inflationary, post-inflationary (misalignment) and post-inflationary (axion-string) scenarios; see Section 3.

testing a broader mass range as well as our uncertainty in the local dark matter energy density. Second, proposed techniques to explore mass ranges inaccessible to microwave cavity-style experiments must be developed into mature production experiments.

The outlook for improving the mass range of cavity haloscopes has, up until recently,

appeared poor: while the axion coupling scales with the mass, the natural cavity size scales as m_a^{-3} and the quantum noise limit scales as m_a , suggesting sensitivity should fall as m_a^{-3} . However, several of the technologies we discussed have recently been demonstrated to considerably mitigate this scaling effect. Multicavity systems can boost the volume scaling by an order of magnitude (or more, limited by mechanical complexity). Quantum detection techniques: Squeezing, qubit, or bolometric-based methods could evade the quantum noise limit issue and potentially reduce noise by perhaps an order of magnitude. Advances in sustaining high-Q for a superconducting cavity in a high magnetic field could increase sensitivity by two orders of magnitude or more, even at higher frequencies. High-field and large-volume magnets are also being developed, but their realization is unlikely to result in an order of magnitude improvement in practical stored energy for axion experiments in the near future. The current DFSZ results from ADMX reach up to $4 \mu\text{eV}$ with a run plan that extends to $10 \mu\text{eV}$, so we shall take $10 \mu\text{eV}$ as a basis for what can be reachable with existing technology (assuming a local dark matter density of $0.45 \text{ GeV}/\text{cm}^3$). Considering sensitivity scaling to degrade as m_a^{-2} with increasing axion mass (including the use of beyond-standard-quantum-limit detectors previously mentioned), and the (admittedly optimistic) four orders of magnitude from improvements from technologies above, we can speculate that haloscopes could reach close to the meV mass scale at DFSZ sensitivity, completely covering post-inflationary misalignment dominated dark matter axion creation scenarios and the upper part of pre-inflationary axion creation scenarios. To achieve this will require a unified effort to combine all demonstrated technological innovations into a suite of cavity experiments that span the frequency range.

The remaining axion parameter space, above an meV and below a μeV , remains to be covered by sensitivity improvements from experiments being currently being developed beyond the cavity haloscopes, or new, as yet-undemonstrated technologies. Here the path forward is somewhat less clear. On the high-mass end, the produced photon wavelength is much smaller than natural experiment scales, so it may be that reflector or thin-film style detectors could be scaled, along with far-IR and THz photodetection technology, to be sensitive to DFSZ-coupled axions. A large dedicated solar experiment or improved astrophysical constraints may probe this region as well. Another direction are short-range axion-mediated forces. On the low-mass end, it is quite likely that LC-circuit style haloscopes can be scaled to reach the DFSZ milestone for many orders of magnitude below the current μeV bounds. At neV -scale axion masses, the most-promising experimental technologies rely on nuclear couplings via the NMR-type measurements, but early demonstrations are as yet far from QCD axion sensitivity. It is clear that covering the entire possible QCD axion mass range will require the support of a broad variety of small-scale demonstrators to illuminate which paths are the shortest to a discovery.

In the event that an axion-like signal is detected, there would immediately be a wealth of information to extract. In most detector configurations, the kinematic distribution of the local dark matter is derivable from the axion line shape (that is, the

local axion phase space) as well as its evolution over time. The axion phase space encodes the infall history of the axion dark matter, which opens the possibility that the axion discovery yields detailed information on the history of our galactic structure formation. Pre- and post-discovery, the particle physics and phenomenology of the axion will require further study, but would already unambiguously establish a new particle physics scale far above the electroweak scale. For an axion detection in a haloscope, for example, it is only the product of the axion-photon coupling-squared and the local dark matter density that is measured; there is no guarantee that this signal comes from a QCD axion instead of, say, an axion-like particle, and there is no way of knowing whether the axion comprises all of the local dark matter or merely a fraction. Further experiments exploring several couplings to fermions, and especially those testing the QCD coupling, will be needed to establish the new particle as the QCD axion and its abundance as the dark matter abundance.

Thus there are considerable theoretical and experimental challenges in the search for the QCD dark-matter axion. Nonetheless, there is room for optimism: The axion continues to be a very attractive particle dark-matter candidate. Sensitivity to the very compelling DFSZ axion coupling has been demonstrated, and production experiments now operate at that sensitivity over very promising axion masses. There is renewed appreciation for QCD axion masses well below and above the microwave cavity QCD axion mass scale, and technologies are being developed that may have the requisite sensitivity in these lower and higher masses. The number of experimenters and experiments are growing, and there continues to be better understanding of axion phenomenology. Overall, the case for the QCD dark-matter axion is strong and the experimental axion search program is accelerating. It may be that a discovery is near.

Acknowledgments

We thank our many colleagues and collaborators for their insights and conversations on QCD axions, and especially David Cyncynates, Ed Hardy, Junwu Huang, Sanjay Reddy, Ben Safdi, Andrew Sonnenschein, Ken Van Tilburg, and Giovanni Villadoro whose exchange of ideas was particularly helpful in the preparation of this review. We thank David Cyncynates, Sanjay Reddy, and Giovanni Villadoro for helpful comments on the manuscript and Ciaran O'Hare for maintaining an online repository of recent axion bounds [37]. M.B. is supported by the U.S. Department of Energy Office of Science under Award Number DE-SC0024375 and the Department of Physics and College of Arts and Science at the University of Washington. G.R. is supported by U.S. Department of Energy Office of Science under Award Number DE-SC0011665. M.B. is also grateful for the hospitality of KITP and Perimeter Institute, where part of this work was carried out. This research was supported in part by grant NSF PHY-2309135 to the Kavli Institute for Theoretical Physics (KITP). Research at Perimeter Institute is supported in part by the Government of Canada through the Department of Innovation, Science and Economic Development and by the Province of Ontario through the Ministry of

Colleges and Universities. This work was also supported by a grant from the Simons Foundation (1034867, Dittrich).

- [1] R. D. Peccei and H. R. Quinn, *CP Conservation in the Presence of Instantons*, *Physical Review Letters* **38** (1977) 1440.
- [2] S. Weinberg, *A New Light Boson?*, *Physical Review Letters* **40** (1978) 223.
- [3] F. Wilczek, *Problems of Strong p and t Invariance in the Presence of Instantons*, *Physical Review Letters* **40** (1978) 279.
- [4] R. D. Peccei and H. R. Quinn, *Constraints Imposed by CP Conservation in the Presence of Instantons*, *Phys. Rev. D* **16** (1977) 1791.
- [5] G. 't Hooft, *Computation of the Quantum Effects Due to a Four-Dimensional Pseudoparticle*, *Phys. Rev. D* **14** (1976) 3432.
- [6] R. Jackiw and C. Rebbi, *Vacuum Periodicity in a Yang-Mills Quantum Theory*, *Phys. Rev. Lett.* **37** (1976) 172.
- [7] C. G. Callan, Jr., R. F. Dashen and D. J. Gross, *Instantons as a Bridge Between Weak and Strong Coupling in QCD*, *Phys. Rev. D* **20** (1979) 3279.
- [8] R. J. Crewther, P. Di Vecchia, G. Veneziano and E. Witten, *Chiral Estimate of the Electric Dipole Moment of the Neutron in Quantum Chromodynamics*, *Phys. Lett. B* **88** (1979) 123.
- [9] M. Pospelov and A. Ritz, *Theta induced electric dipole moment of the neutron via QCD sum rules*, *Phys. Rev. Lett.* **83** (1999) 2526 [[hep-ph/9904483](#)].
- [10] M. Pospelov and A. Ritz, *Theta vacua, QCD sum rules, and the neutron electric dipole moment*, *Nucl. Phys. B* **573** (2000) 177 [[hep-ph/9908508](#)].
- [11] C. Abel et al., *Measurement of the Permanent Electric Dipole Moment of the Neutron*, *Phys. Rev. Lett.* **124** (2020) 081803 [[2001.11966](#)].
- [12] V. V. Flambaum, M. Pospelov, A. Ritz and Y. V. Stadnik, *Sensitivity of EDM experiments in paramagnetic atoms and molecules to hadronic CP violation*, *Phys. Rev. D* **102** (2020) 035001 [[1912.13129](#)].
- [13] C. Vafa and E. Witten, *Parity Conservation in QCD*, *Phys. Rev. Lett.* **53** (1984) 535.
- [14] M. Pospelov and A. Ritz, *Electric dipole moments as probes of new physics*, *Annals Phys.* **318** (2005) 119 [[hep-ph/0504231](#)].
- [15] P. Di Vecchia and G. Veneziano, *Chiral Dynamics in the Large n Limit*, *Nucl. Phys. B* **171** (1980) 253.
- [16] M. Gorghetto and G. Villadoro, *Topological Susceptibility and QCD Axion Mass: QED and NNLO corrections*, *JHEP* **03** (2019) 033 [[1812.01008](#)].
- [17] G. G. di Cortona, E. Hardy, J. P. Vega and G. Villadoro, *The qcd axion, precisely*, *Journal of High Energy Physics* **2016** (2016) .
- [18] S. Dimopoulos, P. H. Frampton, H. Georgi and M. B. Wise, *Automatic invisible axion without domain walls*, *Physics Letters B* **117** (1982) 185.
- [19] H. Georgi and M. B. Wise, *Hiding the invisible axion*, *Physics Letters B* **116** (1982) 123.
- [20] M. B. Wise, H. Georgi and S. L. Glashow, *Su(5) and the invisible axion*, *Phys. Rev. Lett.* **47** (1981) 402.
- [21] J. Preskill, M. B. Wise and F. Wilczek, *Cosmology of the Invisible Axion*, *Phys. Lett.* **B120** (1983) 127.
- [22] L. Abbott and P. Sikivie, *A Cosmological Bound on the Invisible Axion*, *Phys. Lett. B* **120** (1983) 133.
- [23] M. Dine and W. Fischler, *The Not So Harmless Axion*, *Phys. Lett. B* **120** (1983) 137.
- [24] P. Svrcek and E. Witten, *Axions In String Theory*, *JHEP* **06** (2006) 051 [[hep-th/0605206](#)].
- [25] A. Arvanitaki, S. Dimopoulos, S. Dubovsky, N. Kaloper and J. March-Russell, *String Axiverse*, *Phys. Rev.* **D81** (2010) 123530 [[0905.4720](#)].
- [26] A. Hook, *TASI Lectures on the Strong CP Problem and Axions*, *PoS TASI2018* (2019) 004 [[1812.02669](#)].
- [27] L. Di Luzio, M. Giannotti, E. Nardi and L. Visinelli, *The landscape of QCD axion models*, *Phys. Rept.* **870** (2020) 1 [[2003.01100](#)].
- [28] A. Ringwald, *Review on Axions*, 4, 2024, [2404.09036](#).

- [29] P. W. Graham, I. G. Irastorza, S. K. Lamoreaux, A. Lindner and K. A. van Bibber, *Experimental Searches for the Axion and Axion-Like Particles*, *Ann. Rev. Nucl. Part. Sci.* **65** (2015) 485 [1602.00039].
- [30] I. G. Irastorza and J. Redondo, *New experimental approaches in the search for axion-like particles*, *Prog. Part. Nucl. Phys.* **102** (2018) 89 [1801.08127].
- [31] P. Sikivie, *Invisible Axion Search Methods*, *Rev. Mod. Phys.* **93** (2021) 015004 [2003.02206].
- [32] A. Berlin and Y. Kahn, *New Technologies for Axion and Dark Photon Searches*, **2412.08704**.
- [33] D. J. E. Marsh, *Axion Cosmology*, *Phys. Rept.* **643** (2016) 1 [1510.07633].
- [34] C. A. J. O'Hare, *Cosmology of axion dark matter*, *PoS COSMICWISPers* (2024) 040 [2403.17697].
- [35] A. Caputo and G. Raffelt, *Astrophysical Axion Bounds: The 2024 Edition*, *PoS COSMICWISPers* (2024) 041 [2401.13728].
- [36] PARTICLE DATA GROUP collaboration, *Review of particle physics*, *Phys. Rev. D* **110** (2024) 030001.
- [37] C. O'HARE, *cajohare/axionlimits: Axionlimits*, July, 2020. 10.5281/zenodo.3932430.
- [38] C. Bonati, M. D'Elia, M. Mariti, G. Martinelli, M. Mesiti, F. Negro et al., *Axion phenomenology and θ -dependence from $N_f = 2 + 1$ lattice QCD*, *JHEP* **03** (2016) 155 [1512.06746].
- [39] S. Borsanyi et al., *Calculation of the axion mass based on high-temperature lattice quantum chromodynamics*, *Nature* **539** (2016) 69 [1606.07494].
- [40] A. Trunin, F. Burger, E.-M. Ilgenfritz, M. P. Lombardo and M. Müller-Preussker, *Topological susceptibility from $N_f = 2 + 1 + 1$ lattice QCD at nonzero temperature*, *J. Phys. Conf. Ser.* **668** (2016) 012123 [1510.02265].
- [41] E. Berkowitz, M. I. Buchoff and E. Rinaldi, *Lattice QCD input for axion cosmology*, *Phys. Rev. D* **92** (2015) 034507 [1505.07455].
- [42] S. Borsanyi, M. Dierigl, Z. Fodor, S. D. Katz, S. W. Mages, D. Nogradi et al., *Axion cosmology, lattice QCD and the dilute instanton gas*, *Phys. Lett. B* **752** (2016) 175 [1508.06917].
- [43] P. Petreczky, H.-P. Schadler and S. Sharma, *The topological susceptibility in finite temperature QCD and axion cosmology*, *Phys. Lett. B* **762** (2016) 498 [1606.03145].
- [44] F. Burger, E.-M. Ilgenfritz, M. P. Lombardo and A. Trunin, *Chiral observables and topology in hot QCD with two families of quarks*, *Phys. Rev. D* **98** (2018) 094501 [1805.06001].
- [45] C. Bonati, M. D'Elia, G. Martinelli, F. Negro, F. Sanfilippo and A. Todaro, *Topology in full QCD at high temperature: a multicanonical approach*, *JHEP* **11** (2018) 170 [1807.07954].
- [46] M. Dine, P. Draper, L. Stephenson-Haskins and D. Xu, *Axions, Instantons, and the Lattice*, *Phys. Rev. D* **96** (2017) 095001 [1705.00676].
- [47] A. Hook and J. Huang, *Probing axions with neutron star inspirals and other stellar processes*, *JHEP* **06** (2018) 036 [1708.08464].
- [48] T. D. Cohen, R. J. Furnstahl and D. K. Griegel, *Quark and gluon condensates in nuclear matter*, *Phys. Rev. C* **45** (1992) 1881.
- [49] R. Balkin, J. Serra, K. Springmann and A. Weiler, *The QCD axion at finite density*, *JHEP* **07** (2020) 221 [2003.04903].
- [50] M. Kumamoto, J. Huang, C. Drischler, M. Baryakhtar and S. Reddy, *Pi in the Sky: Neutron Stars with Exceptionally Light QCD Axions*, **2410.21590**.
- [51] K. Springmann, M. Stadlbauer, S. Stelzl and A. Weiler, *A Universal Bound on QCD Axions from Supernovae*, **2410.19902**.
- [52] P. W. Graham and S. Rajendran, *New Observables for Direct Detection of Axion Dark Matter*, *Phys. Rev. D* **88** (2013) 035023 [1306.6088].
- [53] D. Budker, P. W. Graham, M. Ledbetter, S. Rajendran and A. O. Sushkov, *Proposal for a cosmic axion spin precession experiment (casper)*, *Phys. Rev. X* **4** (2014) 021030.
- [54] D. F. J. Kimball, S. Afach, D. Aybas, J. W. Blanchard, D. Budker, G. Centers et al., *Overview of the Cosmic Axion Spin Precession Experiment (CASPER)*, *Springer Proc. Phys.* **245** (2020) 105 [1711.08999].

- [55] A. Arvanitaki, A. Madden and K. Van Tilburg, *Piezoaxionic effect*, *Phys. Rev. D* **109** (2024) 072009 [[2112.11466](#)].
- [56] A. Arvanitaki, J. Engel, A. A. Geraci, A. Madden, A. Hepburn and K. Van Tilburg, *The Ferroaxionic Force*, [2411.10516](#).
- [57] J. E. Kim, *Weak Interaction Singlet and Strong CP Invariance*, *Phys. Rev. Lett.* **43** (1979) 103.
- [58] M. A. Shifman, A. I. Vainshtein and V. I. Zakharov, *Can Confinement Ensure Natural CP Invariance of Strong Interactions?*, *Nucl. Phys. B* **166** (1980) 493.
- [59] M. Dine, W. Fischler and M. Srednicki, *A Simple Solution to the Strong CP Problem with a Harmless Axion*, *Phys. Lett. B* **104** (1981) 199.
- [60] A. R. Zhitnitsky, *On Possible Suppression of the Axion Hadron Interactions. (In Russian)*, *Sov. J. Nucl. Phys.* **31** (1980) 260.
- [61] M. Srednicki, *Axion Couplings to Matter. 1. CP Conserving Parts*, *Nucl. Phys. B* **260** (1985) 689.
- [62] H. Georgi, D. B. Kaplan and L. Randall, *Manifesting the Invisible Axion at Low-energies*, *Phys. Lett. B* **169** (1986) 73.
- [63] J. E. Moody and F. Wilczek, *New Macroscopic Forces?*, *Phys. Rev. D* **30** (1984) 130.
- [64] A. Arvanitaki and A. A. Geraci, *Resonantly detecting axion-mediated forces with nuclear magnetic resonance*, *Phys. Rev. Lett.* **113** (2014) 161801.
- [65] ARIADNE collaboration, *Progress on the ARIADNE axion experiment*, *Springer Proc. Phys.* **211** (2018) 151 [[1710.05413](#)].
- [66] P. Agrawal, J. Fan, M. Reece and L.-T. Wang, *Experimental Targets for Photon Couplings of the QCD Axion*, *JHEP* **02** (2018) 006 [[1709.06085](#)].
- [67] P. Agrawal, M. Nee and M. Reig, *Axion couplings in grand unified theories*, *JHEP* **10** (2022) 141 [[2206.07053](#)].
- [68] N. Gendler, D. J. E. Marsh, L. McAllister and J. Moritz, *Glimmers from the axiverse*, *JCAP* **09** (2024) 071 [[2309.13145](#)].
- [69] P. Agrawal, M. Nee and M. Reig, *Axion Couplings in Heterotic String Theory*, [2410.03820](#).
- [70] V. C. Rubin and W. K. Ford, Jr., *Rotation of the Andromeda Nebula from a Spectroscopic Survey of Emission Regions*, *Astrophys. J.* **159** (1970) 379.
- [71] WMAP collaboration, *First year Wilkinson Microwave Anisotropy Probe (WMAP) observations: Determination of cosmological parameters*, *Astrophys. J. Suppl.* **148** (2003) 175 [[astro-ph/0302209](#)].
- [72] J. A. Frieman, S. Dimopoulos and M. S. Turner, *Axions and stars*, *Phys. Rev. D* **36** (1987) 2201.
- [73] G. G. Raffelt and D. S. P. Dearborn, *Bounds on hadronic axions from stellar evolution*, *Phys. Rev. D* **36** (1987) 2211.
- [74] D. S. P. Dearborn, D. N. Schramm and G. Steigman, *Astrophysical constraints on the couplings of axions, majorons, and familons*, *Phys. Rev. Lett.* **56** (1986) 26.
- [75] A. D. Linde, *Inflation and Axion Cosmology*, *Phys. Lett. B* **201** (1988) 437.
- [76] J. March-Russell and H. Tillim, *Axiverse Strings*, [2109.14637](#).
- [77] J. N. Benabou, Q. Bonnefoy, M. Buschmann, S. Kumar and B. R. Safdi, *Cosmological dynamics of string theory axion strings*, *Phys. Rev. D* **110** (2024) 035021 [[2312.08425](#)].
- [78] M. Reece, *Extra-Dimensional Axion Expectations*, [2406.08543](#).
- [79] R. Petrossian-Byrne and G. Villadoro, *Open String Axiverse*, [2503.16387](#).
- [80] V. Loladze, A. Platschorre and M. Reig, *Higher Axion Strings*, [2503.18707](#).
- [81] A. Arvanitaki, S. Dimopoulos, M. Galanis, L. Lehner, J. O. Thompson and K. Van Tilburg, *Large-misalignment mechanism for the formation of compact axion structures: Signatures from the QCD axion to fuzzy dark matter*, *Phys. Rev. D* **101** (2020) 083014 [[1909.11665](#)].
- [82] P. Sikivie, *Of Axions, Domain Walls and the Early Universe*, *Phys. Rev. Lett.* **48** (1982) 1156.
- [83] A. Vilenkin and A. E. Everett, *Cosmic Strings and Domain Walls in Models with Goldstone and Pseudo-Goldstone Bosons*, *Phys. Rev. Lett.* **48** (1982) 1867.
- [84] A. Vilenkin, *Cosmic Strings and Domain Walls*, *Phys. Rept.* **121** (1985) 263.

- [85] R. L. Davis, *Cosmic Axions from Cosmic Strings*, *Phys. Lett. B* **180** (1986) 225.
- [86] T. Vachaspati and A. Vilenkin, *Gravitational Radiation from Cosmic Strings*, *Phys. Rev. D* **31** (1985) 3052.
- [87] D. G. Figueroa, M. Hindmarsh, J. Lizarraga and J. Urrestilla, *Irreducible background of gravitational waves from a cosmic defect network: update and comparison of numerical techniques*, *Phys. Rev. D* **102** (2020) 103516 [[2007.03337](#)].
- [88] C.-F. Chang and Y. Cui, *Gravitational waves from global cosmic strings and cosmic archaeology*, *JHEP* **03** (2022) 114 [[2106.09746](#)].
- [89] M. Gorghetto, E. Hardy and H. Nicolaescu, *Observing invisible axions with gravitational waves*, *JCAP* **06** (2021) 034 [[2101.11007](#)].
- [90] M. Gorghetto, E. Hardy and G. Villadoro, *Axions from Strings: the Attractive Solution*, *JHEP* **07** (2018) 151 [[1806.04677](#)].
- [91] M. Buschmann, J. W. Foster, A. Hook, A. Peterson, D. E. Willcox, W. Zhang et al., *Dark matter from axion strings with adaptive mesh refinement*, *Nature Commun.* **13** (2022) 1049 [[2108.05368](#)].
- [92] M. Buschmann, J. W. Foster and B. R. Safdi, *Early-Universe Simulations of the Cosmological Axion*, *Phys. Rev. Lett.* **124** (2020) 161103 [[1906.00967](#)].
- [93] M. Gorghetto, E. Hardy and G. Villadoro, *More axions from strings*, *SciPost Phys.* **10** (2021) 050 [[2007.04990](#)].
- [94] K. Saikawa, J. Redondo, A. Vaquero and M. Kaltschmidt, *Spectrum of global string networks and the axion dark matter mass*, [2401.17253](#).
- [95] H. Kim, J. Park and M. Son, *Axion dark matter from cosmic string network*, *JHEP* **07** (2024) 150 [[2402.00741](#)].
- [96] J. N. Benabou, M. Buschmann, J. W. Foster and B. R. Safdi, *Axion mass prediction from adaptive mesh refinement cosmological lattice simulations*, [2412.08699](#).
- [97] D. Harari and P. Sikivie, *On the Evolution of Global Strings in the Early Universe*, *Phys. Lett. B* **195** (1987) 361.
- [98] C. Hagmann, S. Chang and P. Sikivie, *Axions from string decay*, *Nucl. Phys. B Proc. Suppl.* **72** (1999) 81 [[hep-ph/9807428](#)].
- [99] R. A. Battye and E. P. S. Shellard, *Global string radiation*, *Nucl. Phys. B* **423** (1994) 260 [[astro-ph/9311017](#)].
- [100] R. A. Battye and E. P. S. Shellard, *Axion string constraints*, *Phys. Rev. Lett.* **73** (1994) 2954 [[astro-ph/9403018](#)].
- [101] M. Gorghetto and E. Hardy, *Post-inflationary axions: a minimal target for axion haloscopes*, *JHEP* **05** (2023) 030 [[2212.13263](#)].
- [102] M. Tegmark, A. Aguirre, M. Rees and F. Wilczek, *Dimensionless constants, cosmology and other dark matters*, *Phys. Rev. D* **73** (2006) 023505 [[astro-ph/0511774](#)].
- [103] C. Hagmann and P. Sikivie, *Computer simulations of the motion and decay of global strings*, *Nucl. Phys. B* **363** (1991) 247.
- [104] V. B. Klaer and G. D. Moore, *The dark-matter axion mass*, *JCAP* **11** (2017) 049 [[1708.07521](#)].
- [105] M. Dine, N. Fernandez, A. Ghalsasi and H. H. Patel, *Comments on axions, domain walls, and cosmic strings*, *JCAP* **11** (2021) 041 [[2012.13065](#)].
- [106] R. L. Davis and E. P. S. Shellard, *Do axions need inflation?*, *Nucl. Phys. B* **324** (1989) 167.
- [107] S. Hoof, J. Riess and D. J. E. Marsh, *Statistical Uncertainties of the $N_{DW} = 1$ QCD Axion Mass Window from Topological Defects*, [2108.09563](#).
- [108] M. S. Turner and F. Wilczek, *Inflationary axion cosmology*, *Phys. Rev. Lett.* **66** (1991) 5.
- [109] M. P. Hertzberg, M. Tegmark and F. Wilczek, *Axion Cosmology and the Energy Scale of Inflation*, *Phys. Rev. D* **78** (2008) 083507 [[0807.1726](#)].
- [110] PLANCK collaboration, *Planck 2018 results. X. Constraints on inflation*, *Astron. Astrophys.* **641** (2020) A10 [[1807.06211](#)].
- [111] S. Chang and K. Choi, *Hadronic axion window and the big bang nucleosynthesis*, *Phys. Lett. B*

- 316** (1993) 51 [[hep-ph/9306216](#)].
- [112] S. Weinberg, *Goldstone Bosons as Fractional Cosmic Neutrinos*, *Phys. Rev. Lett.* **110** (2013) 241301 [[1305.1971](#)].
- [113] C. Brust, D. E. Kaplan and M. T. Walters, *New Light Species and the CMB*, *JHEP* **12** (2013) 058 [[1303.5379](#)].
- [114] P. Graf and F. D. Steffen, *Thermal axion production in the primordial quark-gluon plasma*, *Phys. Rev. D* **83** (2011) 075011 [[1008.4528](#)].
- [115] E. Masso, F. Rota and G. Zsembinszki, *On axion thermalization in the early universe*, *Phys. Rev. D* **66** (2002) 023004 [[hep-ph/0203221](#)].
- [116] A. Salvio, A. Strumia and W. Xue, *Thermal axion production*, *JCAP* **01** (2014) 011 [[1310.6982](#)].
- [117] D. Baumann, D. Green and B. Wallisch, *New Target for Cosmic Axion Searches*, *Phys. Rev. Lett.* **117** (2016) 171301 [[1604.08614](#)].
- [118] A. Notari, F. Rompineve and G. Villadoro, *Improved Hot Dark Matter Bound on the QCD Axion*, *Phys. Rev. Lett.* **131** (2023) 011004 [[2211.03799](#)].
- [119] D. Green, Y. Guo and B. Wallisch, *Cosmological implications of axion-matter couplings*, *JCAP* **02** (2022) 019 [[2109.12088](#)].
- [120] L. Caloni, M. Gerbino, M. Lattanzi and L. Visinelli, *Novel cosmological bounds on thermally-produced axion-like particles*, *JCAP* **09** (2022) 021 [[2205.01637](#)].
- [121] N. Blinov, M. J. Dolan and P. Draper, *Imprints of the Early Universe on Axion Dark Matter Substructure*, *Phys. Rev. D* **101** (2020) 035002 [[1911.07853](#)].
- [122] N. Blinov, M. J. Dolan, P. Draper and J. Kozaczuk, *Dark matter targets for axionlike particle searches*, *Phys. Rev. D* **100** (2019) 015049 [[1905.06952](#)].
- [123] R. T. Co, E. Gonzalez and K. Harigaya, *Axion Misalignment Driven to the Hilltop*, *JHEP* **05** (2019) 163 [[1812.11192](#)].
- [124] F. Takahashi and W. Yin, *QCD axion on hilltop by a phase shift of π* , *JHEP* **10** (2019) 120 [[1908.06071](#)].
- [125] J. Huang, A. Madden, D. Racco and M. Reig, *Maximal axion misalignment from a minimal model*, *JHEP* **10** (2020) 143 [[2006.07379](#)].
- [126] R. T. Co, L. J. Hall and K. Harigaya, *Axion Kinetic Misalignment Mechanism*, *Phys. Rev. Lett.* **124** (2020) 251802 [[1910.14152](#)].
- [127] R. T. Co, L. J. Hall and K. Harigaya, *QCD Axion Dark Matter with a Small Decay Constant*, *Phys. Rev. Lett.* **120** (2018) 211602 [[1711.10486](#)].
- [128] D. Cyncynates, T. Giurgica-Tiron, O. Simon and J. O. Thompson, *Resonant nonlinear pairs in the axiverse and their late-time direct and astrophysical signatures*, *Phys. Rev. D* **105** (2022) 055005 [[2109.09755](#)].
- [129] D. Cyncynates, O. Simon, J. O. Thompson and Z. J. Weiner, *Nonperturbative structure in coupled axion sectors and implications for direct detection*, *Phys. Rev. D* **106** (2022) 083503 [[2208.05501](#)].
- [130] D. Cyncynates and J. O. Thompson, *Heavy qcd axion dark matter from avoided level crossing*, *Phys. Rev. D* **108** (2023) L091703 [[2306.04678](#)].
- [131] P. Agrawal, G. Marques-Tavares and W. Xue, *Opening up the QCD axion window*, *JHEP* **03** (2018) 049 [[1708.05008](#)].
- [132] W. Hu, R. Barkana and A. Gruzinov, *Cold and fuzzy dark matter*, *Phys. Rev. Lett.* **85** (2000) 1158 [[astro-ph/0003365](#)].
- [133] L. Hui, J. P. Ostriker, S. Tremaine and E. Witten, *Ultralight scalars as cosmological dark matter*, *Phys. Rev. D* **95** (2017) 043541 [[1610.08297](#)].
- [134] E. G. M. Ferreira, *Ultra-light dark matter*, *Astron. Astrophys. Rev.* **29** (2021) 7 [[2005.03254](#)].
- [135] L. Hui, *Wave Dark Matter*, *Ann. Rev. Astron. Astrophys.* **59** (2021) 247 [[2101.11735](#)].
- [136] N. Dalal and A. Kravtsov, *Excluding fuzzy dark matter with sizes and stellar kinematics of ultrafaint dwarf galaxies*, *Phys. Rev. D* **106** (2022) 063517 [[2203.05750](#)].

- [137] K. M. Zurek, C. J. Hogan and T. R. Quinn, *Astrophysical Effects of Scalar Dark Matter Miniclusters*, *Phys. Rev. D* **75** (2007) 043511 [[astro-ph/0607341](#)].
- [138] C. J. Hogan and M. J. Rees, *AXION MINICLUSTERS*, *Phys. Lett. B* **205** (1988) 228.
- [139] E. W. Kolb and I. I. Tkachev, *Axion miniclusters and Bose stars*, *Phys. Rev. Lett.* **71** (1993) 3051 [[hep-ph/9303313](#)].
- [140] E. W. Kolb and I. I. Tkachev, *Large amplitude isothermal fluctuations and high density dark matter clumps*, *Phys. Rev. D* **50** (1994) 769 [[astro-ph/9403011](#)].
- [141] E. W. Kolb and I. I. Tkachev, *Nonlinear axion dynamics and formation of cosmological pseudosolitons*, *Phys. Rev. D* **49** (1994) 5040 [[astro-ph/9311037](#)].
- [142] M. Fairbairn, D. J. E. Marsh and J. Quevillon, *Searching for the QCD Axion with Gravitational Microlensing*, *Phys. Rev. Lett.* **119** (2017) 021101 [[1701.04787](#)].
- [143] M. Fairbairn, D. J. E. Marsh, J. Quevillon and S. Rozier, *Structure formation and microlensing with axion miniclusters*, *Phys. Rev. D* **97** (2018) 083502 [[1707.03310](#)].
- [144] M. Gorghetto, E. Hardy and G. Villadoro, *More axion stars from strings*, *JHEP* **08** (2024) 126 [[2405.19389](#)].
- [145] D. A. Dicus, E. W. Kolb, V. L. Teplitz and R. V. Wagoner, *Astrophysical bounds on the masses of axions and higgs particles*, *Physical Review D* **18** (1978) 1829.
- [146] A. Burrows, M. S. Turner and R. P. Brinkmann, *Axions and SN 1987a*, *Phys. Rev. D* **39** (1989) 1020.
- [147] G. G. Raffelt, *Stars as laboratories for fundamental physics: The astrophysics of neutrinos, axions, and other weakly interacting particles*. 5, 1996.
- [148] PARTICLE DATA GROUP collaboration, *Review of Particle Physics*, *PTEP* **2022** (2022) 083C01.
- [149] V. Anastassopoulos, S. Aune, K. Barth, A. Belov, H. Bräuninger, G. Cantatore et al., *New cast limit on the axion–photon interaction*, *Nature Physics* **13** (2017) 584.
- [150] T. Dafni and J. Galán, *Digging into axion physics with (baby)iaxo*, *Universe* **8** (2022) .
- [151] S. Hoof, J. Jaeckel and L. J. Thormaehlen, *Quantifying uncertainties in the solar axion flux and their impact on determining axion model parameters*, *Journal of Cosmology and Astroparticle Physics* **2021** (2021) 006.
- [152] A. Derevianko, V. A. Dzuba, V. V. Flambaum and M. Pospelov, *Axio-electric effect*, *Phys. Rev. D* **82** (2010) 065006 [[1007.1833](#)].
- [153] XENON COLLABORATION collaboration, *Search for new physics in electronic recoil data from xenonnt*, *Phys. Rev. Lett.* **129** (2022) 161805.
- [154] K. Van Tilburg, *Stellar basins of gravitationally bound particles*, *Phys. Rev. D* **104** (2021) 023019 [[2006.12431](#)].
- [155] A. Ayala, I. Domínguez, M. Giannotti, A. Mirizzi and O. Straniero, *Revisiting the bound on axion-photon coupling from Globular Clusters*, *Phys. Rev. Lett.* **113** (2014) 191302 [[1406.6053](#)].
- [156] M. J. Dolan, F. J. Hiskens and R. R. Volkas, *Advancing globular cluster constraints on the axion-photon coupling*, *JCAP* **10** (2022) 096 [[2207.03102](#)].
- [157] M. M. Bertolami, B. Melendez, L. Althaus and J. Isern, *Revisiting the axion bounds from the galactic white dwarf luminosity function*, *Journal of Cosmology and Astroparticle Physics* **2014** (2014) 069.
- [158] J. Isern, S. Catalán, E. García-Berro and S. Torres, *Axions and the white dwarf luminosity function*, *Journal of Physics: Conference Series* **172** (2009) 012005.
- [159] A. H. Córsico, L. G. Althaus, M. M. Miller Bertolami and S. O. Kepler, *Pulsating white dwarfs: new insights*, *Astron. Astrophys. Rev.* **27** (2019) 7 [[1907.00115](#)].
- [160] C. Dessert, A. J. Long and B. R. Safdi, *No Evidence for Axions from Chandra Observation of the Magnetic White Dwarf RE J0317-853*, *Phys. Rev. Lett.* **128** (2022) 071102 [[2104.12772](#)].
- [161] C. Dessert, A. J. Long and B. R. Safdi, *X-ray Signatures of Axion Conversion in Magnetic White Dwarf Stars*, *Phys. Rev. Lett.* **123** (2019) 061104 [[1903.05088](#)].
- [162] C. Dessert, D. Dunsky and B. R. Safdi, *Upper limit on the axion-photon coupling from magnetic*

- white dwarf polarization, *Phys. Rev. D* **105** (2022) 103034 [2203.04319].
- [163] O. Ning, C. Dessert, V. Hong and B. R. Safdi, *Search for Axions from Magnetic White Dwarfs with Chandra*, [2411.05041](#).
- [164] M. S. Turner, *Axions from sn1987a*, *Phys. Rev. Lett.* **60** (1988) 1797.
- [165] G. G. Raffelt, *Astrophysical axion bounds*, *Lect. Notes Phys.* **741** (2008) 51 [hep-ph/0611350].
- [166] J. H. Chang, R. Essig and S. D. McDermott, *Supernova 1987A Constraints on Sub-GeV Dark Sectors, Millicharged Particles, the QCD Axion, and an Axion-like Particle*, *JHEP* **09** (2018) 051 [1803.00993].
- [167] P. Carena, T. Fischer, M. Giannotti, G. Guo, G. Martínez-Pinedo and A. Mirizzi, *Improved axion emissivity from a supernova via nucleon-nucleon bremsstrahlung*, *JCAP* **10** (2019) 016 [1906.11844].
- [168] P. Carena, B. Fore, M. Giannotti, A. Mirizzi and S. Reddy, *Enhanced Supernova Axion Emission and its Implications*, *Phys. Rev. Lett.* **126** (2021) 071102 [2010.02943].
- [169] D. Page, M. V. Beznogov, I. Garibay, J. M. Lattimer, M. Prakash and H.-T. Janka, *NS 1987A in SN 1987A*, *Astrophys. J.* **898** (2020) 125 [2004.06078].
- [170] C. Fransson, M. Barlow, P. Kavanagh, J. Larsson, O. Jones, B. Sargent et al., *Emission lines due to ionizing radiation from a compact object in the remnant of supernova 1987a*, *Science* **383** (2024) 898.
- [171] L. B. Leinson, *Axion mass limit from observations of the neutron star in Cassiopeia A*, *JCAP* **08** (2014) 031 [1405.6873].
- [172] K. Hamaguchi, N. Nagata, K. Yanagi and J. Zheng, *Limit on the Axion Decay Constant from the Cooling Neutron Star in Cassiopeia A*, *Phys. Rev. D* **98** (2018) 103015 [1806.07151].
- [173] B. Posselt and G. G. Pavlov, *Upper limits on the rapid cooling of the Central Compact Object in Cas A*, *Astrophys. J.* **864** (2018) 135 [1808.00531].
- [174] M. V. Beznogov, E. Rrapaj, D. Page and S. Reddy, *Constraints on Axion-like Particles and Nucleon Pairing in Dense Matter from the Hot Neutron Star in HESS J1731-347*, *Phys. Rev. C* **98** (2018) 035802 [1806.07991].
- [175] M. Buschmann, C. Dessert, J. W. Foster, A. J. Long and B. R. Safdi, *Upper Limit on the QCD Axion Mass from Isolated Neutron Star Cooling*, *Phys. Rev. Lett.* **128** (2022) 091102 [2111.09892].
- [176] A. Hook, Y. Kahn, B. R. Safdi and Z. Sun, *Radio Signals from Axion Dark Matter Conversion in Neutron Star Magnetospheres*, *Phys. Rev. Lett.* **121** (2018) 241102 [1804.03145].
- [177] F. P. Huang, K. Kadota, T. Sekiguchi and H. Tashiro, *Radio telescope search for the resonant conversion of cold dark matter axions from the magnetized astrophysical sources*, *Phys. Rev. D* **97** (2018) 123001 [1803.08230].
- [178] M. S. Pshirkov and S. B. Popov, *Conversion of Dark matter axions to photons in magnetospheres of neutron stars*, *J. Exp. Theor. Phys.* **108** (2009) 384 [0711.1264].
- [179] S. J. Witte, D. Noordhuis, T. D. P. Edwards and C. Weniger, *Axion-photon conversion in neutron star magnetospheres: The role of the plasma in the Goldreich-Julian model*, *Phys. Rev. D* **104** (2021) 103030 [2104.07670].
- [180] A. J. Millar, S. Baum, M. Lawson and M. D. Marsh, *Axion-photon conversion in strongly magnetised plasmas*, *Journal of Cosmology and Astroparticle Physics* **2021** (2021) 013 [2107.07399].
- [181] J. W. Foster, Y. Kahn, O. Macias, Z. Sun, R. P. Eatough, V. I. Kondratiev et al., *Green Bank and Effelsberg Radio Telescope Searches for Axion Dark Matter Conversion in Neutron Star Magnetospheres*, *Phys. Rev. Lett.* **125** (2020) 171301 [2004.00011].
- [182] J. W. Foster, S. J. Witte, M. Lawson, T. Linden, V. Gajjar, C. Weniger et al., *Extraterrestrial Axion Search with the Breakthrough Listen Galactic Center Survey*, *Phys. Rev. Lett.* **129** (2022) 251102 [2202.08274].
- [183] R. A. Battye, M. J. Keith, J. I. McDonald, S. Srinivasan, B. W. Stappers and P. Weltevrede, *Searching for time-dependent axion dark matter signals in pulsars*, *Phys. Rev. D* **108** (2023)

- 063001 [2303.11792].
- [184] D. Noordhuis, A. Prabhu, S. J. Witte, A. Y. Chen, F. Cruz and C. Weniger, *Novel Constraints on Axions Produced in Pulsar Polar-Cap Cascades*, *Phys. Rev. Lett.* **131** (2023) 111004 [2209.09917].
- [185] D. Noordhuis, A. Prabhu, C. Weniger and S. J. Witte, *Axion Clouds around Neutron Stars*, *Phys. Rev. X* **14** (2024) 041015 [2307.11811].
- [186] R. Balkin, J. Serra, K. Springmann, S. Stelzl and A. Weiler, *White dwarfs as a probe of exceptionally light QCD axions*, *Phys. Rev. D* **109** (2024) 095032 [2211.02661].
- [187] J. Huang, M. C. Johnson, L. Sagunski, M. Sakellariadou and J. Zhang, *Prospects for axion searches with Advanced LIGO through binary mergers*, *Phys. Rev. D* **99** (2019) 063013 [1807.02133].
- [188] R. Balkin, J. Serra, K. Springmann, S. Stelzl and A. Weiler, *Heavy neutron stars from light scalars*, **2307.14418**.
- [189] A. Gómez-Bañón, K. Bartnick, K. Springmann and J. A. Pons, *Constraining Light QCD Axions with Isolated Neutron Star Cooling*, *Phys. Rev. Lett.* **133** (2024) 251002 [2408.07740].
- [190] J. Zhang, Z. Lyu, J. Huang, M. C. Johnson, L. Sagunski, M. Sakellariadou et al., *First Constraints on Nuclear Coupling of Axionlike Particles from the Binary Neutron Star Gravitational Wave Event GW170817*, *Phys. Rev. Lett.* **127** (2021) 161101 [2105.13963].
- [191] A. Arvanitaki and S. Dubovsky, *Exploring the String Axiverse with Precision Black Hole Physics*, *Phys. Rev.* **D83** (2011) 044026 [1004.3558].
- [192] P. Pani, V. Cardoso, L. Gualtieri, E. Berti and A. Ishibashi, *Perturbations of slowly rotating black holes: massive vector fields in the Kerr metric*, *Phys. Rev.* **D86** (2012) 104017 [1209.0773].
- [193] M. Baryakhtar, R. Lasenby and M. Teo, *Black Hole Superradiance Signatures of Ultralight Vectors*, *Phys. Rev.* **D96** (2017) 035019 [1704.05081].
- [194] W. E. East and F. Pretorius, *Superradiant Instability and Backreaction of Massive Vector Fields around Kerr Black Holes*, *Phys. Rev. Lett.* **119** (2017) 041101 [1704.04791].
- [195] W. E. East, *Superradiant instability of massive vector fields around spinning black holes in the relativistic regime*, *Phys. Rev. D* **96** (2017) 024004 [1705.01544].
- [196] M. Baryakhtar, M. Galanis, R. Lasenby and O. Simon, *Black hole superradiance of self-interacting scalar fields*, *Phys. Rev. D* **103** (2021) 095019 [2011.11646].
- [197] R. Brito, S. Grillo and P. Pani, *Black Hole Superradiant Instability from Ultralight Spin-2 Fields*, *Phys. Rev. Lett.* **124** (2020) 211101 [2002.04055].
- [198] R. Brito, V. Cardoso and P. Pani, *Superradiance*, *Lect. Notes Phys.* **906** (2015) pp.1 [1501.06570].
- [199] A. Arvanitaki, M. Baryakhtar and X. Huang, *Discovering the QCD Axion with Black Holes and Gravitational Waves*, *Phys. Rev.* **D91** (2015) 084011 [1411.2263].
- [200] V. M. Mehta, M. Demirtas, C. Long, D. J. E. Marsh, L. Mcallister and M. J. Stott, *Superradiance Exclusions in the Landscape of Type IIB String Theory*, **2011.08693**.
- [201] S. Hoof, D. J. E. Marsh, J. Sisk-Reynés, J. H. Matthews and C. Reynolds, *Getting More Out of Black Hole Superradiance: a Statistically Rigorous Approach to Ultralight Boson Constraints*, **2406.10337**.
- [202] V. Dergachev and M. A. Papa, *Sensitivity Improvements in the Search for Periodic Gravitational Waves Using O1 LIGO Data*, *Physical Review Letters* **123** (2019) 101101.
- [203] V. Dergachev and M. A. Papa, *Results from an Extended Falcon All-Sky Survey for Continuous Gravitational Waves*, *Phys. Rev. D* **101** (2020) 022001 [1909.09619].
- [204] C. Palomba et al., *Direct constraints on ultra-light boson mass from searches for continuous gravitational waves*, *Phys. Rev. Lett.* **123** (2019) 171101 [1909.08854].
- [205] S. J. Zhu, M. Baryakhtar, M. A. Papa, D. Tsuna, N. Kawanaka and H.-B. Eggenstein, *Characterizing the continuous gravitational-wave signal from boson clouds around Galactic isolated black holes*, *Phys. Rev. D* **102** (2020) 063020 [2003.03359].

- [206] A. Arvanitaki, M. Baryakhtar, S. Dimopoulos, S. Dubovsky and R. Lasenby, *Black Hole Mergers and the QCD Axion at Advanced LIGO*, *Phys. Rev. D* **95** (2017) 043001 [[1604.03958](#)].
- [207] K. K. Y. Ng, O. A. Hannuksela, S. Vitale and T. G. F. Li, *Searching for ultralight bosons within spin measurements of a population of binary black hole mergers*, *Phys. Rev. D* **103** (2021) 063010 [[1908.02312](#)].
- [208] K. K. Y. Ng, S. Vitale, O. A. Hannuksela and T. G. F. Li, *Constraints on Ultralight Scalar Bosons within Black Hole Spin Measurements from the LIGO-Virgo GWTC-2*, *Phys. Rev. Lett.* **126** (2021) 151102 [[2011.06010](#)].
- [209] M. J. Stott and D. J. E. Marsh, *Black hole spin constraints on the mass spectrum and number of axionlike fields*, *Phys. Rev. D* **98** (2018) 083006 [[1805.02016](#)].
- [210] V. Cardoso, O. J. C. Dias, G. S. Hartnett, M. Middleton, P. Pani and J. E. Santos, *Constraining the mass of dark photons and axion-like particles through black-hole superradiance*, *JCAP* **03** (2018) 043 [[1801.01420](#)].
- [211] P. Du, D. Egana-Ugrinovic, R. Essig, G. Fragione and R. Perna, *Searching for ultra-light bosons and constraining black hole spin distributions with stellar tidal disruption events*, *Nature Commun.* **13** (2022) 4626 [[2202.01215](#)].
- [212] S. Ghosh, E. Berti, R. Brito and M. Richartz, *Follow-up signals from superradiant instabilities of black hole merger remnants*, *Phys. Rev. D* **99** (2019) 104030 [[1812.01620](#)].
- [213] K. Riles, *Searches for continuous-wave gravitational radiation*, *Living Rev. Rel.* **26** (2023) 3 [[2206.06447](#)].
- [214] R. Brito, S. Ghosh, E. Barausse, E. Berti, V. Cardoso, I. Dvorkin et al., *Stochastic and resolvable gravitational waves from ultralight bosons*, *Phys. Rev. Lett.* **119** (2017) 131101 [[1706.05097](#)].
- [215] R. Brito, S. Ghosh, E. Barausse, E. Berti, V. Cardoso, I. Dvorkin et al., *Gravitational wave searches for ultralight bosons with LIGO and LISA*, *Phys. Rev. D* **96** (2017) 064050 [[1706.06311](#)].
- [216] L. Tsukada, T. Callister, A. Matas and P. Meyers, *First search for a stochastic gravitational-wave background from ultralight bosons*, *Phys. Rev. D* **99** (2019) 103015 [[1812.09622](#)].
- [217] LIGO SCIENTIFIC, VIRGO, KAGRA collaboration, *All-sky search for gravitational wave emission from scalar boson clouds around spinning black holes in ligo o3 data*, *Physical Review D* **105** (2022) [[2111.15507](#)].
- [218] M. Isi, L. Sun, R. Brito and A. Melatos, *Directed searches for gravitational waves from ultralight bosons*, *Phys. Rev. D* **99** (2019) 084042 [[1810.03812](#)].
- [219] D. Jones, L. Sun, N. Siemonsen, W. E. East, S. M. Scott and K. Wette, *Methods and prospects for gravitational-wave searches targeting ultralight vector-boson clouds around known black holes*, *Phys. Rev. D* **108** (2023) 064001 [[2305.00401](#)].
- [220] D. Baumann, H. S. Chia and R. A. Porto, *Probing Ultralight Bosons with Binary Black Holes*, *Phys. Rev. D* **99** (2019) 044001 [[1804.03208](#)].
- [221] O. A. Hannuksela, K. W. K. Wong, R. Brito, E. Berti and T. G. F. Li, *Probing the existence of ultralight bosons with a single gravitational-wave measurement*, *Nature Astron.* **3** (2019) 447 [[1804.09659](#)].
- [222] D. Baumann, G. Bertone, J. Stout and G. M. Tomaselli, *Ionization of gravitational atoms*, *Phys. Rev. D* **105** (2022) 115036 [[2112.14777](#)].
- [223] D. Baumann, G. Bertone, J. Stout and G. M. Tomaselli, *Sharp Signals of Boson Clouds in Black Hole Binary Inspirals*, *Phys. Rev. Lett.* **128** (2022) 221102 [[2206.01212](#)].
- [224] V. Cardoso, S. Chakrabarti, P. Pani, E. Berti and L. Gualtieri, *Floating and sinking: The Imprint of massive scalars around rotating black holes*, *Phys. Rev. Lett.* **107** (2011) 241101 [[1109.6021](#)].
- [225] J. Zhang and H. Yang, *Gravitational floating orbits around hairy black holes*, *Phys. Rev. D* **99** (2019) 064018 [[1808.02905](#)].

- [226] J. Zhang and H. Yang, *Dynamic Signatures of Black Hole Binaries with Superradiant Clouds*, *Phys. Rev. D* **101** (2020) 043020 [[1907.13582](#)].
- [227] E. Payne, L. Sun, K. Kremer, P. D. Lasky and E. Thrane, *The Imprint of Superradiance on Hierarchical Black Hole Mergers*, *Astrophys. J.* **931** (2022) 79 [[2107.11730](#)].
- [228] H. Yoshino and H. Kodama, *Bosenova collapse of axion cloud around a rotating black hole*, *Prog. Theor. Phys.* **128** (2012) 153 [[1203.5070](#)].
- [229] A. Gruzinov, *Black Hole Spindown by Light Bosons*, [1604.06422](#).
- [230] H. Omiya, T. Takahashi, T. Tanaka and H. Yoshino, *Impact of multiple modes on the evolution of self-interacting axion condensate around rotating black holes*, *JCAP* **06** (2023) 016 [[2211.01949](#)].
- [231] S. Collaviti, L. Sun, M. Galanis and M. Baryakhtar, *Observational prospects of self-interacting scalar superradiance with next-generation gravitational-wave detectors*, *Class. Quant. Grav.* **42** (2025) 025006 [[2407.04304](#)].
- [232] H. Omiya, T. Takahashi, T. Tanaka and H. Yoshino, *Deci-Hz gravitational waves from the self-interacting axion cloud around a rotating stellar mass black hole*, *Phys. Rev. D* **110** (2024) 044002 [[2404.16265](#)].
- [233] M. P. Hertzberg and E. D. Schiappacasse, *Scalar dark matter clumps with angular momentum*, *JCAP* **08** (2018) 028 [[1804.07255](#)].
- [234] S. Sen, *Plasma effects on lasing of a uniform ultralight axion condensate*, *Phys. Rev. D* **98** (2018) 103012 [[1805.06471](#)].
- [235] J. W. Foster, N. L. Rodd and B. R. Safdi, *Revealing the Dark Matter Halo with Axion Direct Detection*, *Phys. Rev. D* **97** (2018) 123006 [[1711.10489](#)].
- [236] J. E. Kim, *Light pseudoscalars, particle physics and cosmology*, *Physics Reports* **150** (1987) 1.
- [237] H.-Y. Cheng, *The strong cp problem revisited*, *Physics Reports* **158** (1988) 1.
- [238] L. J. Rosenberg and K. A. van Bibber, *Searches for invisible axions*, *Physics Reports* **325** (2000) 1.
- [239] NOMAD collaboration, *Search for eV (pseudo)scalar penetrating particles in the SPS neutrino beam*, *Phys. Lett. B* **479** (2000) 371.
- [240] J. Jaeckel and M. Spannowsky, *Probing MeV to 90 GeV axion-like particles with LEP and LHC*, *Phys. Lett. B* **753** (2016) 482 [[1509.00476](#)].
- [241] S. Knapen, T. Lin, H. K. Lou and T. Melia, *Searching for Axionlike Particles with Ultraperipheral Heavy-Ion Collisions*, *Phys. Rev. Lett.* **118** (2017) 171801 [[1607.06083](#)].
- [242] CMS collaboration, *Evidence for light-by-light scattering and searches for axion-like particles in ultraperipheral PbPb collisions at $\sqrt{s_{NN}} = 5.02$ TeV*, *Phys. Lett. B* **797** (2019) 134826 [[1810.04602](#)].
- [243] D. Aloni, C. Fanelli, Y. Soreq and M. Williams, *Photoproduction of Axionlike Particles*, *Phys. Rev. Lett.* **123** (2019) 071801 [[1903.03586](#)].
- [244] ATLAS collaboration, *Measurement of light-by-light scattering and search for axion-like particles with 2.2 nb^{-1} of Pb+Pb data with the ATLAS detector*, *JHEP* **03** (2021) 243 [[2008.05355](#)].
- [245] NA64 collaboration, *Search for Axionlike and Scalar Particles with the NA64 Experiment*, *Phys. Rev. Lett.* **125** (2020) 081801 [[2005.02710](#)].
- [246] F. Capozzi, B. Dutta, G. Gurung, W. Jang, I. M. Shoemaker, A. Thompson et al., *New constraints on ALP couplings to electrons and photons from ArgoNeuT and the MiniBooNE beam dump*, *Phys. Rev. D* **108** (2023) 075019 [[2307.03878](#)].
- [247] BESIII collaboration, *Search for diphoton decays of an axionlike particle in radiative J/ψ decays*, *Phys. Rev. D* **110** (2024) L031101 [[2404.04640](#)].
- [248] F. Reines, H. S. Gurr and H. W. Sobel, *Detection of $\bar{\nu}_e - e$ scattering*, *Phys. Rev. Lett.* **37** (1976) 315.
- [249] F. Reines, H. W. Sobel and H. S. Gurr, *Stability of the neutrino*, *Phys. Rev. Lett.* **32** (1974) 180.
- [250] T. W. Donnelly, S. J. Freedman, R. S. Lytel, R. D. Peccei and M. Schwartz, *Do axions exist?*

- Phys. Rev. D* **18** (1978) 1607.
- [251] P. Bosetti, H. Deden, M. Deutschmann, P. Fritze, H. Grässler, W. Krenz et al., *Observation of prompt neutrinos from 400 gev proton-nucleus collisions*, *Physics Letters B* **74** (1978) 143.
- [252] A. F. Rothenberg, *A Search for Unknown Sources of Neutrino Like Particles*, Stanford University, Ph.D. thesis, 1972.
- [253] A. F. Rothenberg, "SLAC report SLAC-R-0147: A Search for Unknown Sources of Neutrino-Like Particles." 1972.
- [254] A. F. Rothenberg, "Stanford University, Physics Department report RX-1311." 1972.
- [255] B. Kim and C. Stamm, *Axion production in high-energy proton-nucleon scattering and an estimate of its mass*, *Physics Letters B* **105** (1981) 55.
- [256] P. Alibrán, N. Armenise, R. Arnold, J. Bartley, E. Bellotti, D. Bertrand et al., *Observation of an excess of ν_e , $\$nu_e\$ events in a beam dump experiment at 400 gev$* , *Physics Letters B* **74** (1978) 134.
- [257] T. Hansl, M. Holder, J. Knobloch, J. May, H. Paar, P. Palazzi et al., *Results of a beam dump experiment at the cern sps neutrino facility*, *Physics Letters B* **74** (1978) 139.
- [258] T. Cowan, H. Backe, K. Bethge, H. Bokemeyer, H. Folger, J. S. Greenberg et al., *Observation of correlated narrow-peak structures in positron and electron spectra from superheavy collision systems*, *Phys. Rev. Lett.* **56** (1986) 444.
- [259] G. Taubes, *The one that got away?*, *Science* **275** (1997) 148
[<https://www.science.org/doi/pdf/10.1126/science.275.5297.148>].
- [260] E. M. Riordan, M. W. Krasny, K. Lang, P. de Barbaro, A. Bodek, S. Dasu et al., *Search for short-lived axions in an electron-beam-dump experiment*, *Phys. Rev. Lett.* **59** (1987) 755.
- [261] C. Han, M. L. López-Ibáñez, A. Melis, O. Vives and J. M. Yang, *Anomaly-free leptophilic axionlike particle and its flavor violating tests*, *Phys. Rev. D* **103** (2021) 035028.
- [262] J. D. Bjorken, S. Ecklund, W. R. Nelson, A. Abashian, C. Church, B. Lu et al., *Search for neutral metastable penetrating particles produced in the slac beam dump*, *Phys. Rev. D* **38** (1988) 3375.
- [263] M. Sivertz, J. Lee-Franzini, J. E. Horstkotte, C. Klopfenstein, R. D. Schamberger, L. J. Spencer et al., *Upper limit for axion production in radiative Υ decay*, *Phys. Rev. D* **26** (1982) 717.
- [264] M. S. Alam, S. E. Csorna, A. Fridman, L. Garren, M. D. Mestayer, R. S. Panvini et al., *Search for axion production in Υ decay*, *Phys. Rev. D* **27** (1983) 1665.
- [265] C. Edwards, R. Partridge, C. Peck, F. C. Porter, D. Antreasyan, Y. F. Gu et al., *Upper limit for $\frac{J}{\Psi} \rightarrow \gamma + axion$* , *Phys. Rev. Lett.* **48** (1982) 903.
- [266] B. Niczyporuk, Z. Jakubowski, T. Żeludziejewicz, G. Folger, B. Lurz, H. Vogel et al., *Experimental upper limits for hadronic and axion decays of the $\gamma(1s)$* , *Zeitschrift für Physik C Particles and Fields* **17** (1983) 197.
- [267] G. Mageras, P. Franzini, P. M. Tuts, S. Youssef, T. Zhao, J. Lee-Franzini et al., *Search for light short-lived particles in radiative upsilon decays*, *Phys. Rev. Lett.* **56** (1986) 2672.
- [268] T. Bowcock, R. T. Giles, J. Hassard, K. Kinoshita, F. M. Pipkin, R. Wilson et al., *Upper limits for the production of light short-lived neutral particles in radiative Υ decay*, *Phys. Rev. Lett.* **56** (1986) 2676.
- [269] P. Sikivie, *Experimental tests of the "invisible" axion*, *Phys. Rev. Lett.* **51** (1983) 1415.
- [270] P. Sikivie, *Experimental tests of the "invisible" axion - correction*, *Phys. Rev. Lett.* **52** (1984) 695.
- [271] L. Krauss, J. Moody, F. Wilczek and D. E. Morris, *Calculations for Cosmic Axion Detection*, *Phys. Rev. Lett.* **55** (1985) 1797.
- [272] P. Sikivie, *Detection Rates for 'Invisible' Axion Searches*, *Phys. Rev. D* **32** (1985) 2988.
- [273] E. I. Gates, G. Gyuk and M. S. Turner, *The local halo density*, *The Astrophysical Journal* **449** (1995) L123.
- [274] P. F. de Salas and A. Widmark, *Dark matter local density determination: recent observations and future prospects*, *Reports on Progress in Physics* **84** (2021) 104901.

- [275] S. De Panfilis, A. C. Melissinos, B. E. Moskowitz, J. T. Rogers, Y. K. Semertzidis, W. Wuensch et al., *Limits on the Abundance and Coupling of Cosmic Axions at $4.5\text{-Microev} < m(a) < 5.0\text{-Microev}$* , *Phys. Rev. Lett.* **59** (1987) 839.
- [276] C. Hagmann, P. Sikivie, N. S. Sullivan and D. B. Tanner, *Results from a search for cosmic axions*, *Phys. Rev. D* **42** (1990) 1297.
- [277] R. Khatiwada, D. Bowring, A. S. Chou, A. Sonnenschein, W. Wester, D. V. Mitchell et al., *Axion dark matter experiment: Detailed design and operations*, *Review of Scientific Instruments* **92** (2021) 124502 [<https://doi.org/10.1063/5.0037857>].
- [278] A. K. Yi, S. Ahn, c. Kutlu, J. Kim, B. R. Ko, B. I. Ivanov et al., *Axion dark matter search around $4.55 \mu\text{eV}$ with dine-fischler-srednicki-zhitnitskii sensitivity*, *Phys. Rev. Lett.* **130** (2023) 071002.
- [279] L. Zhong, S. Al Kenany, K. M. Backes, B. M. Brubaker, S. B. Cahn, G. Carosi et al., *Results from phase 1 of the haystac microwave cavity axion experiment*, *Phys. Rev. D* **97** (2018) 092001.
- [280] A. Quiskamp, B. T. McAllister, P. Altin, E. N. Ivanov, M. Goryachev and M. E. Tobar, *Direct search for dark matter axions excluding alpogenesis in the $63\text{- to }67\text{-}\mu\text{eV}$ range with the organ experiment*, *Science Advances* **8** (2022) eabq3765 [<https://www.science.org/doi/pdf/10.1126/sciadv.abq3765>].
- [281] D. Alesini, C. Braggio, G. Carugno, N. Crescini, D. D'Agostino, D. Di Gioacchino et al., *Search for invisible axion dark matter of mass $m_a = 43\mu\text{eV}$ with the quax- a_γ experiment*, *Phys. Rev. D* **103** (2021) 102004.
- [282] J. L. Ouellet, C. P. Salemi, J. W. Foster, R. Henning, Z. Bogorad, J. M. Conrad et al., *First results from abracadabra-10 cm: A search for sub- μeV axion dark matter*, *Phys. Rev. Lett.* **122** (2019) 121802.
- [283] S. DePanfilis, A. C. Melissinos, B. E. Moskowitz, J. T. Rogers, Y. K. Semertzidis, W. U. Wuensch et al., *Limits on the abundance and coupling of cosmic axions at $4.5 < m_a < 5.0\mu\text{eV}$* , *Phys. Rev. Lett.* **59** (1987) 839.
- [284] C. B. Adams et al., *Axion Dark Matter*, in *Snowmass 2021*, 3, 2022, **2203.14923**.
- [285] DMRADIO COLLABORATION collaboration, *Projected sensitivity of dmradio- m^3 : A search for the qcd axion below $1\mu\text{eV}$* , *Phys. Rev. D* **106** (2022) 103008.
- [286] P. Brun, , A. Caldwell, L. Chevalier, G. Dvali, P. Freire et al., *A new experimental approach to probe QCD axion dark matter in the mass range above $40 \mu\text{eV}$* , *The European Physical Journal C* **79** (2019) .
- [287] C. Hagmann, D. Kinion, W. Stoeffl, K. van Bibber, E. Daw, H. Peng et al., *Results from a high-sensitivity search for cosmic axions*, *Phys. Rev. Lett.* **80** (1998) 2043.
- [288] W. Heitler, *The Quantum Theory of Radiation*. Oxford University Press, Oxford, UK, 1954.
- [289] M.-O. André, M. Mück, J. Clarke, J. Gail and C. Heiden, *Radio-frequency amplifier with tenth-kelvin noise temperature based on a microstrip direct current superconducting quantum interference device*, *Applied Physics Letters* **75** (1999) 698 [https://pubs.aip.org/aip/apl/article-pdf/75/5/698/10181781/698_1_online.pdf].
- [290] S. J. Asztalos, G. Carosi, C. Hagmann, D. Kinion, K. van Bibber, M. Hotz et al., *Squid-based microwave cavity search for dark-matter axions*, *Phys. Rev. Lett.* **104** (2010) 041301.
- [291] ADMX COLLABORATION collaboration, *Search for invisible axion dark matter with the axion dark matter experiment*, *Phys. Rev. Lett.* **120** (2018) 151301.
- [292] ADMX COLLABORATION collaboration, *Axion dark matter experiment: Run 1b analysis details*, *Phys. Rev. D* **103** (2021) 032002.
- [293] *Searching for the dark: The hunt for axions*, *Scientific American* **318** (2018) 50.
- [294] E. Lentz, T. Quinn, L. Rosenberg, Leslie and M. Tremmel, *A new signal model for axion cavity searches from n -body simulations*, *The Astrophysical Journal* **845** (2017) .
- [295] ADMX COLLABORATION collaboration, *Search for invisible axion dark matter in the $3.3 - 4.2 \mu\text{eV}$ mass range*, *Phys. Rev. Lett.* **127** (2021) 261803.

- [296] O. Kwon, D. Lee, W. Chung, D. Ahn, H. Byun, F. Caspers et al., *First results from an axion haloscope at capp around 10.7 μeV* , *Phys. Rev. Lett.* **126** (2021) 191802.
- [297] S. Ahn, J. Kim, B. I. Ivanov, O. Kwon, H. Byun, A. F. van Loo et al., *Extensive search for axion dark matter over 1 ghz with capp's main axion experiment*, *Phys. Rev. X* **14** (2024) 031023.
- [298] A. K. Yi, S. Ahn, c. Kutlu, J. Kim, B. R. Ko, B. I. Ivanov et al., *Axion dark matter search around 4.55 μeV with dine-fischler-srednicki-zhitnitskii sensitivity*, *Phys. Rev. Lett.* **130** (2023) 071002.
- [299] J. Jeong, S. Youn, S. Bae, J. Kim, T. Seong, J. E. Kim et al., *Search for invisible axion dark matter with a multiple-cell haloscope*, *Phys. Rev. Lett.* **125** (2020) 221302.
- [300] K. M. Backes, D. A. Palken, S. A. Kenany, B. M. Brubaker, S. B. Cahn, A. Droster et al., *A quantum enhanced search for dark matter axions*, *Nature* **590** (2021) 238 [2008.01853].
- [301] B. M. Brubaker et al., *First results from a microwave cavity axion search at 24 μeV* , *Phys. Rev. Lett.* **118** (2017) 061302 [1610.02580].
- [302] HAYSTAC collaboration, *New results from HAYSTAC's phase II operation with a squeezed state receiver*, *Phys. Rev. D* **107** (2023) 072007 [2301.09721].
- [303] A. Álvarez Melcón, S. Arguedas Cuendis, J. Baier, K. Barth, H. Bräuninger, S. Calatroni et al., *First results of the cast-rades haloscope search for axions at 34.67 μeV* , *Journal of High Energy Physics* **2021** (2021) 75.
- [304] R. Barbieri, C. Braggio, G. Carugno, C. S. Gallo, A. Lombardi, A. Ortolan et al., *Searching for galactic axions through magnetized media: the QUAX proposal*, *Phys. Dark Univ.* **15** (2017) 135 [1606.02201].
- [305] N. Crescini, D. Alesini, C. Braggio, G. Carugno, D. Di Gioacchino, C. S. Gallo et al., *Operation of a ferromagnetic axion haloscope at $m_a = 58\mu\text{ eV}$* , *The European Physical Journal C* **78** (2018) 703.
- [306] QUAX COLLABORATION collaboration, *Axion search with a quantum-limited ferromagnetic haloscope*, *Phys. Rev. Lett.* **124** (2020) 171801.
- [307] QUAX COLLABORATION collaboration, *Search for axion dark matter with the quax-lnf tunable haloscope*, *Phys. Rev. D* **110** (2024) 022008.
- [308] Y. Lee, B. Yang, H. Yoon, M. Ahn, H. Park, B. Min et al., *Searching for invisible axion dark matter with an 18 t magnet haloscope*, *Phys. Rev. Lett.* **128** (2022) 241805.
- [309] H. Yoon, M. Ahn, B. Yang, Y. Lee, D. Kim, H. Park et al., *Axion haloscope using an 18 t high temperature superconducting magnet*, *Phys. Rev. D* **106** (2022) 092007.
- [310] R. Gupta, M. Anerella, J. Cozzolino, P. Joshi, S. Joshi, S. Plate et al., *Status of the 25 t, 100 mm bore hts solenoid for an axion dark matter search experiment*, *IEEE Transactions on Applied Superconductivity* **29** (2019) 1.
- [311] S. Hahn, K. Kim, K. Kim, X. Hu, T. Painter, I. Dixon et al., *45.5-tesla direct-current magnetic field generated with a high-temperature superconducting magnet*, *Nature* **570** (2019) 496.
- [312] C. M. Caves, *Quantum limits on noise in linear amplifiers*, *Phys. Rev. D* **26** (1982) 1817.
- [313] S. K. Lamoreaux, K. A. van Bibber, K. W. Lehnert and G. Carosi, *Analysis of single-photon and linear amplifier detectors for microwave cavity dark matter axion searches*, *Phys. Rev. D* **88** (2013) 035020.
- [314] H. Zheng, M. Silveri, R. T. Brierley, S. M. Girvin and K. W. Lehnert, *Accelerating dark-matter axion searches with quantum measurement technology*, 2016.
- [315] A. V. Dixit, S. Chakram, K. He, A. Agrawal, R. K. Naik, D. I. Schuster et al., *Searching for Dark Matter with a Superconducting Qubit*, *Phys. Rev. Lett.* **126** (2021) 141302 [2008.12231].
- [316] K. Wurtz, B. Brubaker, Y. Jiang, E. Ruddy, D. Palken and K. Lehnert, *Cavity entanglement and state swapping to accelerate the search for axion dark matter*, *PRX Quantum* **2** (2021) 040350.
- [317] S. Posen, M. Checchin, O. S. Melnychuk, T. Ring, I. Gonin and T. Khabiboulline, *Measurement of High Quality Factor Superconducting Cavities in Tesla-Scale Magnetic Fields for Dark-Matter Searches*, *Phys. Rev. Applied* **20** (2023) 034004 [2201.10733].

- [318] D. Ahn, O. Kwon, W. Chung, W. Jang, D. Lee, J. Lee et al., *Biaxially Textured $YBa_2Cu_3O_{7-x}$ Microwave Cavity in a High Magnetic Field for a Dark-Matter Axion Search*, *Phys. Rev. Applied* **17** (2022) L061005 [2103.14515].
- [319] D. Ahn, O. Kwon, W. Chung, W. Jang, D. Lee, J. Lee et al., *Maintaining high Q -factor of superconducting $YBa_2Cu_3O_{7-x}$ microwave cavity in a high magnetic field*, 1904.05111.
- [320] R. Cervantes et al., *Search for 70 μ eV Dark Photon Dark Matter with a Dielectrically Loaded Multiwavelength Microwave Cavity*, *Phys. Rev. Lett.* **129** (2022) 201301 [2204.03818].
- [321] R. Cervantes et al., *ADMX-Orpheus first search for 70 μ eV dark photon dark matter: Detailed design, operations, and analysis*, *Phys. Rev. D* **106** (2022) 102002 [2204.09475].
- [322] M. Baryakhtar, J. Huang and R. Lasenby, *Axion and hidden photon dark matter detection with multilayer optical haloscopes*, *Phys. Rev. D* **98** (2018) 035006.
- [323] J. Chiles et al., *New Constraints on Dark Photon Dark Matter with Superconducting Nanowire Detectors in an Optical Haloscope*, *Phys. Rev. Lett.* **128** (2022) 231802 [2110.01582].
- [324] M. Lawson, A. J. Millar, M. Pancaldi, E. Vitagliano and F. Wilczek, *Tunable axion plasma haloscopes*, *Phys. Rev. Lett.* **123** (2019) 141802.
- [325] ALPHA collaboration, *Searching for dark matter with plasma haloscopes*, *Phys. Rev. D* **107** (2023) 055013 [2210.00017].
- [326] MADMAX WORKING GROUP collaboration, *Dielectric Haloscopes: A New Way to Detect Axion Dark Matter*, *Phys. Rev. Lett.* **118** (2017) 091801 [1611.05865].
- [327] B. A. dos Santos Garcia, D. Bergermann, A. Caldwell, V. Dabhi, C. Diaconu, J. Diehl et al., *First search for axion dark matter with a madmax prototype*, 2024.
- [328] P. Sikivie, N. Sullivan and D. B. Tanner, *Proposal for axion dark matter detection using an lc circuit*, *Phys. Rev. Lett.* **112** (2014) 131301.
- [329] S. Chaudhuri, P. W. Graham, K. Irwin, J. Mardon, S. Rajendran and Y. Zhao, *Radio for hidden-photon dark matter detection*, *Phys. Rev. D* **92** (2015) 075012 [1411.7382].
- [330] J. L. Ouellet, C. P. Salemi, J. W. Foster, R. Henning, Z. Bogorad, J. M. Conrad et al., *Design and implementation of the abracadabra-10 cm axion dark matter search*, *Phys. Rev. D* **99** (2019) 052012.
- [331] C. P. Salemi, J. W. Foster, J. L. Ouellet, A. Gavin, K. M. W. Pappas, S. Cheng et al., *Search for low-mass axion dark matter with abracadabra-10 cm*, *Phys. Rev. Lett.* **127** (2021) 081801.
- [332] N. Crisosto, P. Sikivie, N. S. Sullivan, D. B. Tanner, J. Yang and G. Rybka, *ADMX SLIC: Results from a superconducting lc circuit investigating cold axions*, *Phys. Rev. Lett.* **124** (2020) 241101.
- [333] A. V. Gramolin, D. Aybas, D. Johnson, J. Adam and A. O. Sushkov, *Search for axion-like dark matter with ferromagnets*, *Nature Phys.* **17** (2021) 79 [2003.03348].
- [334] Y. Kahn, B. R. Safdi and J. Thaler, *Broadband and resonant approaches to axion dark matter detection*, *Physical Review Letters* **117** (2016) .
- [335] M. Silva-Feaver et al., *Design Overview of DM Radio Pathfinder Experiment*, *IEEE Trans. Appl. Supercond.* **27** (2017) 1400204 [1610.09344].
- [336] DMRADIO collaboration, *Proposal for a definitive search for GUT-scale QCD axions*, *Phys. Rev. D* **106** (2022) 112003 [2203.11246].
- [337] DMRADIO collaboration, *Electromagnetic modeling and science reach of DMRadio- m^3* , 2302.14084.
- [338] M. Goryachev, B. T. McAllister and M. E. Tobar, *Axion detection with precision frequency metrology*, *Physics of the Dark Universe* **26** (2019) 100345.
- [339] C. Thomson, M. Goryachev, B. T. McAllister and M. E. Tobar, *Corrigendum to “axion detection with precision frequency metrology” [phys. dark universe 26 (2019) 100345]*, *Physics of the Dark Universe* **32** (2021) 100787.
- [340] A. Berlin, R. T. D’Agnolo, S. A. R. Ellis, C. Nantista, J. Neilson, P. Schuster et al., *Axion Dark Matter Detection by Superconducting Resonant Frequency Conversion*, *JHEP* **07** (2020) 088 [1912.11048].

- [341] A. Berlin, R. T. D’Agnolo, S. A. R. Ellis and K. Zhou, *Heterodyne broadband detection of axion dark matter*, *Phys. Rev. D* **104** (2021) L111701 [2007.15656].
- [342] R. Lasenby, *Microwave cavity searches for low-frequency axion dark matter*, *Phys. Rev. D* **102** (2020) 015008 [1912.11056].
- [343] J. Jaeckel and J. Redondo, *Resonant to broadband searches for cold dark matter consisting of weakly interacting slim particles*, *Phys. Rev. D* **88** (2013) 115002 [1308.1103].
- [344] D. Horns, J. Jaeckel, A. Lindner, A. Lobanov, J. Redondo and A. Ringwald, *Searching for WISPy Cold Dark Matter with a Dish Antenna*, *JCAP* **1304** (2013) 016 [1212.2970].
- [345] FUNK EXPERIMENT collaboration, *Limits from the Funk Experiment on the Mixing Strength of Hidden-Photon Dark Matter in the Visible and Near-Ultraviolet Wavelength Range*, *Phys. Rev. D* **102** (2020) 042001 [2003.13144].
- [346] BREAD collaboration, *Broadband Solenoidal Haloscope for Terahertz Axion Detection*, *Phys. Rev. Lett.* **128** (2022) 131801 [2111.12103].
- [347] G. Hoshino et al., *First Axion-Like Particle Results from a Broadband Search for Wave-Like Dark Matter in the 44 to 52 μeV Range with a Coaxial Dish Antenna*, **2501.17119**.
- [348] S. A. Hoedl, F. Fleischer, E. G. Adelberger and B. R. Heckel, *Improved constraints on an axion-mediated force*, *Phys. Rev. Lett.* **106** (2011) 041801.
- [349] W.-T. Ni, S.-s. Pan, H.-C. Yeh, L.-S. Hou and J. Wan, *Search for an axionlike spin coupling using a paramagnetic salt with a dc squid*, *Phys. Rev. Lett.* **82** (1999) 2439.
- [350] P.-H. Chu, A. Dennis, C. B. Fu, H. Gao, R. Khatiwada, G. Laskaris et al., *Laboratory search for spin-dependent short-range force from axionlike particles using optically polarized ^3He gas*, *Phys. Rev. D* **87** (2013) 011105.
- [351] J. Lee, A. Almasi and M. Romalis, *Improved limits on spin-mass interactions*, *Phys. Rev. Lett.* **120** (2018) 161801.
- [352] H. Fosbinder-Elkins, Y. Kim, J. Dargert, M. Harkness, A. A. Geraci, E. Levenson-Falk et al., *A method for controlling the magnetic field near a superconducting boundary in the ariadne axion experiment*, *Quantum Science and Technology* **7** (2022) 014002 [1710.08102].
- [353] C. Lohmeyer, N. Aggarwal, A. Arvanitaki, A. Brown, A. Fang, A. Geraci et al., *Microwave cavities and detectors for axion research*, *Springer International Publishing eBooks* (2020) .
- [354] V. Gkika, Y. Kim, A. Matlashov, Y. C. Shin, Y. Semertzidis, R. Cantor et al., *Optimization of High-Sensitivity SQUID Gradiometer for ARIADNE at CAPP*, *J. Low Temp. Phys.* **216** (2024) 386.
- [355] A. Garcon, D. Aybas, J. W. Blanchard, G. Centers, N. L. Figueroa, P. W. Graham et al., *The cosmic axion spin precession experiment (CASPER): a dark-matter search with nuclear magnetic resonance*, *Quantum Science and Technology* **3** (2017) 014008.
- [356] D. Aybas, J. Adam, E. Blumenthal, A. V. Gramolin, D. Johnson, A. Kleyheeg et al., *Search for axionlike dark matter using solid-state nuclear magnetic resonance*, *Phys. Rev. Lett.* **126** (2021) 141802.
- [357] C. Abel, N. J. Ayres, G. Ban, G. Bison, K. Bodek, V. Bondar et al., *Search for axionlike dark matter through nuclear spin precession in electric and magnetic fields*, *Phys. Rev. X* **7** (2017) 041034.
- [358] D. Aybas, H. Bekker, J. W. Blanchard, D. Budker, G. P. Centers, N. L. Figueroa et al., *Quantum sensitivity limits of nuclear magnetic resonance experiments searching for new fundamental physics*, *Quantum Science and Technology* **6** (2021) 034007.
- [359] A. O. Sushkov, O. P. Sushkov and A. Yaresko, *Effective electric field: Quantifying the sensitivity of searches for new P, T -odd physics with $\text{EuCl}_3 \cdot 6\text{H}_2\text{O}$* , *Phys. Rev. A* **107** (2023) 062823 [2304.08461].
- [360] A. J. Winter, T. Marić, V. A. Balabanova, J. Ádám, G. Randall, A. Wickenbrock et al., *Calibration of the Solid-State Nuclear Magnetic Resonance Search for Axion-Like Dark Matter*, *Annalen Phys.* **536** (2024) 2300252.
- [361] T. Wu et al., *Search for Axionlike Dark Matter with a Liquid-State Nuclear Spin*

- Comagnetometer*, *Phys. Rev. Lett.* **122** (2019) 191302 [1901.10843].
- [362] T. Wu, J. W. Blanchard, G. P. Centers, N. L. Figueroa, A. Garcon, P. W. Graham et al., *Search for axionlike dark matter with a liquid-state nuclear spin comagnetometer*, *Phys. Rev. Lett.* **122** (2019) 191302.
- [363] A. Garcon, J. W. Blanchard, G. P. Centers, N. L. Figueroa, P. W. Graham, D. F. J. Kimball et al., *Constraints on bosonic dark matter from ultralow-field nuclear magnetic resonance*, *Science Advances* **5** (2019) eaax4539 [<https://www.science.org/doi/pdf/10.1126/sciadv.aax4539>].
- [364] I. M. Bloch, G. Ronen, R. Shaham, O. Katz, T. Volansky and O. Katz, *New constraints on axion-like dark matter using a floquet quantum detector*, *Science Advances* **8** (2022) eabl8919 [<https://www.science.org/doi/pdf/10.1126/sciadv.abl8919>].
- [365] J. Lee, M. Lisanti, W. A. Terrano and M. Romalis, *Laboratory Constraints on the Neutron-Spin Coupling of feV-Scale Axions*, *Phys. Rev. X* **13** (2023) 011050 [2209.03289].
- [366] NASDUCK collaboration, *Constraints on axion-like dark matter from a SERF comagnetometer*, *Nature Commun.* **14** (2023) 5784 [2209.13588].